PITPNA AND PITPNB COOPERATE IN MAINTAINING NSCS SELF-RENEWAL VIA GOLPH3-DEPENDENT NOTCH SIGNALING DURING MOUSE BRAIN DEVELOPMENT.

A Dissertation

by

SEONG KWON HUR

Submitted to the Office of Graduate and Professional Studies of
Texas A&M University
in partial fulfillment of the requirements for the degree of

DOCTOR OF PHILOSOPHY

Chair of Committee,	Vytas A. Bankaitis
Committee Members,	Robin Fuchs-Young
	Siegfried Musser
	David W. Threadgill
Head of Program,	Warren Zimmer

December 2018

Major Subject: Medical Sciences

ABSTRACT

Phosphatidylinositol (PtdIns) transfer proteins (PITPs) stimulate PtdIns-4-Hydroxy Kinases, generating a lipid signaling in eukaryotic cells, but the biological outcomes of these signaling pathways remain unclear. Herein, we exploit genetic techniques, shRNA, and an *in utero* electroporation approach to investigate the role of PITP-dependent inositol lipid signaling in the embryonic neural stem cell (NSC) pool. The chief discoveries of this work are 1) that two type-1 START-like PITPs, PITPNA and PITPNB are specifically required for maintaining the NSC pool (meaning that the functional role of PITPNA/PITPNB in NSCs self-renewing cannot be accounted for by a simple PtdIns-gradient model) and 2) PITPNA and PITPNB are specifically required to cooperate in maintaining neural stem cell (NSCs) self-renewal via a PtdIns-4-P and GOLPH3-dependent mechanism, a critical process for proper neuronal development.

This discovery is the culmination of a number of smaller discoveries. First, we found that the combination of a *Pitpna* null mouse line and *Pitpnb* silencing evokes a dramatic depletion of NSC reserves via accelerating asymmetric differentiation cell division in embryonic brain (see 2.4.1, 2.4.2). While a plasmid that is isogenic to the wild-type PITPNA or PITPNB rescued this NSC depletion, PITPNA mutant clones that prevent phosphatidylinositol or phosphatidylcholine binding failed to rescue the NSC depletion during *in utero* electroporation experiments (see 2.4.3). Moreover, neither Sec14p, (a structurally unrelated yeast PITP with similar lipid-binding/transfer activities and cellular localization) nor PITPNC1 (a mouse homolog of PITPNA/PITPNB that also shows similar PtdIns-transfer activity but with PtdOH as the secondary ligand), restored the NSC pool in *Pitpna*$^{-/-}$ embryos expressing *Pitpnb* shRNA (see

2.4.4). We observed that GOLPH3-dependent Golgi positioning is required for controlling NSC self-renewing and maintaining the NSC pool, and that shRNA for GOLPH3 yielded a similar NSC pool reduction phenotype to PITPNA/PITPNB$^{-/-}$ (see 2.4.5, 2.4.6). Furthermore, we confirmed that PITP deficiencies cause a significant reduction of the Notch intracellular domain (NICD) in embryonic NSCs (see 2.4.7). We propose a mechanism where PITPNA/PITPNB drive PtdIns-4-P-dependent recruitment of GOLPH3 to Golgi membranes so as to promote an asymmetric Golgi network where Notch receptor is maturated to control the NSC self-renewing.

DEDICATION

This dissertation is dedicated to my family. I would like to express my deepest thanks to my wife, Chihea Moon and my 4 adorable kids. Without her love, devoted support, and patience, I could not move forward and achieve anything. I sincerely appreciate her and hold her close to my heart.

ACKNOWLEDGEMENTS

I enthusiastically and thankfully write this page to acknowledge all researchers and scientists who have assisted and taught me to perform research in the field of molecular and cellular biology. Without their devoted contributions, the studies I am about to describe in this dissertation could not be accomplished.

First, I would like to express immeasurable gratitude to my mentor and dissertation committee chair, Dr. Vytas A. Bankaitis. He has offered excellent academic advice and thoughtful guidance. He trained me to develop novel research ideas, design research studies, test hypotheses, analyze the data, and interpret findings accurately and properly. He has always supported studies academically and monetarily for the lab. He supported me to present my study findings at department seminars, internal conferences, and international conferences, and he always spent a lot of time going over the presentation to make sure the contents, findings, interpretations, and approach were delivered correctly. I greatly appreciate Dr. Bankaitis's extraordinary supervision.

I also wish to express my appreciation to the dissertation committee members, Dr. Robin Fuchs-Young, Dr. Siegfried M. Musser and Dr. David W. Threadgill, for sharing many ideas and valuable suggestions on my research that improved the quality of my research and presentation. I was so lucky to have thesis advisers like you.

I also would like to thank all the current and alumni members in Dr. Bankaitis' lab, Dr. Zhigang Xie, Dr. Mark McDermott, Dr. Ashutosh Tripathi, Dr. Aby Grabon, Dr. Danish Khan, Yiwei Miao, Yuanlong Shao, Yaxi Wang, Elliot Martinez, Benjamin Osborn, Dongju Lee, Angela Arabiotorre for being awesome colleagues and friends during my unforgettable time in

the Dr. Bankaitis lab. I really appreciate your willingness to help and share me reagents, ideas, and research experiences, it was great encouragement to me.

Finally, I would like to express my gratitude to my parents, JayHurn Hur and KwangJa Kim; and my parents-in-law, KyeongSoo Kim who have encouraged and unconditionally supported me. I could not have done my Ph.D. without their love, unconditional support, and patience.

CONTRIBUTORS AND FUNDING SOURCES

This work was supported by a dissertation committee consisting of Professor Vytas Bankaitis, Professor Robin Fuchs-Young, and Professor Siegfried Musser of the Department of Molecular and Cellular Medicine, and Professor David W. Threadgill of the Department of Veterinary Pathobiology.

Some plasmids described in Chapter II were provided by Zhigang Xie of the Department of Molecular and Cellular Medicine and were published in Developmental Cell, March 26, 2018. All other work conducted for the dissertation was completed by the student independently.

This work was funded by grants from the NIH (R01GM112591) and The Robert A. Welch Foundation (BE-0017).

NOMENCLATURE

ADP	Adenosine diphosphate
AP1	Adaptor protein complex 1
ARF	ADP ribosylation factor
ATP	Adenosine triphosphate
BAR	Bin, Amphiphysin, Rvs; Membrane binding domain
CAG	Chicken beta actin promoter (Strong synthetic promoter)
CERT	Ceramide transfer protein
COPI	Coat protein complex
CRD	Chylomicron retention disease
DCC	Deleted in colorectal cancer
DAG	Diacylglycerol
EEA1	Early Endosome Antigen 1
ER	Endoplasmic reticulum
EGFP	Enhanced green fluorescent protein
FAPP	Four phosphate adaptor protein
FYVE	Fab1, YOTB, VAC1, EEA1
GEF	Guanine nucleotide exchange factor
GFP	Green fluorescent protein
GGA	Golgi Associated, Gamma Adaptin Ear Containing protein
GM130	Golgin subfamily A member 2, cis-Golgi marker protein
GOLPH3	Golgi phosphoprotein 3

GSK3	Glycogen synthase kinase 3
GTP	Guanosine-5'-triphosphate
HES1	Hairy and enhancer of split-1, transcriptional factor
IPC	Intermediate progenitor cells
INM	Interkinetic nuclear migration
INPP1	Inositol polyphosphate-1-phosphatase
INPP5E	Inositol polyphosphate-5-phosphatase
Ins	Inositol
$InsP_3$	Ins-1,4,5-triphosphate
InsP	D-*myo*-inositol-1-phosphate
IUE	*in utero* electroporation
JNK	c-Jun N-terminal kinases
MEFs	Mouse embryonic fibroblasts
NICD	Notch intracellular domain
NSC	Neural stem cell
OSBP	Oxysterol-binding protein
Pax6	Paired box protein Pax-6; NSC marker
PCP	Planer cell polarity
PIP_2	phosphatidylinositol bisphosphate
PITP	Phosphatidyl inositol transfer protein
PITPNA	Phosphatidyl inositol transfer protein alpha
PITPNB	Phosphatidyl inositol transfer protein beta
PITPNC1	Phosphatidyl inositol transfer protein NC1, RdgB

PI3Ks	Phosphatidylinositol -3-phosphate kinases
PI4Ks	Phosphatidylinositol 4-OH kinases
PLC	Phospholipase C
PtdCho	Phosphatidyl choline
PtdIns	Phosphatidyl inositol
PtdOH	Phosphatidic acid
PH	Pleckstrin homology
PKC	Protein kinase C
PTEN	PtdIns-3,4,5-P3 phosphatase
PX	phosphoinositide-binding structural domain
Rac1	Ras-related C3 botulinum toxin substrate 1
RAS	A protein superfamily of small GTPases
RhoA	Ras homolog gene family, member A
ROCK	Rho-associated protein kinase
SGMS1	Sphingomyelin synthase 1
shRNA	Short hairpin RNA
START	StAR-related lipid transfer
Tbr2	T-box brain protein 2
TGN	Trans Golgi network
Fab1	Phosphatidylinositol 3-phosphate 5-kinase
VAC1	Vesicle transport protein
Wnt	signaling glycoproteins

TABLE OF CONTENTS

LIST OF FIGURES

CHAPTER I

INTRODUCTION

1.1 Inositol signaling

Over the past 30 years, the roles of phosphorylated D-*myo*-inositol (Ins-phosphates) and phosphatidylinositol (a lipid comprised of inositol bound to diacylglycerol via a phosphodiester bond) within cellular signal transduction have been well studied (Di Paolo and De Camilli, 2006; Fruman et al., 1998; Michell, 2008). The inositol (Ins) and phosphoinositide (PtdIns) signaling pathways regulate diverse cellular events in eukaryotic cells, and disturbances in these signaling pathways are the fundamental causes of many diseases, including cancer and neurological diseases.

1.1.1 Inositol is a signaling scaffold

The inositol and phosphoinositide signaling pathways are major signaling pathways for intracellular regulatory systems. Phosphoinositides accomplish dual signaling roles in the inositol signaling pathway. First, phosphoinositides are the source from which several important signaling molecules are generated. For example, Phosphatidylinositol-4,5-bisphosphate is commonly hydrolyzed by phospholipase C (PLC) to produce the versatile second messenger diacylglycerol (DAG) and soluble Ins-1,4,5-triphosphate ($InsP_3$) (Rhee, 2001; Suh et al., 2008). In this case, the diacylglycerol second messenger activates protein kinase C (PKC) to phosphorylate diverse proteins in a signaling cascade, and the soluble $InsP_3$ opens the gates of

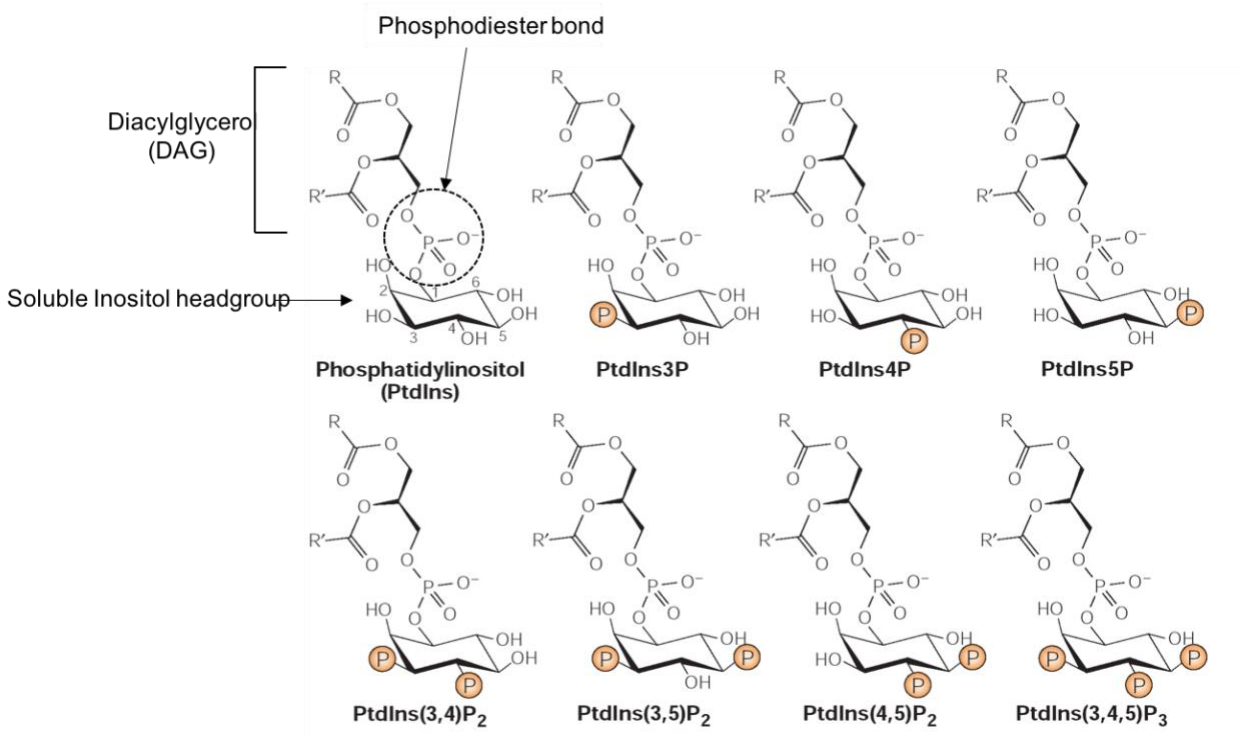

Figure 1. Mammalian cells generate 7 chemically distinct phosphoinositides.

The inositol head group is a 6-carbon ring structure, where each carbon site has a hydroxyl group that can be phosphorylated. The soluble group is connected to the diacylglycerol group by a phosphodiester bond.

intracellular calcium channels and serves as the precursor of other soluble Ins-phosphates. (Berridge and Irvine, 1984; Odom et al., 2000). Second, in addition to their roles as precursors for other second messenger molecules, phosphoinositides have their own innate signaling capabilities. Within mammalian cells, only 7 chemically distinct phosphoinositides (PtdIns-3-P, PtdIns-4-P, PtdIns-5-P, PtdIns(3,5)P_2, PtdIns(4,5)P_2, PtdIns(3,4)P_2, and PtdIns(3,4,5)P_3) (Fig. 1) are generated, but each are recognized by effector proteins that encode specific phosphoinositide-binding domains, such as pleckstrin homology (PH) domains, Fab1, YOTB, VAC1 and EEA1 (FYVE) domains, PX domains, and BAR domains (Balla, 2005; Bankaitis et al., 2010; Lemmon, 2008; McLaughlin and Murray, 2005). Despite the limited number of phosphoinositides, the biological outcomes of phosphoinositide signaling are extremely diverse, even within a given cellular compartment. However, the mechanism by which this diversity in biological outcomes is attained from such limited molecules still remains a mystery.

1.1.2 PtdIns-4-P signaling and its role in proper intracellular trafficking

PtdIns-4-P is produced by phosphatidylinositol 4-OH kinases (PI4Ks) by phosphorylation of PtdIns on the 4-OH position of the inositol head group (Fig 1). Mammals have two classes of PI4Ks: the type II (PI4KIIα, PI4KIIβ) and type III (PI4KIIIα and PI4KIIIβ) PI4Ks, which have different domain group (Boura and Nencka, 2015). The type II kinases mainly localize to Golgi and endosomal membranes (Clayton et al., 2013; Salazar et al., 2005), although others demonstrate that PI4KIIα primarily localizes to the TGN and minor at the ER membranes (Waugh et al., 2003). The mammalian type III PI4Ks variously localize to the cytosol, nucleolus, the cis-Golgi, and the ER (Balla et al., 2000; Dumaresq-Doiron et al., 2010; Kakuk et al., 2006; Nakatsu et al., 2012). As a result, PtdIns-4-P pools are present on the TGN, the plasma

membrane and the early, late and lysosomal endosomal membranes (Hammond et al., 2014; Hammond et al., 2009; Nakatsu et al., 2012; Sridhar et al., 2013).

Studies in *S. cerevisiae* were the first to show that PtdIns-4-P regulates Golgi trafficking - hypomorphic PtdIns-4-OH kinase mutants (which are therefore defective in PtdIns-4-P production) display a secretory pathway disruption phenotype (Hama et al., 1999; Walch-Solimena and Novick, 1999). Several studies in other eukaryotic systems have observed various Golgi-related PtdIns-4-P effectors which regulate vesicle budding, maintenance of Golgi structure and non-vesicular lipid transport, indicating a ubiquitous role for PtdIns-4-P signaling across higher eukaryotes (D'Angelo et al., 2007; Dippold et al., 2009b; Godi et al., 2004; Toth et al., 2006; Wang et al., 2003).

1.1.3 PtdIns-4-P effector proteins and their roles in signal interpretation

The TGN/endosomal networks operate as an intracellular regulatory core, in which cargo sorting, and therefore nutrient sorting and post-translational modification, is controlled by lipid signaling. The role of lipid signaling, including PttdIns-4-P signaling, between the trans-Golgi network (TGN) and the endosomal membrane, as well as its effects on vesicular and non-vesicular trafficking, is well-documented (Balla, 2013; Bankaitis et al., 1990; Bankaitis et al., 2012; Gu et al., 2001; Mellman, 1996; Roth, 2004). Proteins that have an observable change in activity as a result of binding to PtdIns-4-P are known as effector proteins. These effectors include two main classes - the adaptor and coat complexes group (i.e., AP-1 and GGA), and the lipid-transfer proteins group (i.e., CERT , FAPP, OSBP) (D'Angelo et al., 2008).

The adaptor and coat complexes group covers a diverse family of proteins that control vesicular transport. ARF-GTP, one of best-described effectors, collaborates with PtdIns-4-P to

employ vesicle biogenesis players, such as clathrin adaptor protein complex 1 (AP-1), Rab GTPase/Rab guanine nucleotide exchange factor (GEFs), and the GGA adaptor proteins, which control trafficking between TGN and lysosome (Demmel et al., 2008; Heldwein et al., 2004; Wang et al., 2007).

The lipid transfer proteins group instead includes a number of proteins known to play a role in non-vesicular transport. An example of this family includes the four phosphate adaptor proteins (FAPPs), which interact with both ARF-GTPase and PtdIns-4-P through their plekstrin homology (PH) domain at TGN to regulate the process of membrane tubulation and post-Golgi trafficking (Cao et al., 2009; Godi et al., 2004). Meanwhile, CERT is responsible for the non-vesicular transfer of ceramide from the ER, where ceramide is synthesized, to the Golgi complex (Hanada et al., 2003). In the Golgi, CERT binds to PtdIns-4-P, which serves as a signal to deposit bound ceramide into the Golgi membrane, allowing it to be used for the production of sphingomyelin through sphingomyelin synthase 1 (SGMS1).

In addition to these broad families, there are a number of known PtdIns-4-P binding proteins whose function remains unknown. GOLPH3, a known PtdIns-4-P binding protein that is known to localize to the Golgi and then to help Golgi formation (Dippold et al., 2009a; Wood et al., 2009), has remained one of these. However, given the evidence presented later in this work, we propose that GOLPH3 plays a vital role as a PtdIns-4-P effector protein in Golgi PtdIns-4-P signaling during embryonic brain development (see 2.4.6).

1.2 PtdIns 4-OH kinases are a biologically insufficient enzyme

PtdIns-4-P signaling is often investigated under the lens of understanding the PtdIns 4-OH kinases (PI4Ks) and phosphatases. However, PtdIns 4-OH kinases are known to be inefficient

regulators of the PtdIns-4-P signaling because the enzyme, on its own, is biologically insufficient for generation of the PtdIns-4-P signal due to the ubiquitous presence of phosphoinositide phosphatases and PtdIns-4-P-binding proteins that, in effect, erase minor or accidental signals (Bankaitis et al., 2010; Grabon et al., 2015; Schaaf et al., 2008).

To overcome this effect, PI4Ks utilize a number of assistant proteins to allow them the ability to find or access PtdIns, thereby boosting PtdIns-4-P production to enable a meaningful PtdIns-4-P signal. Phosphatidylinositol transfer proteins (PITPs), a family of proteins ubiquitous across eukaryotes, are strong and efficient regulators of PtdIns-4-P signaling. These proteins boost PtdIns-4-P production by simulating PtdIns-4-OH kinases, which is enough to overcome the activity of erasers to induce PtdIns-4-P signaling. Moreover, PITPs appear to not only play a key role in regulating PtdIns-4-P signaling via activation of the PtdIns-4-OH kinase, but they also can, in part, explain the diversity of biological outcomes which arise from PtdIns-4-P signaling.

1.3 Phosphatidylinositol transfer proteins (PITPs)

Phosphatidylinositol transfer proteins (PITPs) are highly conserved in all eukaryotes. The ‘classical’ PITPs have the energy-independent ability to transport PtdIns and another lipid, Phosphatidylcholine (PtdCho), between membranes in vitro. These PITPs bind PtdIns and PtdCho in a mutually exclusive manner. Within these proteins, the binding affinity for PtdIns is much stronger than for PtdCho, and the transfer rate of PtdIns is approx. 20-fold greater than that of PtdCho (Wirtz, 1991). The ‘non-classical’ PITPs preserve the ability to transport PtdIns but have the ability to bind and transfer other second lipids instead of PtdCho (Li et al., 2000; Nile et al., 2010; Phillips et al., 2006b; Routt et al., 2005).

PITPs divide into two distinct branches, which are the yeast Sec14-like PITPs and the START-like (StAR-related lipid transfer domain) PITPs. The Sec14 –like PITPs comprise 6 members including the founding member, which is the major yeast PITP Sec14 (Bankaitis et al., 1990; Cleves et al., 1991). According to recent studies, the Sec14-like PITPs include both classical and non-classical PITPs. Sec14-like PITPs are a useful example of how the classical and non-classical PITPs of Sec14-like proteins provide diversity in lipid binding to induce diverse biological outcomes for phosphoinositide signaling (Grabon et al., 2015; Huang et al., 2016). The detailed mechanisms of how these proteins fulfill their functions remain unclear.

On the other hand, the START-like PITPs are still poorly unknown in terms of their biological functions compared to the Sec14-like PITPs. In mammals there are 5 known START-like PITPs, which break down into two types: type-1 PITPs and type-2 PITPs. There are three type-1 PITPs (PITPNA, PITPNB and PITPNC1) and two type-2 PITPs. Type-1 PITPs are relatively small and are homologous to one another, while type-2 PITPs are larger and harbor a homologous domain to type-1 PITPs, but include additional structural and functional domains.

Adding to the confusion, type-1 PITPs are divided into two classes based on the secondary lipids that they bind in addition to PtdIns: Class I PITPs (comprised of PITPNA, PITPNB) bind PtdCho (like Sec14) and the Class II PITPs (PITPNC1) bind Phosphatidic Acid (PtdOH) (Cockcroft and Carvou, 2007; Nile et al., 2010). Although this dissertation focuses on the Class I START-like PITPs (PITPNA/PITPNB) found in mammalian cells, their distinction is important for some experiments presented in this work.

1.3.1 Biochemical properties of Class I START-like PITPs

PITPNA and PITPNB are encoded on separate chromosomes, but they share 77% primary sequence identity and 94% amino acid similarity. They exhibit the classical PITP features of PtdIns and PtdCho binding and transfer activities in vitro (De Vries et al., 1996; de Vries and Beart, 1995; Yoder et al., 2001), and they stimulate PtdIns-4-P production (Ile et al., 2010). PITPNB can be expressed in two spliced forms (sp1 and sp2) by alternative mRNA splicing, which only differ at the C-terminal 16-17 amino acids (Morgan et al., 2006; Phillips et al., 2006a). Crystal structural analysis of both PITPNA and PITPNB indicates that although they are structurally unrelated to Sec14-like PITPs, PtdIns and PtdCho undertake very similar positions within their single large lipid-binding cavity (Figure 2) (Schouten et al., 2002; Tilley et al., 2004; Yoder et al., 2001). The five hydroxyl sites of the inositol ring headgroup individually interact with four amino acids that are common to the two proteins (T59, K61, E86 and N90). Residue C95 is important for PtdCho binding of PITPNA (Alb et al., 1995; Tilley et al., 2004; Yoder et al., 2001).

Recently, *in silico* molecular dynamics simulation studies have generated a detailed view into the expected mechanisms by which Type1-START-like PITPs exchange PtdIns/PtdCho molecules between membranes (Grabon et al., 2017). Importantly, these simulations indicate a mechanism wherein the lipid is briefly exposed to the cytosolic environment, enabling the aforementioned activation of PtdIns-4-OH kinases, a model known as the *lipid presentation model*. This model could provide an explanation for the diversity of PI-4-P signaling outcomes, as interaction with the kinase or other scaffold proteins may provide a level of specificity in the signaling as a part of the lipid interaction. However, this model is contrary to the currently-accepted model of PITP function known as the *lipid gradient model*, wherein the role of PITPs is

to simply ensure distribution of PtdIns and other lipid molecules throughout the cell for cellular signaling. This dissertation contains *in vivo* evidence that directly contradicts the lipid gradient model, as PITPs which bind and transfer the same lipid molecules within the same cellular compartments from different species are incapable of replacing one another, indicating a specific need for some protein element, separate from lipid transfer, which is necessary for proper embryonic development.

1.3.2 Cellular functions of Type 1 START-like PITPs

The cellular functions of type 1 PITPs are not well documented, although some clues exist as to their function. Chromaffin cell line studies have shown that PITPNA stimulates Ca^{2+}-activated secretion via the secretory vesicle (Hay et al., 1995; Hay and Martin, 1993). Also, data from a cell-free system derived from a neuroendocrine cell line, which had an embryonic origin from the neural crest, indicated that PITPNA is required for secretory vesicle formation from neuroendocrine TGN (Ohashi et al., 1995). PITPNA also interacts with netrin receptor DCC (deleted in colorectal cancer) and stimulates hydrolysis of phosphatidylinositol bisphosphate (PIP_2) by PLCβ or PLCγ1 (Kauffmann-Zeh et al., 1995; Xie et al., 2005). Gene silencing experiments have shown that PITPNB plays a crucial role in regulating nuclear envelope shape and is essential for COPI-mediated backward membrane trafficking from the cis-Golgi membrane to the endoplasmic reticulum (ER) (Carvou et al., 2010).

1.4 Type-1 START-like PITP-associated disease

The connection between PtdIns-4-P production via the biochemical properties of type-1 START-like PITPs and specific biological outcomes has not yet been resolved. However, it is

unambiguously clear that PITPNA is a critical gene for the survival of vertebrate organisms. In mice, PITPNA deficiency, caused by an engineered deletion that eliminates three exons encoding essential functional elements of the PITPNA, are born alive but suffer neonatal lethality due to multiple pathologies, including spinocerebellar neurodegenerative disease, deranged intestinal and hepatic lipid metabolism, and catastrophic hypoglycemia (Alb et al., 2003). In zebrafish retina development, PITPNB is primarily essential for the biogenesis and maintenance of the double cone photoreceptor cell outer segments (Ile et al., 2010). Recently, the mammalian PITPNC1 was revealed to have a PtdOH binding activity to become PtdIns/PtdOH transfer proteins (Garner et al., 2012). Interest in PITPNC1 is also rising in cancer biology - PITPNC1 is downregulated by the microRNA MIR-126, which is a tumor suppressor, and PITPNC1 promotes metastasis of multiple types of cancer (Halberg et al., 2016; Png et al., 2011).

1.4.1 Histological Analysis of neurodegenerative diseases in PITPNA Knockout mice

PITPNA null mice reveal strong inflammation and myelination defects in the cervical and lumbar spinal cord (Alb et al., 2003). In addition, the white matter of the spinal cord is clearly reduced, many neurons are damaged in PITPNA null mice, and inflammation occurs over the entire spinal cord. The response hits the motor neurons in the spinal cord, which are vacuolated and present an aponecrotic process, which is a form of cell death associated with low cellular ATP and a high ADP level. Demyelination occurred in both white and gray matter areas of *Pitpna*$^{0/0}$ mice, particularly in the dorsal spinal columns, and degeneration in the non-neuronal area and axonal swelling were also observed (Alb et al., 2003). Additional consequences are the activation of microglia and astrocytes in the cerebellum, and significant vacuolations of the smooth ER region in cerebellar neurons (Alb et al., 2003).

The phenotypes exhibited by the null mice include not only the spinocerebellar neurodegenerative disease but also glucose homeostasis and Chylomicron Retention Disease (CRD) defects, making it difficult to distinguish whether the spinocerebellar degeneration is a primary phenotype or a secondary consequence of the hypoglycemia and CRD. Previous work determined that given threshold levels of PITPNA activity, the degenerative phenotypes persist while the hypoglycemia and CRD are alleviated, although the beginning of the neurodegeneration disease is delayed without hypoglycemia and CRD (Alb et al., 2007). The combined data imply that the neurological disease is an clear pathology resulting from PITPNA null mice (Nile et al., 2010).

1.4.2 PITP-associated neurological disease

PITPNA is especially highly produced in the brain and cerebellum. In rat brain development, PITPNA is highly expressed in most neurons of all brain regions from embryogenesis until the neonatal developmental stages. In the adult rat, PITPNA is particularly highly expressed in the hippocampus and cerebellum (Imai et al., 1997; Nyquist and Helmkamp, 1989; Utsunomiya et al., 1997). Our PITPNA-deficient mouse model indicated, consistent with these expression reports, a crucial role for PITPNA in maintaining the integrity of the spinocerebellar system (Alb et al., 2003).

PITPNA null (*Pitpna*$^{0/0}$) mice are born alive at the expected normal frequencies from *Pitpna*$^{+/0}$ cross breeding but usually die within 5-7 days of birth. Sometimes, the *Ptipna*$^{0/0}$ homozygotes can live for 9-14 days after birth (Alb et al., 2003). The failure of the *Ptipna*$^{0/0}$ homozygotes to thrive is observed in the form of obvious tremors and weakened motor activity (Alb et al., 2003). The other category of PITPNA-deficient mice is an insertion of an IAP

retrotransposon, which encodes a splicing trap into an intron of the PITPNA gene (Hamilton et al., 1997; Weimar et al., 1982). The vibrato homozygous mice, which express only 20% of wild-type levels of wild-type PITPNA, live for 30~35 days after birth in the inbred C57BL/B6J (Hamilton et al., 1997). Rapid whole-body tremor is observed in the homozygous *Vb* mice. Genetic modifiers extend the lifespan of *Vb/Vb* homozygotes. Some outbred with A/J or even inbred A/J, which harbors *Vb/Vb* gene, have lifespans extending beyond 1 year, while A/J-mediated *Vb* insertion does not elevate the PITPNA expression level (Concepcion et al., 2011).

The neurodegenerative disease of the *Vb* mouse can be divided into three phases. In the early stage, phase I, the 'true vibrator' phenotype can be observed, which is defined by high-frequency tremors that begin approximately 14 days after the birth of $Pitpna^{Vb/Vb}$ homozygotes. Phase II describes a 'degenerative' phase defined by ataxia and action tremors. The animal's voluntary movements, such as posture, balance, and coordination, are affected by coarse tremors in phase II symptoms. Neurons in the spinal cord and the cerebellum are vacuolated and display dilation of the endoplasmic reticulum (ER) membrane system (Weimar et al., 1982). In phase III, breathing is irregular and labored. $Pitpna^{Vb/Vb}$ homozygote mice have been observed to remain in this stage continuously for several hours before death and typically enter into this stage at approximately 30-33 days after birth (Weimar et al., 1982).

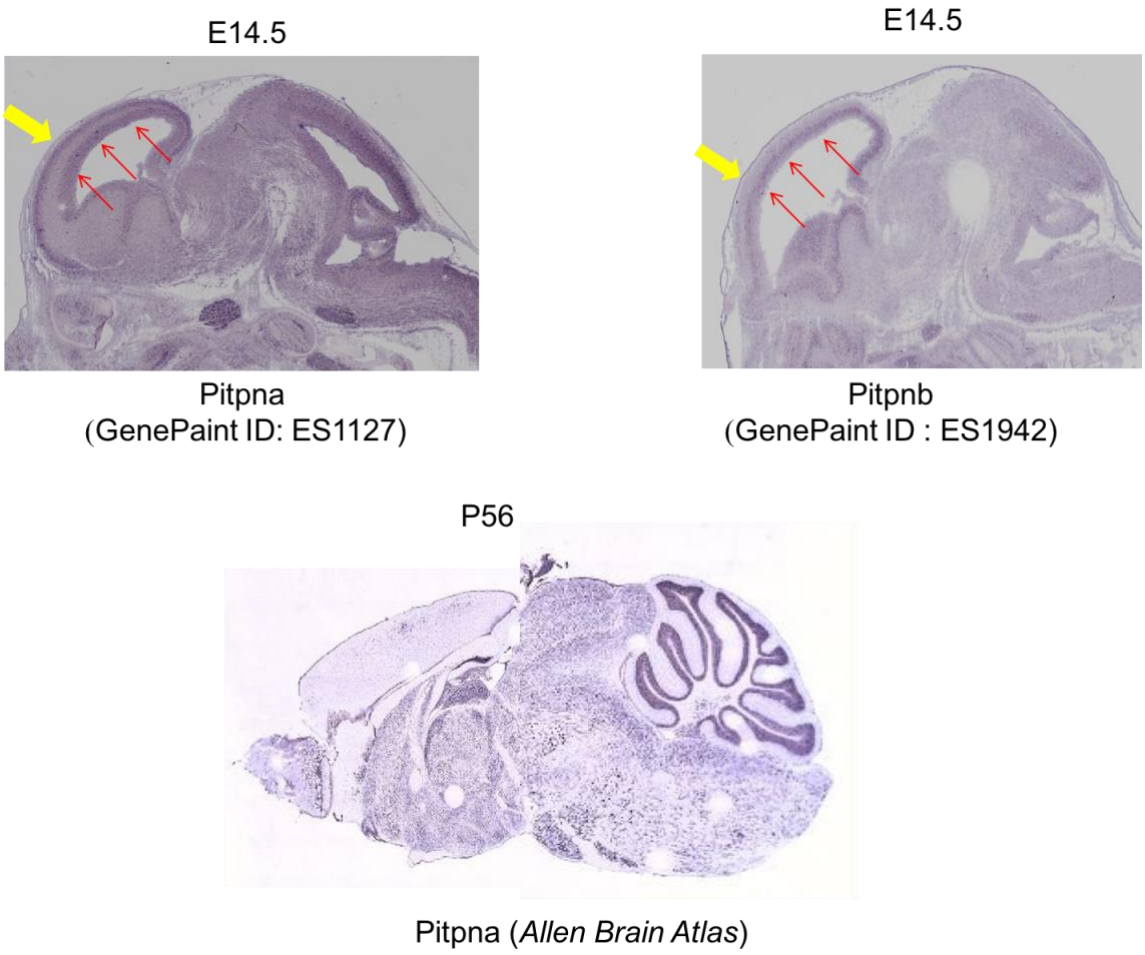

Figure 2. PITPs mRNA expression in brain tissue during mouse brain development.

In-situ hybridization data (sources : Gene paint , Allen Brain Atlas) shows that type 1 PITPs are highly expressed in the neocortical region (yellow arrow), especially ventricular zone (VZ, red arrow) of the neocortex during embryonic stages, while in the neonatal stage, the cerebellum highly expresses PITPs.

1.4.3 PITP expression in brain tissue during mouse brain development

The loss-of-function studies for individual Class 1 START-like PITPs provide some common findings that deficiencies of these proteins can be related to two physiological consequences. One is a neurological issue and the other is a developmental issue. So, we looked at PITP expression levels across mouse developmental stages in an in-situ hybridization database (*Genepaint, Allen Brain Atlas).* We confirmed that Type 1 PITPs are highly expressed in the neocortical region during embryonic stages, while in the adult stage, the cerebellum highly expresses PITPs (Figure 2). Especially, red arrows indicate that ventricular zone (VZ) is highly producing both type 1 PITPs. The VZ is almost entirely populated by neural stem cells (NSCs). In addition to, this data is very appreciated, expression pattern of *Pitpna* in adult stage shows a consistent region with the spinocerebellar neurodegenerative phenotype and defective neuron and glia cells in the cerebellum of *Pitpna* KO mice analysis.

1.5 Embryonic neocortex and Neural Stem Cells (NSCs)

The embryonic neocortex highly expresses both Pitpna and Pitpnb. In particular, the ventricular zone of the neocortex, which has the most abundant PITPs, is a striking region for the study of type 1 PITPs. The neocortex is a principal region in the mammalian brain for high-level brain functions such as memory, cognition, perception, learning, consciousness and language. The mammalian neocortex is a 6-layered structure in which each layer comprises different types of neurons. These neurons are generated from a pool of neural stem cells (NSCs) and intermediate progenitor cells in a temporally and anatomically controlled manner during the embryonic stage (Bjornsson et al., 2015; Sun and Hevner, 2014). For proper neocortical development, the NSC pool needs to be correctly maintained by controlling the balance between

self-renewal and differentiation of NSCs (Doe, 2008). Interference with this NSC homeostasis causes neocortical malformation and impairment of the higher-level functions controlled by the neocortex (Sun and Hevner, 2014).

1.5.1 Embryonic Neural Stem Cells

There are a couple of types of neural stem cells and progenitor cells in the embryonic neocortex. Especially in the mouse embryonic neocortex, only neuroepithelial cells and radial glial cells meet the standards for neural stem cells, which have the capacity for self-renewal and multi-step differentiation (Bjornsson et al., 2015; Kriegstein and Alvarez-Buylla, 2009; Sun and Hevner, 2014). Embryonic neural stem cells exhibit several cellular features that can be observed only in an *in vivo* system. First, NSCs have an apicobasal polarity. An individual NSC spans the entire neocortex, with an apical process contacting the ventricular surface and a basal process contacting the pial surface. Second, NSCs exhibit nuclear movement at different phases of the cell cycle, known as Interkinetic Nuclear Migration (INM). NSC nuclei undergoing S-phase remain at the basal side of the ventricular zone, while during the M phase, nuclei stay along the surface of the ventricle, and NSC nuclei in phases G1 and G2 migrate between the S and M phase locations in the mid region (Conti et al., 2005; Glaser and Brustle, 2005; Sauer and Walker, 1959; Sidman et al., 1959) (Figure 3). Third, the cell cycle length of embryonic NSCs is variable. The cell cycle of NSCs is relatively short during the early neurogenesis stages, whereas later neurogenesis stages increase the cell cycle length of NSCs (Doe, 2008; Miyama et al., 1997). Fourth, symmetric and asymmetric neural stem cell divisions in the ventricular zone are critical features during embryonic neurogenesis. NSCs have the ability to maintain the NSC pool via symmetric self-renewal and generating intermediate progenitor cells (IPCs) and neurons via

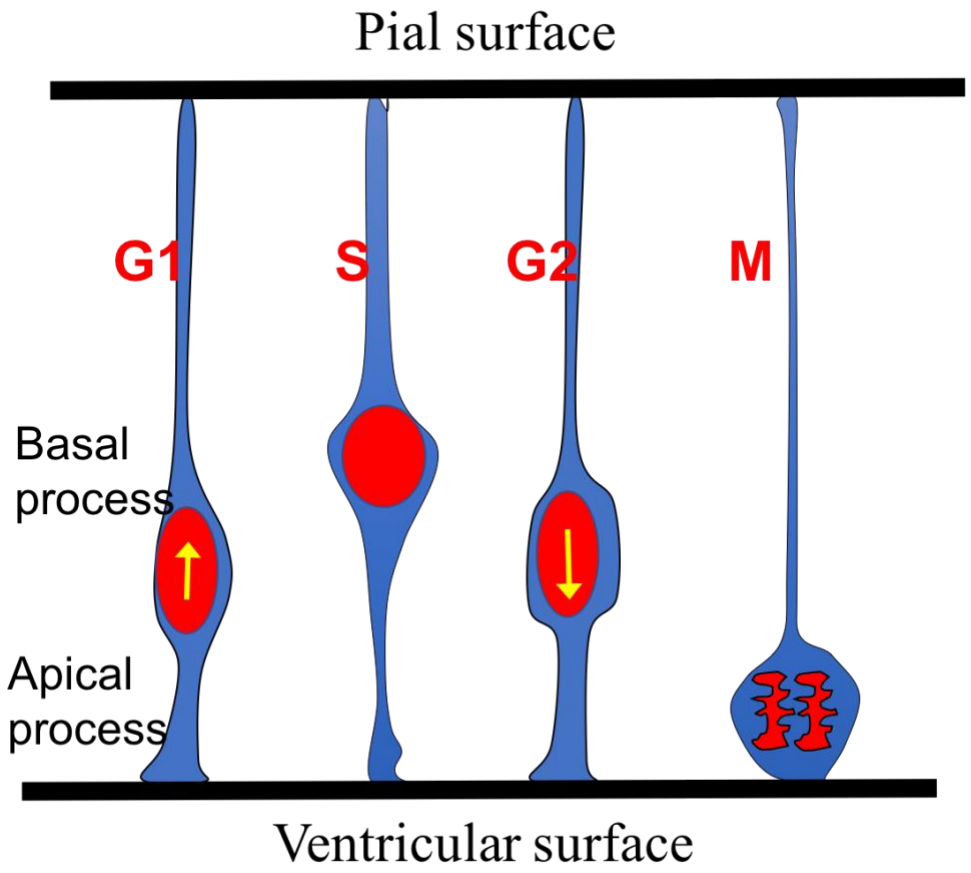

Figure 3. Interkinetic nuclear migration in NSCs in the mouse embryonic neocortex.

NSC nuclei undergoing S-phase remain at the basal side of the ventricular zone, while during M phase, nuclei stay along the surface of the ventricle, and NSC nuclei in phases G1 and G2 migrate between the S and M phase locations in the mid-region.

asymmetric cell divisions to develop the mouse neocortex (Doe, 2008; Kriegstein and Alvarez-Buylla, 2009). These key NSC features imply a limitation of the experimental strategy, which is to study embryonic NSCs while preserving the physiological NSC niche. Thus, the NSC primary culture system, which is widely utilized (i.e. Organoid, Neurosphere), does not preserve these key features (Artegiani et al., 2012; Kriegstein and Alvarez-Buylla, 2009; LoTurco et al., 2009).

1.5.2 Inositol lipid signaling in NSCs

The key features of embryonic NSCs are cell polarity, cell migration, membrane trafficking, gene transcription and mRNA translation, are associated with inositol lipid signaling (Balla, 2013; Grabon et al., 2015; Xie et al., 2018). Inositol lipid signaling is associated with regulating these embryonic NSC key features and plays critical roles in the neocortical development. Furthermore, recent studies reported that mutations in genes related with inositol lipid signaling lead to neocortical developmental brain disorders. For instance, mutations in PTEN (which encodes a PtdIns-3,4,5-P3 phosphatase), PLCB1 (which encodes a PIP-specific phospholipase C), INPP1(which encodes an inositol polyphosphate-1-phosphatase), PI3K (which encodes a PtdIns-3-phosphate kinase), and INPP5E (which encodes an inositol polyphosphate-5-phosphatase) are associated with autism and/or mental retardation (Bourgeron, 2009; Christian et al., 2008; Serajee et al., 2003; Zhou and Parada, 2012). However, many studies about role of these genes in developmental brain disorders have unfortunately employed differentiated neurons or adults NSCs (Bourgeron, 2009; Zhou and Parada, 2012) due to the experimental limitations associated with embryonic NSC studies even though PTEN plays a critical role in regulating embryonic NSCs homeostasis (Groszer et al., 2001).

1.6 Murine PITPNA and PITPNB functional redundancy in embryonic development

START-like PITPs share 77% primary sequence; however, it remains unknown how these proteins are associated with diverse cellular functions or whether these two PITPs act in a functional redundant manner are still unknown. At any rate, our previous report with respect to *Pitpna* null mice phenotypes showed that PITPNA is essential for some physiological roles in mice (Alb et al., 2003). *Pitpna* null mice are born and die within 10 days after born with diverse disease phenotypes (Alb et al., 2003). Moreover, the vibrator homozygous mice, which express only 20% of wild-type levels of wild-type PITPNA, live for 30~35 days after birth while rapid whole-body tremor is observed (Hamilton et al., 1997). Early attempt to generate *Pitpnb* null mice or null embryonic stem cells was failed. Recently, using a TALEN mutagenesis strategy we finally generated *Pitpnb* mice homozygous for a reading frameshift that eliminates production of PITPNB in all tissues. The *Pitpnb* null mice were born alive but, unlike *Pitpna* null mice, there is no obvious disease phenotype. We attempted to generate *Pitpna/Pitpnb* double whole body Knockout(KO) mouse to test potential issues of functional redundancy. However, of the 60 P0 neonates and 79 E12.5 embyos analyzed from intercross $Pitpna^{+/-}$ $Pitpnb^{+/-}$, there were none of recovered progenies determined either $Pitpna^{-/-}$ $Pitpnb^{-/-}$ or $Pitpna^{+/-}$ $Pitpnb^{-/-}$ genotypes and also of 12 E11.5 embryos which is ongoing analysis. If there is no genetic interation between two sets of null alleles, the expected recoveries of $Pitpna^{-/-}$ $Pitpnb^{-/-}$ genotype was 3.8 and 4.9 for the 60 P0 and 79 E12.5 cohorts, and of $Pitpna^{+/-}$ $Pitpnb^{-/-}$ genotype was 7.5 and 9.9 for that cohorts. Thus, combined whole body PITPNA/PITPNB deficiency prohibited successful completion of early embryonic development in the mouse with the critical failure occurring prior to E11.5, and a single functional *Pitpna* allele was insufficient to rescue developmental failure.

1.7 Dissertation Goal

Inositol lipid signaling plays a crucial role in diverse cellular events which are associated with brain development (Bourgeron, 2009; Christian et al., 2008; Serajee et al., 2003; Zhou and Parada, 2012), and there are much evidence that type 1 START-like PITPs are deeply associated with neurological disorders throughout development (Imai, Tanaka, Fukusato, Yamashita, & Hosaka, 1997; Nyquist & Helmkamp, 1989; Hamilton et al., 1997; Weimar, Lane, & Sidman, 1982). Thus, understanding how PITP-dependent PtdIns-4-P signaling is stimulated, and the role of this signaling pathway in supporting and controlling mouse brain development has been the primary focus of my doctoral experience and, consequently, this dissertation.

In order to achieve this goal, there are a number of technical problems that are known to be barriers of embryonic NSC study that we first aimed to resolve. For example, although it is easier to analyze embryonic stem cells *in vitro*, this environment fails to provide meaningful information regarding neuronal development. As such, an appropriate physiological setting, which preserves the embryonic NSC features, needed to be identified for complex NSC study. This was complicated by the early embryonic lethality associated with *Pitpna* and *Pitpnb*, requiring the use of a conditional tissue-specific double knockout strategy to investigate type 1 START-like-PITPs in the developing embryonic neocortex. Deployment of the neocortical specific double knockout progeny (genotype: $Pitpna^{fl/fl}\ Pitpnb^{fl/fl}\ Emx1^{Cre/+\ or\ Cre/Cre}$) showed that PITPNA/PITPNB control radial polarity of neural stem cells (NSCs) via a PtdIns-4-P and GOLPH3-dependent mechanism that promotes asymmetric Golgi distribution into the apical processes of NSCs during early embryonic neurogenesis (Xie et al., 2018). However, $Emx1^{Cre}$-mediated simultaneous deletion of *Pitpna* and *Pitpnb* led to disruption of the neocortical structure and rapid onset of cell death, preventing detailed analysis of the role of these PITPs in

embryonic NSCs (Xie et al., 2018). Thus, we employed an alternative strategy, in utero electroporation (IUE), to analyze NSC homeostasis defects in a PITPA/PITPB-deficient neocortex while preserving the normal physiological NSC niche. IUE allowed us to investigate detailed mechanisms of how PITPs-dependent PtdIns-4-P signaling support NSC homeostasis and determine which signaling pathways are associated with PITP-dependent PtdIns-4-P signaling.

CHAPTER II

PITPNA AND PITPNB COOPERATE IN MAINTAINING NSCS SELF-RENEWAL VIA GOLPH3-DEPENDENT NOTCH SIGNALING DURING MOUSE BRAIN DEVELOPMENT

2.1 Overview

Phosphatidylinositol (PtdIns) transfer proteins (PITPs) stimulate PtdIns-4-P synthesis and signaling in eukaryotic cells. However, the precise nature of the associated signaling pathways, and of the biological outcomes associated with PITP activities remain unclear. Herein, we show that two type-1 START-like PITPs, PITPNA and PITPNB, cooperate in maintaining neural stem cell (NSC) self-renewal via a PtdIns-4-P and GOLPH3-dependent mechanism that promotes Notch signaling in embryonic NSCs. We have exploited an *in utero* electroporation approach to investigate the role of PITP-dependent inositol lipid signaling in the embryonic NSC pool. By silencing *Pitpnb* with shRNA in a *Pitpna* null mouse line we evoked a dramatic depletion of the NSC pool achieved through acceleration asymmetric differentiation of cell division in the embryonic brain. *In utero* electroporation delivery of plasmids isogenic to wild-type PITPNA or PITPNB rescued the NSC depletion resulting from eviction of both PITPs. However, a PITPNA mutant clone deficient in phosphatidylinositol or phosphatidylcholine binding failed to rescue NSC depletion. Moreover, neither Sec14p, the major yeast PITP, which possesses the same lipid-binding/transfer activities but is structurally unrelated to type1 PITPs, nor PITPNC1, a homolog of PITPNA/PITPNB that also shows PtdIns-transfer activity but which uses a different second lipid, PtdOH, restored the NSC pool. These data reveal that PITPNA/PITPNB are specifically required for maintaining the NSC pool and additionally demonstrate that the function role of

PITPNA/PITPNB in NSC self-renewal cannot be accounted for by simple PtdIns-4-P transfer as proposed in PtdIns-gradient models. We observed GOLPH3-dependent Golgi positioning which was required for controlling NSC self-renewal, and for maintaining the NSC pool. Furthermore, we confirmed that PITP deficiencies evokes a significant reduction of the Notch intracellular domain (NICD) in embryonic NSC. We propose a mechanism where PITPNA/PITPNB drive PtdIns-4-P-dependent recruitment of GOLPH3 to Golgi membranes so as to promote an asymmetric Golgi network where the Notch receptor matures to control NSC self-renewal.

2.2 Introduction

The higher-level functions of the mammalian brain are enabled by the structure known as the neocortex. During neocortical development, neural stem cells (NSCs) differentiate into a variety of cell types that distribute in such a way as to create a six-layered structure capable of unparalleled neuronal connections that enable complex functions such as sensory perception, motor control, learning, conscious thought, and language. The development of the neocortex (which typically occurs during mouse embryonic stages E11.5-E17.5) is a delicate balancing act requiring that neural stem cells (NSCs) must differentiate into intermediate progenitor cells (IPCs), polarized neurons, glial cells, and other cell types in a regionally and temporally restricted fashion, while NSCs must be replenished and correctly distributed during this time, requiring complex control mechanisms which maintain the balance between differentiation and self-renewal of the neural stem cell population so that the appropriate number and types of neocortical cells can produced (Bjornsson et al., 2015; Gage and Temple, 2013). Even subtle derangements of NSC homeostasis can result in developmental neuropsychiatric disorders (Gage and Temple, 2013; Taverna et al., 2014).

Given the importance of this developmental process, NSCs have been the subject of intensive study. NSCs exhibit a few key features during early embryonic neurogenesis: (i) NSCs have an apicobasal polarity that permits them to span the entire neocortex; (ii) NSCs suffer cell-cycle-dependent nuclear movements called interkinetic nuclear migration; and (iii) the cell cycles of these NSCs are relatively short, especially during early neurogenesis. While these key histological features of NSCs have been very well studied, their relation to intracellular NSC homeostasis remains poorly understood.

Given the ubiquity of inositol lipid signaling within mammalian cells, and the diverse biological outcomes of these pathways (such as gene transcription, mRNA translation, membrane receptor signaling, membrane trafficking, cell migration, and the establishment and maintenance of cell polarity), phosphoinositide (PIP) signaling may be an important avenue for understanding this key developmental process (Balla, 2013; Grabon et al., 2015). Mammalian cells produce seven distinct PIP signals (PtdIns-3-P, PtdIns-4-P, PtdIns-5-P, PtdIns-3,5-P_2, PtdIns-4,5-P_2, PtdIns-3,4-P_2, PtdIns-3,4,5-P_3) from phosphatidylinositol, many of which are known play a role in cell development processes. NSCs are no exception - mutations in the genes controlling inositol lipid signaling, such as *PTEN* (PtdIns-3,4,5-P_3 phosphatase), *PLCB1* (PIP-specific phospholipase C), *INPP1* (inositol polyphosphate-1-phosphatase), and *INPP5E* (inositol polyphosphate-5-phosphatase) are all linked with autism and mental retardation (Bourgeron, 2009; Christian et al., 2008; Jacoby et al., 2009; Serajee et al., 2003; Zhou and Parada, 2012).

In addition to the PIP signaling proteins, phosphatidylinositol (PtdIns)-transfer proteins (PITPs) are highly-conserved proteins across eukaryotes, and have been revealed to be key regulators of phosphoinositide metabolism by controlling the diverse outcomes of phosphoinositide signaling. PITPs are thus named because of their characteristic ability to enable

the ATP-hydrolysis-independent transfer of PtdIns and other lipids, such as phosphatidylcholine (PtdCho), between membranes *in vitro* (Cockcroft and Carvou, 2007; Wirtz, 2006). PITPs are also known to play other important roles. PITPs fall into two distinct families based on their structural features: Sec14-like PITPs, and PITPs of the StART-related lipid transfer (StART) protein superfamily. Sec14-like PITPs make up a superfamily that includes the mammalian retinaldehyde binding proteins, Rho-GEF, Ras-GAPs, tyrosine phosphatase and other phosphoinositide-binding proteins (Bankaitis et al., 2010; Phillips et al., 2006b; Saito et al., 2007). The interface between these effectors and phosphoinositide signaling are regulated by Sec14-like PITPs to induce diverse biological outcomes of phosphoinositide signaling in response to PtdIns-4-phosphate production (Bankaitis et al., 2010; Ile et al., 2006; Schaaf et al., 2008). In contrast, the physiological functions of the StART-like PITPs are less well known. The StART-like PITP family is subdivided into type 1 and 2 StART-like PITPs. Within mammals, the type 1 StART-like PITPs are known as PITPNA and PITPNB. Both type1 PITPs have an approximate molecular weight of 35 kDa, share 77% primary sequence identity, stimulate PtdIns-4-phosphate production in cells (Ile et al., 2010), and exhibit PtdIns and PtdCho binding and transfer activities in vitro (De Vries et al., 1996; de Vries and Beart, 1995; Yoder et al., 2001).

In the aforementioned research, the relative ease of studying isolated adult neurons and adult specimens with developmental brain disorders has meant that this important family of proteins has been studied in a non-developmental context. As such, the role of PITPs in embryonic development had remained unclear. Very recently, by using *Cre*-mediated deletion of *Pitpna* and *Pitpnb*, we published that PITPNA and PITPNB act in a redundant fashion to stimulate PtdIns-4-phosphate production in embryonic mouse neocortex NSCs, maintaining the

apical distribution of the Golgi body and radial alignment of the NSCs within the neocortex of mouse embryos (Xie et al., 2018). Unfortunately, *Emx1*^{Cre}-mediated simultaneous deletion of *Pitpna* and *Pitpnb* led to disruption of the neocortical structure and rapid onset of cell death, preventing detailed analysis of the role of these PITPs in NSC self-renewal (Xie et al., 2018). In electroporation experiments where Cre plasmid-mediated deletion of *Pitpna* and *Pitpnb* only occurred in a subset of neocortical cells, neocortical structure was preserved and cell death did not increase during neurogenesis (Xie et al., 2018). However, Cre plasmid-mediated depletion of endogenous PITPNA and PITPNB proteins would be relatively slow because of the time required for Cre expression and Cre-mediated excision of targeted DNA sequence. In light of these caveats, we designed an alternative strategy to analyze NSC self-renewal defects under conditions where PITPNA/PITPNB-deficiencies were more rapidly induced. In this work, we introduced a *Pitpnb* shRNA plasmid (mixed with an EGFP plasmid to mark transfected cells) into the neocortex of mouse embryos derived from heterozygous crosses of *Pitpna* whole body knockout mice (*Pitpna*$^{+/-}$ *X Pitpna*$^{+/-}$) (Alb et al., 2003). In transfected *Pitpna*$^{-/-}$ embryos, the endogenous PITPNA protein would be already absent at the time of the experiment, and *Pitpnb* shRNA would directly target *Pitpnb* mRNA to induce relatively rapid reduction of endogenous protein. Our findings indicate that the simultaneous removal of NSC PITPs resulted in irregular NSC differentiation, suggesting a significant developmental role for this family of proteins in the maintenance of the delicate balance between NSC differentiation and self-renewal.

2.3 Experimental Procedures

2.3.1 Plasmids

Plasmids for expressing EGFP, mCherry, PITPNA, PITPNA^{T59D}, PITPNA^{C95T}, EGFP-GM130, GOLPH3, GOLPH3^{R90L} under CAG promoter were previously described (Xie et al., 2018; Xie et al., 2016). The plasmid for expressing PITPNA^{T59D}, PITPNA^{C95T} was generated by introducing the T59D, C95T mutation via site-directed mutagenesis into the pCAX-PITPNA plasmid. To generate plasmid for expressing mouse *Golph3, Pitpnb* (isoform 2) and *Pitpnc1* (isoform 1), the coding sequences of these gene were amplified from neocortical tissues of E14.5 mouse embryos by reverse transcription (RT)-PCR using iScript Select cDNA Synthesis Kit (BIO-RAD) and Phusion high-fidelity DNA polymerase (New England Biolabs), and inserted into the pCAX vector. The shRNA construct for silencing mouse *Pitpnb, golph3* were generated by inserting annealed oligonucleotides, which contained hairpin sequences targeting specific regions in mouse *Pitpnb*, into the BamHI/Hind III sites of pSilencer 2.0-U6. The targeting sequence was 5'-CGGATATTTACGAACTTAC-3' for *Pitpnb* shRNA and 5'-GAAACGTACGGGAACGATTAG-3' for golph3 shRNA. For shRNA rescue experiments, silent mutations were introduced into pCAX-PITPNB (5'-CGGATATTTACGAACTTAC-3' was mutated to 5'-CGCATCTTCACAAATTTAC-3') pCAX-GOLPH3 (5'-GAAACGTACGGG AACGATTAG-3' was mutated to 5'-GAAATGTCCGTGAGCGTTTAG-3') via site-directed mutagenesis.

2.3.2 Antibodies

The antibodies used include: rabbit polyclonal anti-PITPNA (ProteinTech), rabbit

polyclonal anti-PITPNB (Hamilton et al., 1997), rabbit polyclonal anti-GOLPH3 (Abcam), rabbit polyclonal anti-activated Caspase 3 (Cell Signaling), chicken polyclonal anti-GFP (Aves Labs), goat polyclonal anti-GFP (Abcam), rabbit polyclonal anti-mCherry (Abcam), mouse monoclonal anti-Pax6 (Developmental Studies Hybridoma Bank), rabbit polyclonal anti-Tbr2 (Abcam), rabbit monoclonal anti-Cleaved Notch(Val1744; Cell Signaling) and rabbit polyclonal anti-HES1 (GeneTex) and rabbit anti-Ser10-phosphorylated histone H3 (Genscript). Secondary antibodies were from Jackson Immuno Research Laboratories, Inc (West Grove, PA) with minimal species cross reactivity.

2.3.3 Animals and Genotyping

Mice were inbred in the animal facility of Texas A&M University Health Science Center and handled in accordance with National Institute of Health and institutional guidelines on the care and use of animals. Tissues obtained from tails of mice were used for genomic DNA preparation and PCR genotyping. Genotyping primers and the length of PCR products for mice with systemic deletion of *Pitpna* were: AB-2 (5'-GCGAGGCATCACTCTTCCCCTC-3') for *Pitpna*$^{+/+}$ genotype(expected PCR products sizes: 550bp), PG-1(5'-GAATGTGTGCGAGGCCAGAGG-3') for the *Pitpna*$^{-/-}$ genotype(expected PCR products sizes : <500bp) and common reverse primer AB-1B (5'-CACCATCCCCCACGGTGACTG-3'). Primers and the length of the PCR products for other alleles were: Delta13-F3 (5'-AGCCTACATCAATTATATGTAATGTATATACA-3') and Delta13-R1 (5'-GCAAAAATACTTACCTCTTGAACAG-3') for systemic *Pitpnb* deletion (expected PCR product sizes: 100bp for wild-type allele and 87bp for deleted allele). aLOX1 (5'-CTTCCTCTGCCTTGTAATCCTGAG-3') and SDL1 (5'-

GAACAAGAAACTATCCAGCAGACAGACT-3') for *Pitpna* floxed allele (expected PCR product sizes: 303bp for non-floxed allele and 365bp for floxed allele; bLOX1 (5'-GAGGACTGCTGTGTCTGCTGC-3') and SDL2 (5'-GTTTAGCTATGTAAGGGTTACTGT GCA-3') for *Pitpnb* floxed allele (expected PCR product sizes: 347bp for non-floxed allele and 415bp for floxed allele); Emx1-1 (5'-AAGGTGTGGTTCCAGAATCG-3') and Emx1-2 (5'-CTCTCCACCAGAAGGCTGAG-3') for wild-type Emx1 allele (no Cre knockin; expected PCR product size: 378bp); and Cre1 (5'-GCGGTCTGGCAGTAAAAACTATC-3') and Cre2 (5'-GTGAAACAGCATTGCTGT CACTT-3') for Cre knock-in allele (expected PCR product size: 102bp).

2.3.4 In Utero Electroporation (IUE)

The IUE procedure was performed in accordance with National Institute of Health and institutional guidelines on the care and use of animals. Briefly, timed-pregnant female mice were anesthetized, and laparotomy was performed to expose the uteri. Sterile plasmid solutions were injected into the brain of embryos through the uterine wall, and electric pulses were then delivered across the head of embryos. After electroporation, the uteri were returned to the abdominal cavity of the pregnant female, the incision was sutured, and the pregnant female was allowed to recover at a warm location. The mass ratios of the plasmids used for in utero electroporation were: 1:3 for pCAX-EGFP and shRNA plasmid (control or *Pitpnb* shRNA), 1:3:3 for pCAX-EGFP, shRNA plasmid (Control or *Pitpnb* shRNA or *golph3* shRNA), and PITP rescue plasmid (pCAX-PITPNA, pCAX-PITPNB, pCAX-PITPNA^{T59D}, or pCAX-PITPNA^{C95T}, pCAX-GOLPH3, pCAX-GOLPH3^{R90L}), and 1:1:2:2 for experiments using pCAX-mCherry, pCAX-EGFP-GM130, *Pitpnb* shRNA, and pCAX-PITPNA.

2.3.5 Tissue Preparation, Immunostaining, and Confocal Microscopy

Forebrain hemispheres of electroporated mouse embryos were harvested as previously described (Xie et al., 2016). The lateral ventricle was exposed by removal of the hippocampal tissue, the remaining forebrain hemisphere was then fixed in 2% paraformaldehyde for 20-25min at room temperature. The fixed hemispheres were soaked with 20% sucrose (prepared in PBS) for cryoprotection and then embedded in Tissue-Tek OCT. Cryosections (30~40μm) were prepared and used for immunostaining. Antibodies were diluted in 1xPBS containing 3% bovine serum albumin and 0.2% Triton-X-100. Primary antibody incubation was performed at room temperature for overnight, and secondary antibody incubation was performed at room temperature for 2h. DAPI was used to label the nucleus. Confocal images were obtained on a Nikon TiE confocal microscope using the NIS-Elements software.

2.3.6 Attractene transfection *in vivo* and cell pair analysis

Attractene (Qiagen) is a nonliposomal lipid transfection reagent. Attractene-mediated in vivo transfection was performed similarly as the in utero electroporation procedure except that plasmid solution was mixed with Attractene reagent before being injected into the lateral ventricle of embryos and that no electric pulses were delivered after plasmid injection. The plasmid solution was prepared at the mass ratio of 1:3 (EGFP:shRNA). The plasmid solution was mixed with Attractene reagent at the ratio of 0.4μg total DNA (in 7.5μl sterile dH2O) to 1.5μl Attractene. The plasmid/Attractene mixture was kept at room temperature for 10-30min before injection (~2μl injected per embryo). A mixture of the Attractene reagent (Qiagen) and plasmids (0.4-0.5μg DNA in 7.5μl ddH2O was mixed with 1.5μl Attractene) was injected into the lateral

ventricle of E13.5 mouse embryos, and the injected embryos were harvested 20h later. Transfected forebrain hemispheres were fixed 2% paraformaldehyde (prepared in PBS) for 20min, and cryosections (30μm) were prepared and used for Pax6, Tbr2 and EGFP immunostaining. Cell identity was analyzed only for $EGFP^+$ cell pairs (which were derived from a single $EGFP^+$ cell via one round of division), but not single $EGFP^+$ cells (which had not divided during the 20h period), or a cluster of more than two $EGFP^+$ cells (which were derived from a single $EGFP^+$ cell via more than one round of division).

2.3.7 Statistical Analysis

Statistical analysis was performed using the GraphPad Prism software. Student's t-test (unpaired, two-tailed) was used to compare the results from two different groups. One-way ANOVA was used to compare results from three or more groups.

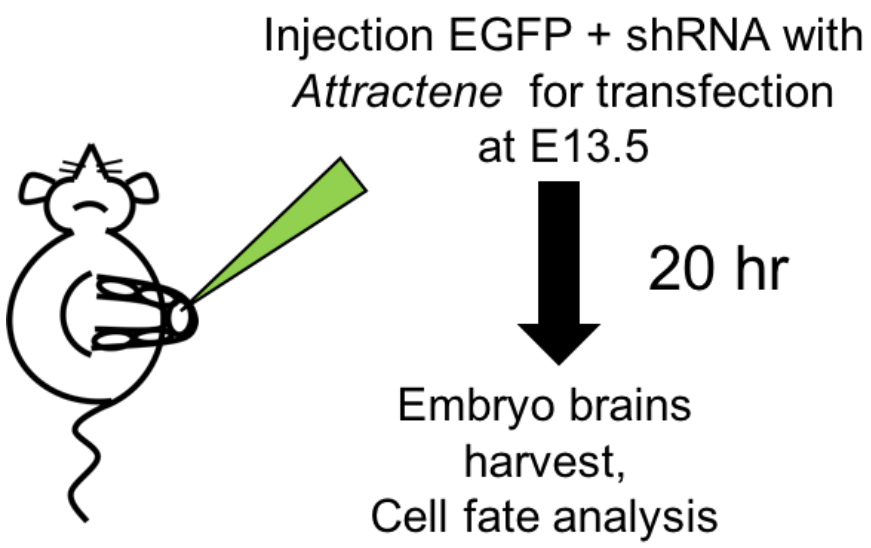

Figure 4. Attractene transfection In Vivo and cell pair analysis.

Attractene (Qiagen) is a nonliposomal lipid transfection reagent. Attractene-mediated in vivo transfection was performed similarly as the in utero electroporation procedure except that plasmid solution was mixed with Attractene reagent before being injected into the lateral ventricle of embryos and that no electric pulses were delivered after plasmid injection. A mixture of the Attractene reagent (Qiagen) and plasmids (0.4-0.5μg DNA in 7.5μl ddH2O was mixed with 1.5μl Attractene) was injected into the lateral ventricle of E13.5 mouse embryos, and the injected embryos were harvested 20h later.

2.4 Results

2.4.1 PITPNA and PITPNB support NSC self-renewing division in embryonic mouse neocortex

Our first application of this strategy was a daughter cell pair analysis to assess whether PITPNA/PITPNB-deficiencies affected the division mode of NSCs in the neocortex. In this experiment, a mixture of control or *Pitpnb* shRNA with EGFP plasmid was introduced into the neocortex of E13.5 mouse embryos via Attractene co-injection, a method for achieving low transfection efficiency throughout the ventricular zone of the neocortex (Xie et al., 2016) (Figure 4). Transfected embryos were sacrificed 20h after plasmid/Attractene injection, and the identity of EGFP+ cell pairs, presumably derived from the division of a single NSC, was determined based on the expression of the NSC marker Pax6 and the IPC marker Tbr2. Consistent with our previous observations (Xie et al., 2016), all of the cells among the cell pairs were either NSCs ($Pax6^{+}Tbr2^{-}$) or IPCs ($Pax6^{-or+}Tbr2^{+}$) (Figure 5). In the control group (*Pitpna*$^{+/+}$ with control shRNA), the majority of cell pairs were either NSC/NSC (27.14 ± 7.26%, mean ± SD, n = 4 embryos) (Figure 6, 9) or NSC/IPC (58.04 ± 6.83%, n = 4 embryos) (Figure 7, 9), and only a minority of cell pairs were IPC/IPC (14.82 ± 4.9%, n = 4 embryos) (Figure 8, 9). Single PITP deficiencies (*Pitpna*$^{-/-}$ embryos transfected with control shRNA, or *Pitpna*$^{+/+ \text{ or } +/-}$ embryos transfected with *Pitpnb* shRNA) did not alter the fraction of different types of cell pairs. However, the combination of *Pitpna* deletion and *Pitpnb* shRNA (*Pitpna*$^{-/-}$ embryos transfected with *Pitpnb* shRNA) led to marked increase in the fraction of IPC/IPC pairs (37.13 ± 4.26, n = 7 embryos, $p<0.0001$)

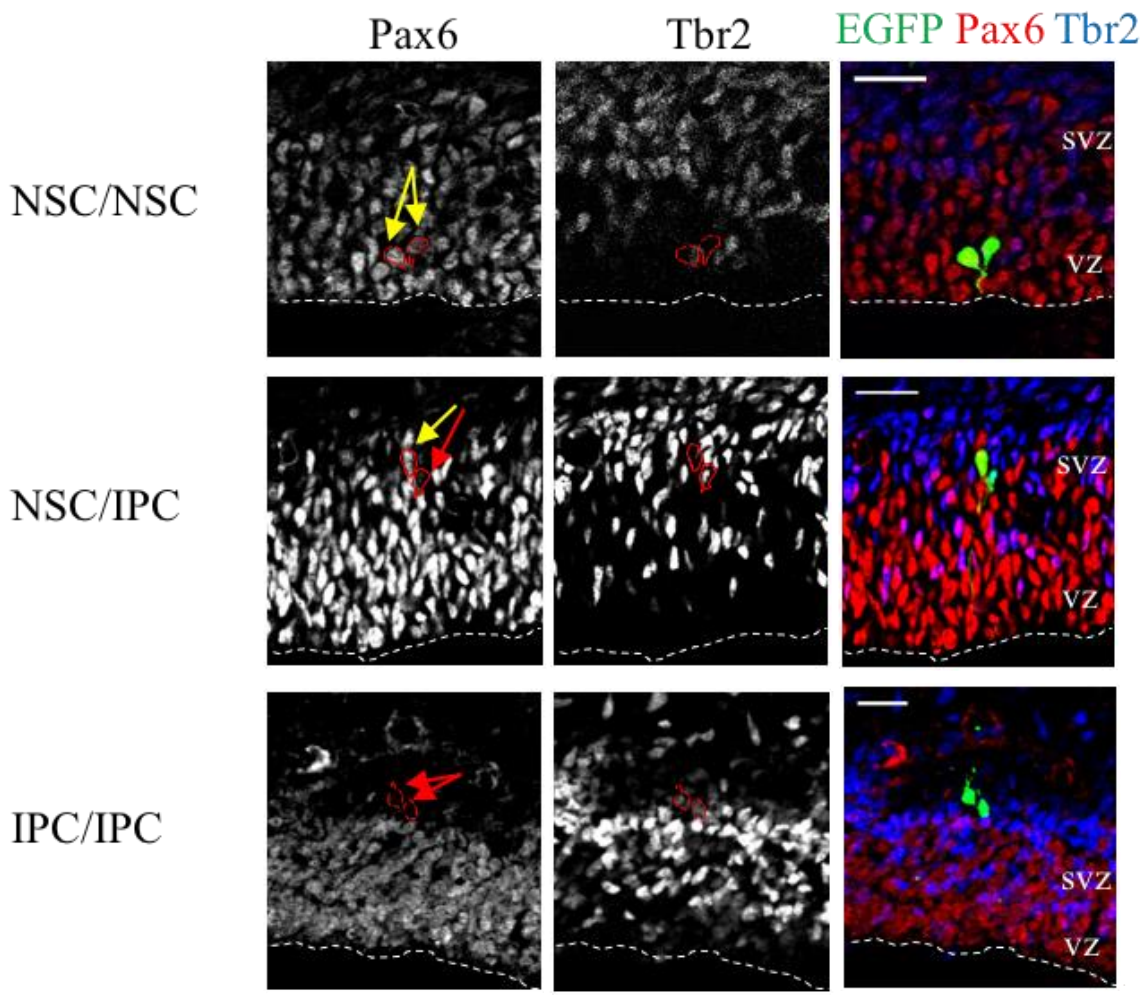

Figure 5. Representative confocal images showing modes of cell division.

Cell identity was analyzed only for EGFP^{+} cell pairs (which were derived from a single EGFP^{+} cell via one round of division) based on the expression of the NSC marker Pax6 and the IPC marker Tbr2 (NSCs is identified by Pax6^{+}Tbr2^{-} and IPCs is identified by Pax6^{-or+}Tbr2^{+}). Representative confocal images showing neighboring EGFP+ cell pairs NSC/NSC, NSC/IPC, and IPC/IPC. Yellow arrows indicate NSCs and red arrows indicate IPCs. Scale bars: 20μm.

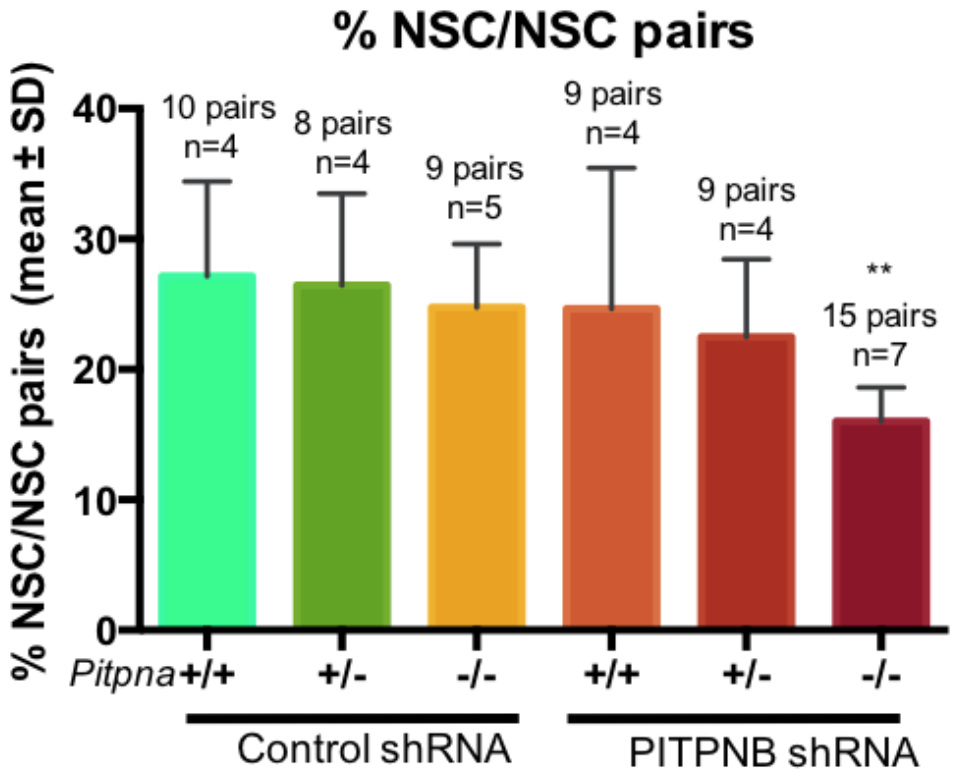

Figure 6. Quantification of symmetric self-renewing divisions.

In the control group (*Pitpna*$^{+/+}$ with control shRNA), the majority of cell pairs were NSC/NSC (27.14 ± 7.26%, mean ± SD, n = 4 embryos in 4 litters). Combination of *Pitpna* deletion and *Pitpnb* shRNA (*Pitpna*$^{-/-}$ embryos transfected with *Pitpnb* shRNA) significantly decreased the fraction of NSC/NSC pairs (16.02 ± 2.25, n = 7 embryos in 6 litters, $p<0.01$ compared to control).

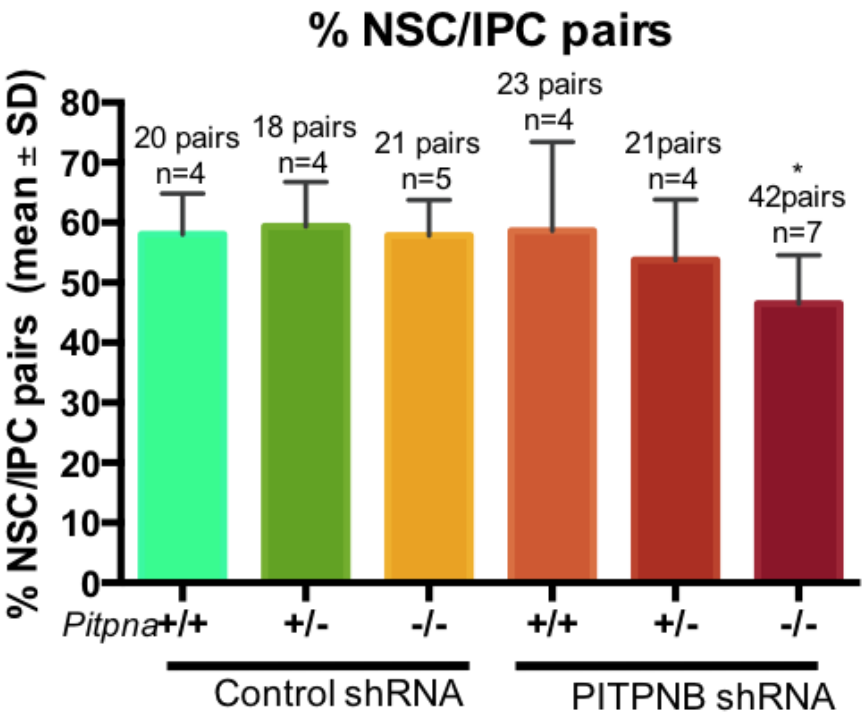

Figure 7. Quantification of asymmetric divisions

In the control group (*Pitpna*$^{+/+}$ with control shRNA), the majority of cell pairs were NSC/IPC (58.04 ± 6.83%, n = 4 embryos in 4 litters). Combination of *Pitpna* KO and *Pitpnb* shRNA (*Pitpna*$^{-/-}$ embryos transfected with *Pitpnb* shRNA) led to a trend toward decreased fraction of NSC/IPC pairs (47.54 ± 8.03, n = 7 embryos in 6 litters, $p<0.05$ compared to control, one-way ANOVA) were also observed in the *Pitpnb* shRNA mice.

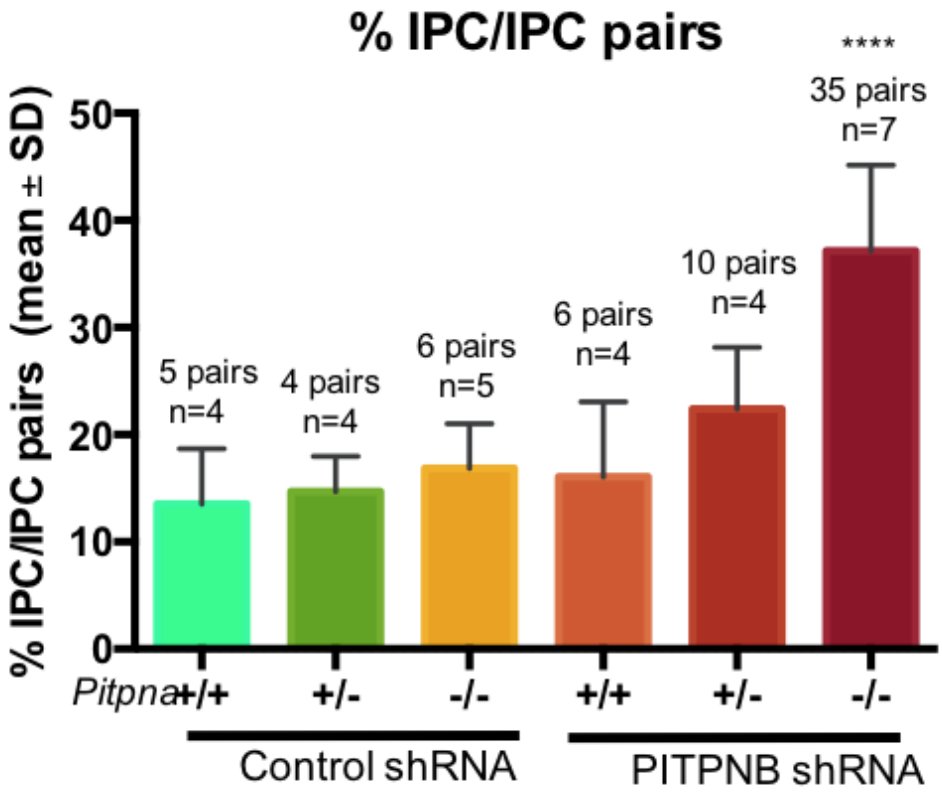

Figure 8. Quantification of symmetric differentiation divisions

In the control group (*Pitpna*$^{+/+}$ with control shRNA), a minority of (13.52 ± 5.16%, n = 4 embryos in 4 litters) cell pairs were IPC/IPC. Single PITP deficiencies (*Pitpna*$^{-/-}$ embryos transfected with control shRNA, or *Pitpna*$^{+/+ \text{ or } +/-}$ embryos transfected with *Pitpnb* shRNA) did not alter the fraction of different types of cell pairs. However, combination of *Pitpna* deletion and *Pitpnb* shRNA (*Pitpna*$^{-/-}$ embryos transfected with *Pitpnb* shRNA) led to marked increase in the fraction of IPC/IPC pairs (37.13 ± 7.99, n = 7 embryos in 6 litters, $p<0.0001$ compared to control, one-way ANOVA).

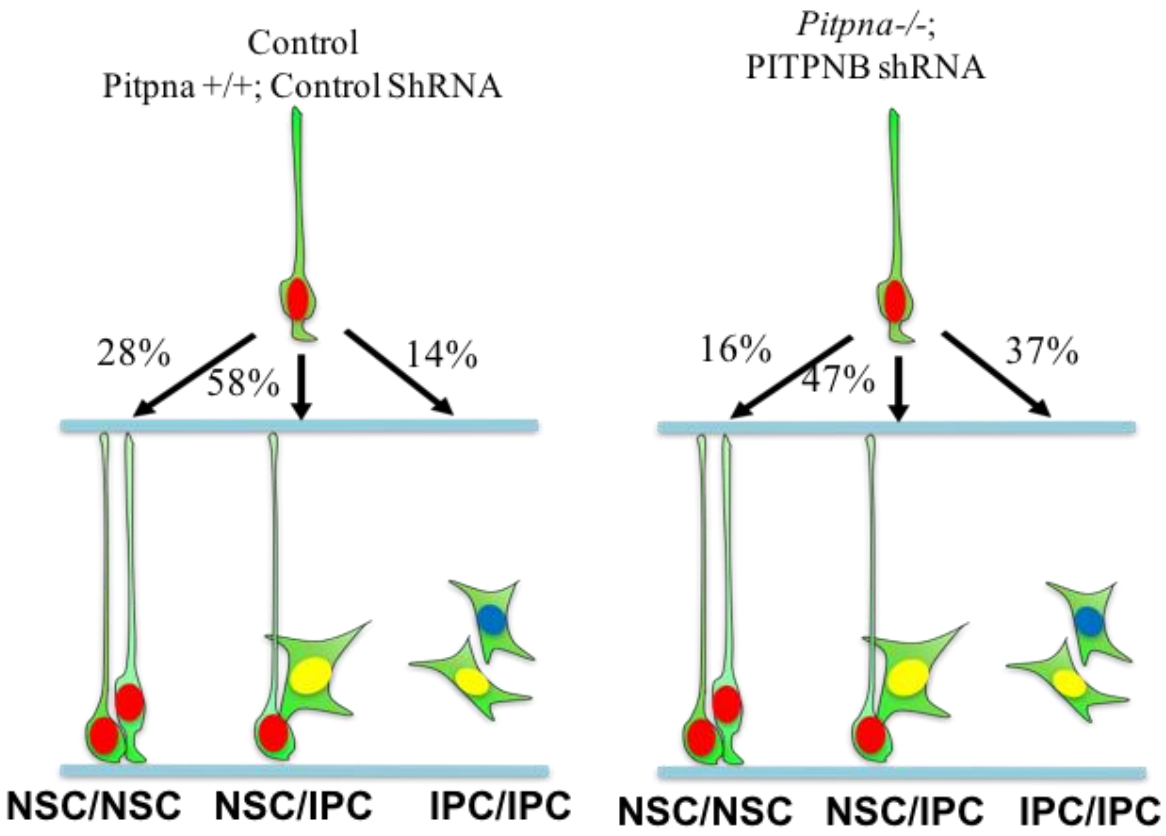

Figure 9. The cell pairs model shows the rate of each NSC cell division mode.

Combination of *Pitpna* deletion and *Pitpnb* shRNA (*Pitpna*$^{-/-}$ embryos transfected with *Pitpnb* shRNA) led to significant increase in the fraction of IPC/IPC pairs (37.13 ± 4.26, n =7 embryos in 6 litters, $p<0.0001$ compared to control, one-way ANOVA). A corresponding significant decrease in the fraction of NSC/NSC pairs (16.03 ± 2.80, n=7 embryos in 6 litters, $p<0.01$ compared to control) and a trend toward decreased fraction of NSC/IPC pairs (47.54 ± 8.03, n=7 embryos in 6 litters, $p<0.05$ compared to control, one-way ANOVA) was also observed in the *Pitpnb* shRNA mice.

compared to control which is 14%, one-way ANOVA) (Figure 8, 9). A corresponding significant decrease in the fraction of NSC/NSC pairs (16.03 ± 2.80, n=7 embryos, $p<0.01$ compared to control which is 28%, one-way ANOVA) (Figures 7 and 10) and a trend toward decreased fraction of NSC/IPC pairs (47.54 ± 9.69, n=7 embryos, $p<0.05$ compared to control which is 58%, one-way ANOVA) was also observed in the *Pitpnb* shRNA mice (Figures 8 and 10). These data suggest that in a *Pitpna* null background the *Pitpnb* shRNA accelerates differentiation divisions of NSCs. Thus, PITPNA and PITPNB may be instrumental for self-renewing divisions of NSCs that generate at least one daughter NSC (Figure 9).

2.4.2 PITPNA and PITPNB maintain the NSC pool in embryonic mouse neocortex

Results from our cell pair analysis predict that PITPNA/PITPNB-deficiencies would lead to diminished NSC pool after several rounds of NSC division. To test this prediction, we introduced an EGFP plasmid together with control or *Pitpnb* shRNA into the neocortex of E12.5 mouse embryos derived from *Pitpna* heterozygous crosses by in utero electroporation and sacrificed the electroporated embryos 3 days later to analyze the NSC pool. Analyses were not performed at later time points because significant loss of plasmids in transfected cells would occur after more rounds of cell divisions. Compared with the control group (*Pitpna*$^{+/+}$ embryos electroporated with control shRNA), a significant reduction of the NSC pool ($Pax6^{+}Tbr2^{-}$ pool) among $EGFP^{+}$ cells was observed in the PITPNA/PITPNB double deficiency group (i.e. *Pitpna*$^{-/-\ or\ +/-}$)

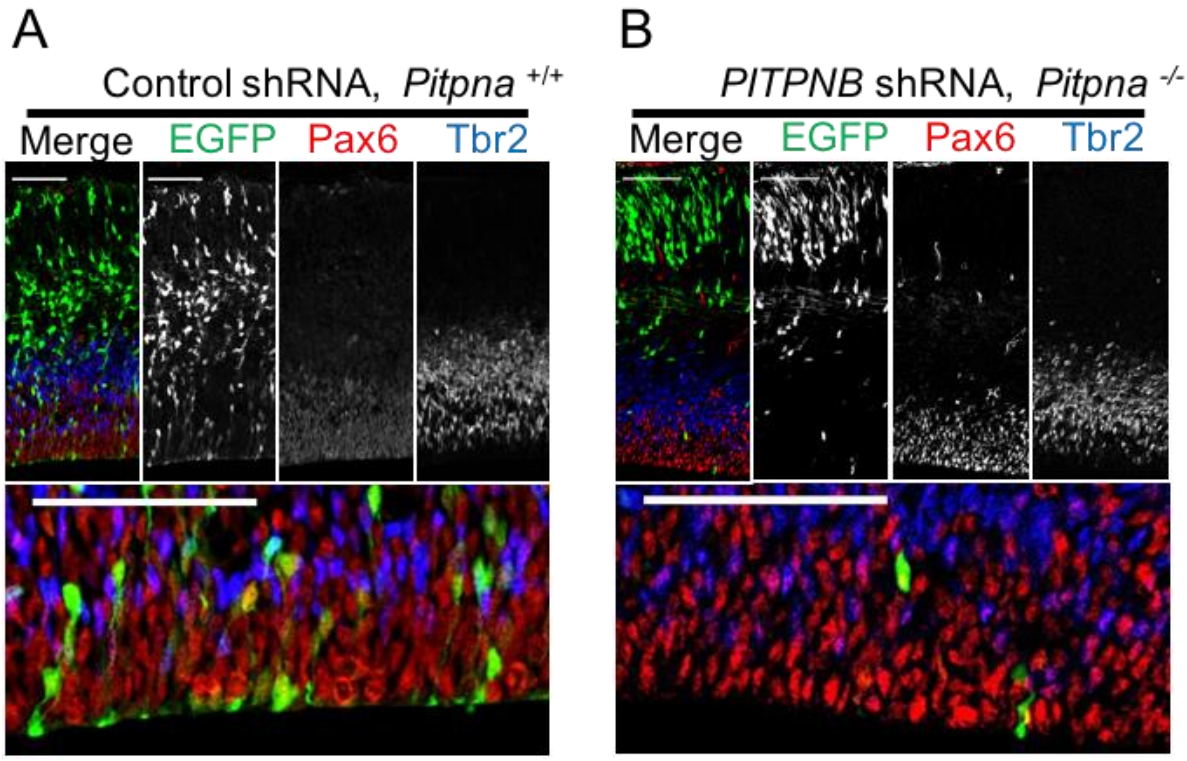

Figure 10. PITPNA/PITPNB deficiencies control the size of the NSC pool in mouse embryonic neocortex. Mouse embryos (progeny of *Pitpna*$^{+/-}$) were co-electroporated with an EGFP plasmid, and either control or a *Pitpnb* shRNA plasmid, at E12.5. The mice were sacrificed at E15.5 and *Pitpna* genotype was confirmed. (A) shows representative confocal images of mouse embryonic neocortex as a control and (B) panel shows representative confocal images of mouse embryonic neocortex with double PITP deficiencies to identify NSCs and IPCs. Areas of the ventricular zone (Pax6^{+} layer) are shown at higher magnification in bottom panels. Scale bars: 50μm.

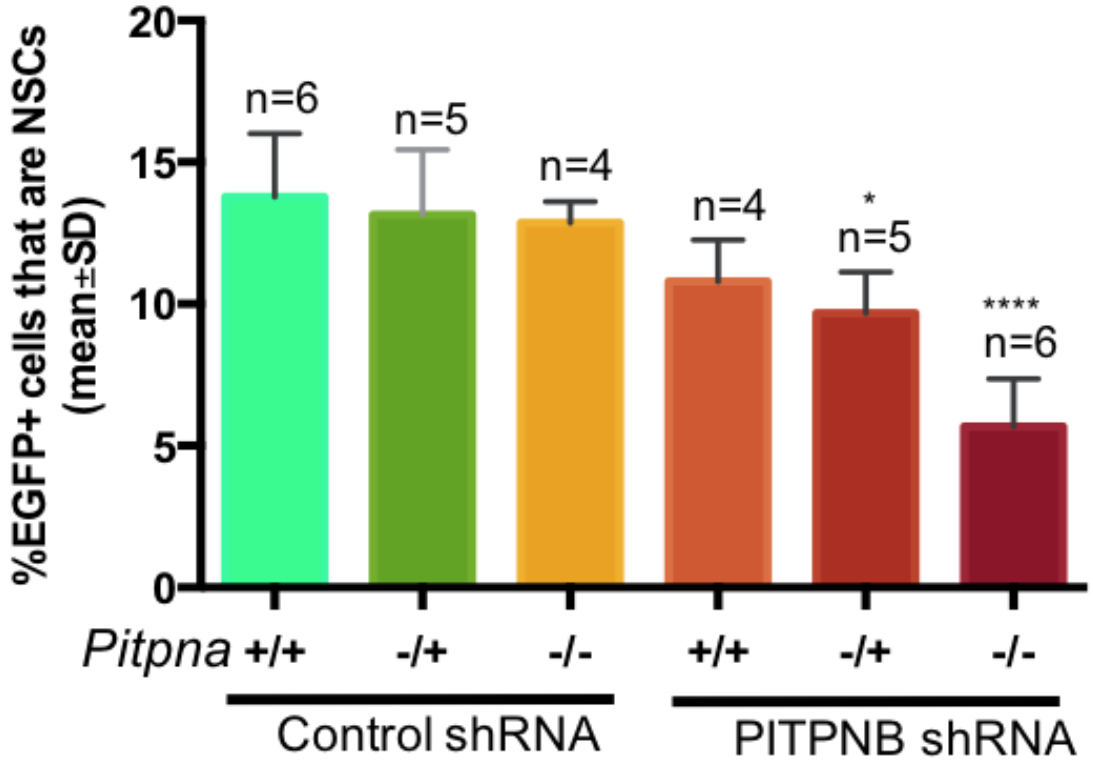

Figure 11. Transfected NSCs pool were quantified.

Compared with the control group (*Pitpna*$^{+/+}$ embryos electroporated with control shRNA), a significant reduction of the NSC pool (Pax6^{+}Tbr2^{-} pool) among EGFP^{+} cells were observed in the PITPNA/PITPNB double deficiency group (i.e. *Pitpna*$^{-/- \text{ or } -/+}$ embryos electroporated with *Pitpnb* shRNA), but not in any other groups, including *Pitpna*$^{-/-}$ embryos electroporated with control shRNA, or *Pitpna*$^{+/+}$ embryos electroporated with *Pitpnb* shRNA, ****p<0.0001 compared to control, one-way ANOVA.

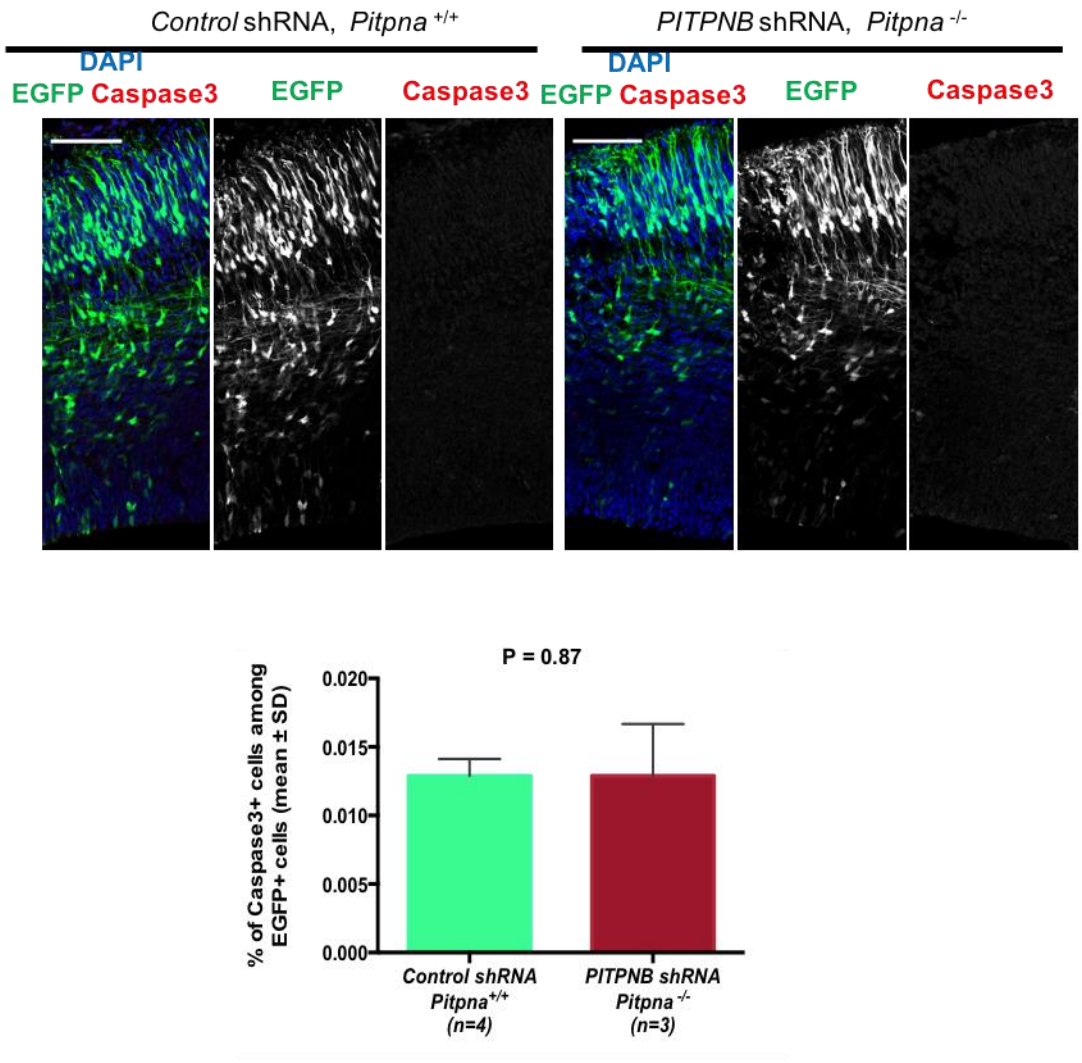

Figure 12. PITPNA/PITPNB deficiencies do not induce apoptosis in embryonic neocortex.

Left panel shows representative confocal images of mouse embryonic neocortex as a control and right panel shows double PITP deficiencies to determine whether they induce apoptosis in NSCs of mouse embryonic neocortex. Below panel shows quantification based on $EGFP^+$ $Caspase3^+$ $P > 0.05$ compared to control, one-way ANOVA. Scale bars: 50μm.

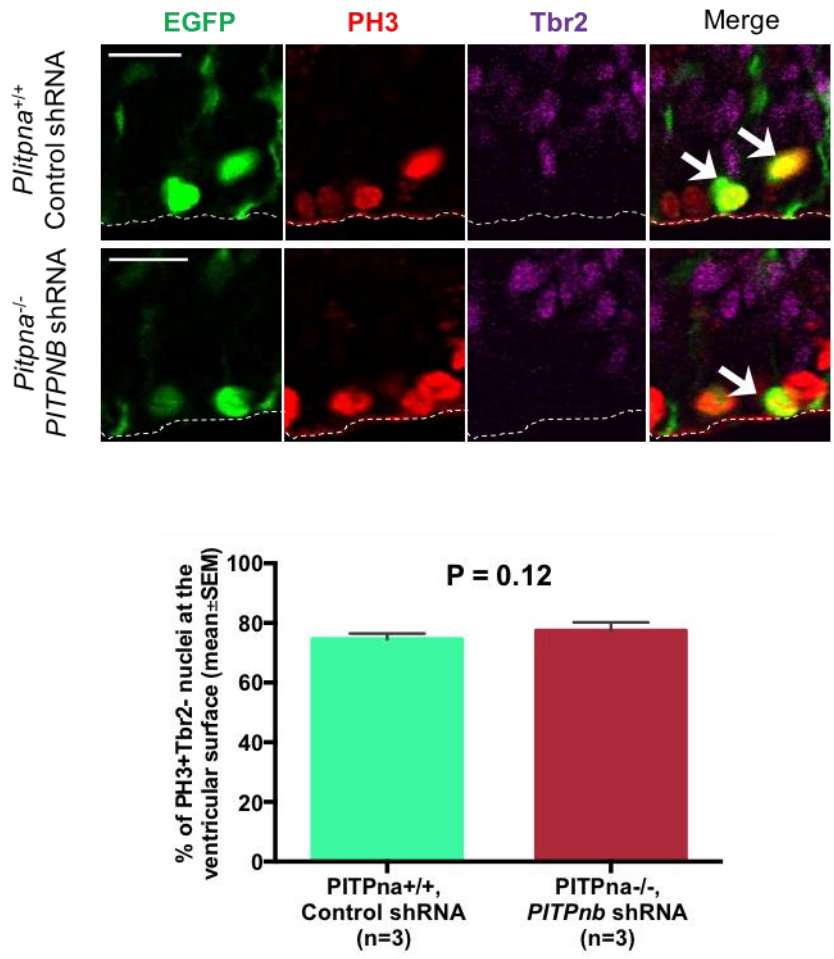

Figure 13. PITPNA/PITPNB deficiencies do not affect mitosis in NSCs.

Double PITP deficiencies do not affect the ability of NSCs to place their nucleus at the ventricular surface during mitosis. Mitotic nuclei were identified via immunostaining of Ser10-phosphorylated histone H3 (PH3). Immunostaining of Tbr2 was performed to exclude IPCs from the analysis. Scale bars: 10 μm. Quantification based on $EGFP^{+}Tbr2^{-}$ shows that most $EGFP^{+}Tbr2^{-}$ mitotic nuclei (indicated by arrows) are located at the ventricular surface in both the control and double PITP deficiency group. Student's t-test. Scale bars: 10μm.

embryos electroporated with *Pitpnb* shRNA) (Figure 10), but not in any other groups, including *Pitpna*$^{-/-}$ embryos electroporated with control shRNA, or *Pitpna*$^{+/+}$ embryos electroporated with *Pitpnb* shRNA (Figure 11). The PITPNA/PITPNB double deficiency group neither exhibited increased fraction of EGFP^{+} cells with condensed or fragmented nuclei, nor showed increased fraction of EGFP^{+} cells expressing activated Caspase 3, an apoptosis marker (Figure 12). Based on these data, we conclude that the diminished NSC pool in the PITPNA/PITPNB double deficiency group results from impaired self-renewal of NSCs, but not from increased cell death of NSCs. NSCs in *Pitpna*$^{-/-}$ embryos expressing *Pitpnb* shRNA did not exhibit abnormalities in mitotic index (i.e., percentage of cells at the M-phase), location of mitotic nuclei at the ventricular surface (Figure 13).

2.4.3 Lipid binding/transfer activities of PITPs are required for maintaining the NSC pool

PtdIns- and PtdCho-binding/transfer are signature biochemical activities of PITPNA and PITPNB. To determine whether these activities are required for supporting the NSC pool, we performed functional rescue experiments in which a rescue plasmid for expressing wild-type or mutant PITPNA/PITPNB deficient in PtdIns- or PtdCho-binding/transfer was introduced into PITPNA/PITPNB double deficiency embryos. In these experiments, the rescue plasmid was co-electroporated with an EGFP plasmid and the *Pitpnb* shRNA into the neocortex of E12.5 mouse embryos derived from *Pitpna* heterozygous crosses, and electroporated embryos were sacrificed 3 days later for analysis of NSCs. Quantification of Pax6 and Tbr2 immunoreactivity revealed that the NSC pool in *Pitpna*$^{-/-}$ embryos expressing *Pitpnb* shRNA was restored by expression of either wild type PITPNA or PITPNB (Figure 14,17), but not by expression of PITPNA deficient

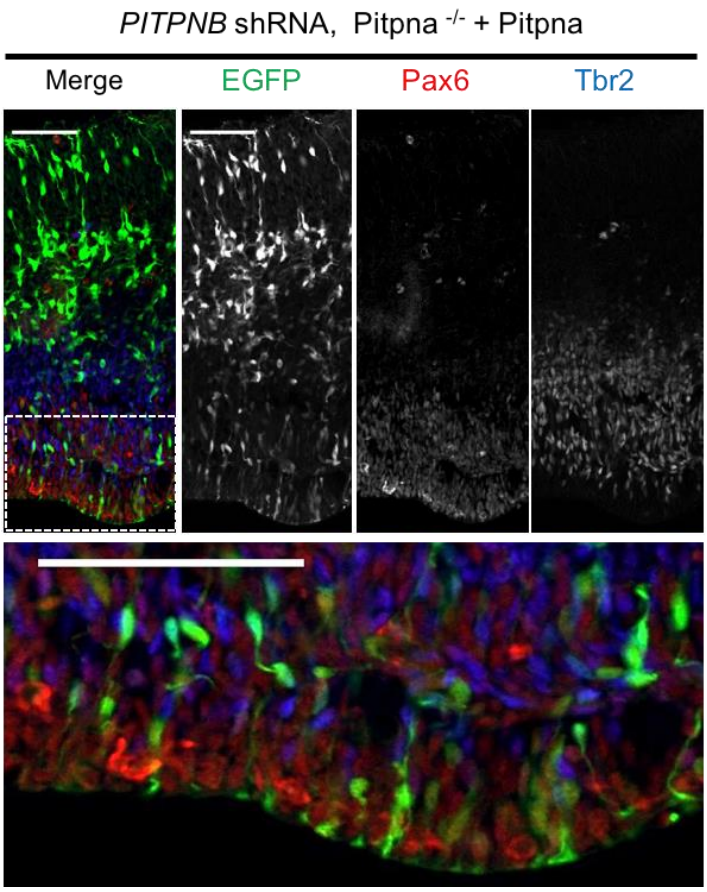

Figure 14. PITPNA rescue PITPNA/PITPNB-deficiency-induced NSC reduction in mouse embryonic neocortex.

Mouse embryos (progeny of *Pitpna*$^{+/-}$) were co-electroporated at E12.5 and sacrificed at E15.5. For the rescue experiments, a plasmid used to express PITPNA, was co-electroporated with *Pitpnb* shRNA and EGFP plasmid and selected pups with genotype *Pitpna*$^{-/-}$. Representative confocal images. Area of the ventricular zone (Pax6^{+} layer) is shown at higher magnification in the bottom panels to identify NSCs. PITPNA rescued PITPNA/PITPNB-deficiency-induced NSC reduction. Scale bars: 50μm.

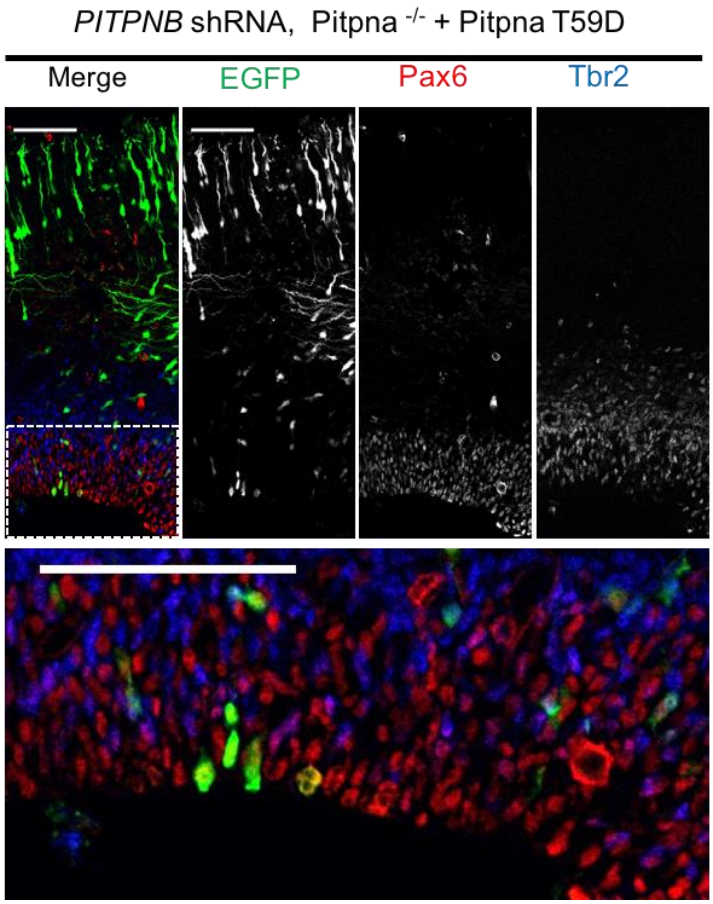

Figure 15. PtdIns binding inhibition mutant PITPNA did not rescue PITPNA/PITPNB-deficiency-induced NSC reduction in mouse embryonic neocortex.

Mouse embryos (progeny of *Pitpna*$^{+/-}$) were co-electroporated at E12.5 and sacrificed at E15.5. For the rescue experiments, a plasmid used to express PITPNA^{T59D}, was co-electroporated with *Pitpnb* shRNA and EGFP plasmid and selected pups with genotype *Pitpna*$^{-/-}$. Representative confocal images. Area of the ventricular zone (Pax6^{+} layer) is shown at higher magnification in the bottom panels to identify NSCs. PITPNA mutants (T59D [PtdIns binding site mutant]) did not rescue double-PITP-deficiency-induced NSC reduction. Scale bars: 50μm.

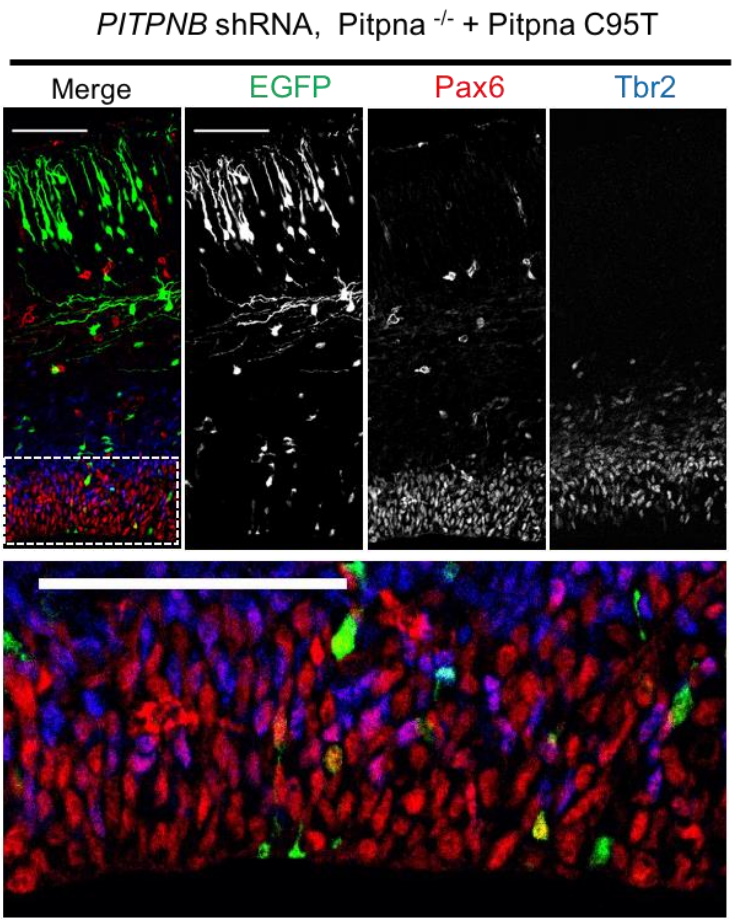

Figure 16. PtdCho binding inhibition mutant PITPNA did not rescue PITPNA/PITPNB-deficiency-induced NSC reduction in mouse embryonic neocortex.

Mouse embryos (progeny of *Pitpna*$^{+/-}$) were co-electroporated at E12.5 and sacrificed at E15.5. For the rescue experiments, a plasmid used to express PITPNA^{C95T}, was co-electroporated with *Pitpnb* shRNA and EGFP plasmid and selected pups with genotype *Pitpna*$^{-/-}$. Representative confocal images. Area of the ventricular zone (Pax6^{+} layer) is shown at higher magnification in the bottom panels to identify NSCs. PITPNA mutants (C95T [PtdCho binding site mutant]) did not rescue double-PITP-deficiency-induced NSC reduction. Scale bars: 50μm.

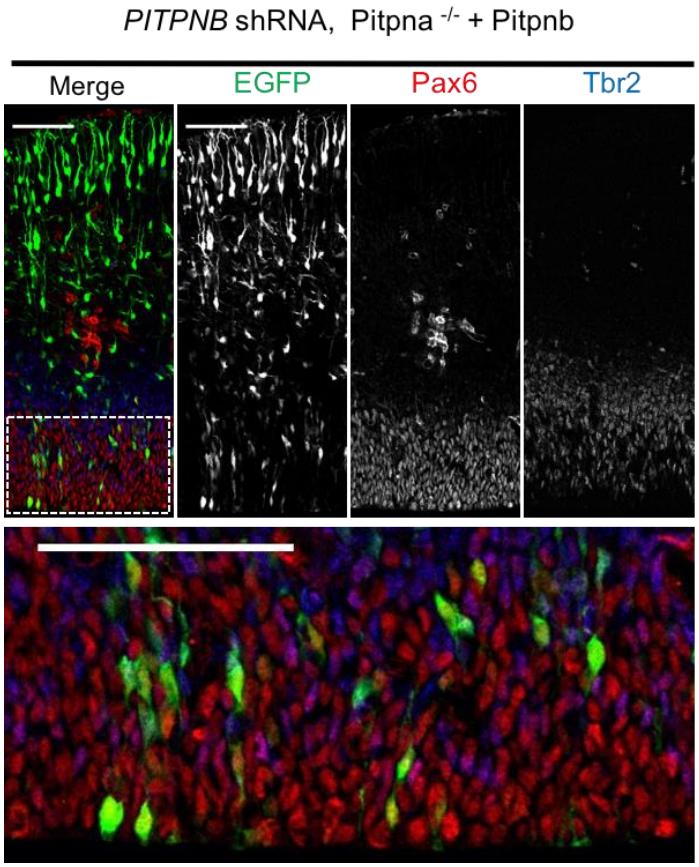

Figure 17. PITPNB rescue PITPNA/PITPNB-deficiency-induced NSC reduction in mouse embryonic neocortex.

Mouse embryos (progeny of *Pitpna*$^{+/-}$) were co-electroporated at E12.5 and sacrificed at E15.5. For the rescue experiments, a plasmid used to express shRNA-resistant wild-type PITPNB, was co-electroporated with *Pitpnb* shRNA and EGFP plasmid and selected pups with genotype *Pitpna*$^{-/-}$. Representative confocal images. Area of the ventricular zone (Pax6^{+} layer) is shown at higher magnification in the bottom panels to identify NSCs. PITPNB rescued PITPNA/PITPNB-deficiency-induced NSC reduction. Scale bars: 50μm.

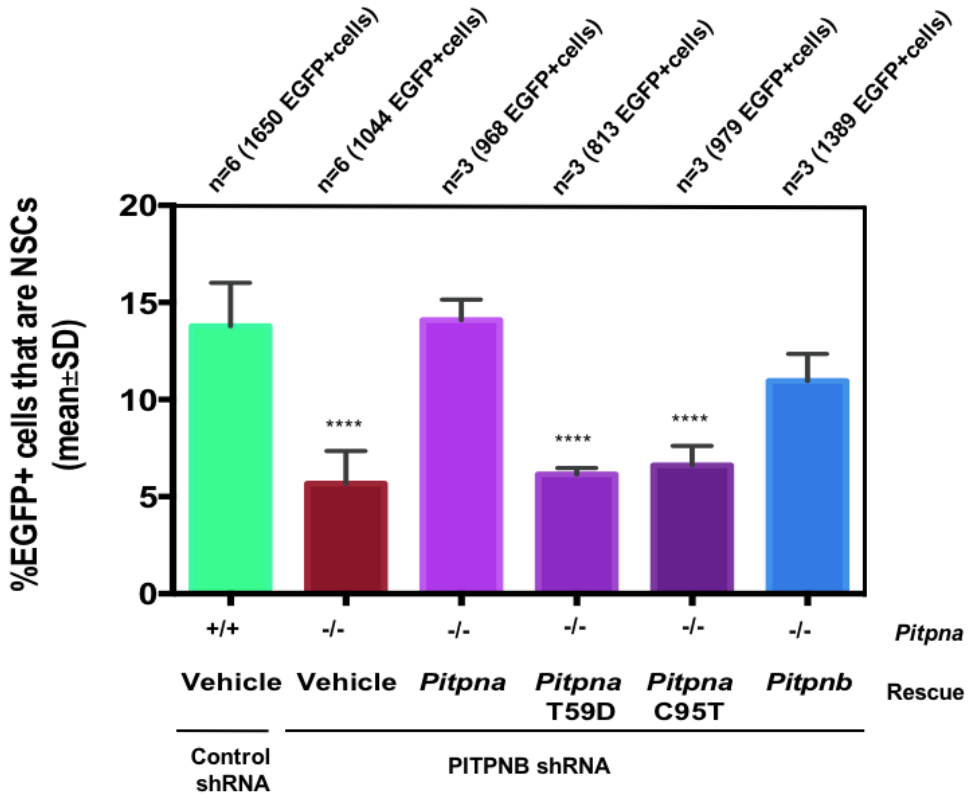

Figure 18. Class I StART-like PITPs rescue the depletion of NSC pool but the PtdIns/PtdCho exchange inhibition mutant PITPNA did not rescue PITPNA/PITPNB-deficiency-induced NSC reduction in mouse embryonic neocortex.

Mouse embryos (progeny of *Pitpna*$^{+/-}$) were co-electroporated at E12.5 and sacrificed at E15.5. For the rescue experiments, a plasmid used to express PITPNA, PITPNA $^{T59D, C95T}$ and shRNA-resistant wild-type PITPNB was co-electroporated with *Pitpnb* shRNA and EGFP plasmid and selected pups with genotype *Pitpna*$^{-/-}$. Quantification of EGFP+ NSCs **** $p<0.0001$, ***$p<0.001$ compared to control, one-way ANOVA.

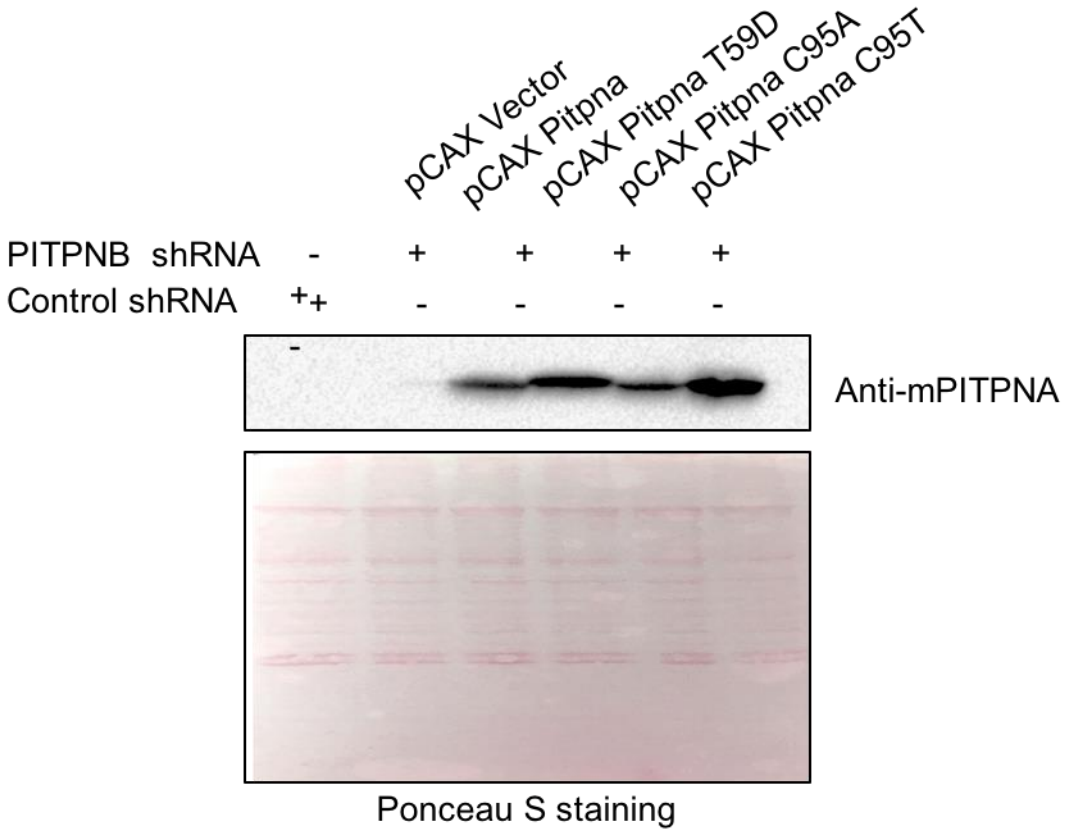

Figure 19. Plasmids expressing PITPNA, PITPNAT59D and PITPNAC95A were stable proteins in Western blot analysis.

PITP rescue plasmids (pCax-Pitpna and pCax-Pitpna^{T59A}, pCax-Pitpna^{C95A}) were confirmed that their proteins expressed very well in Western blot analysis of HEK293T cell line.

in PtdIns-binding/transfer (T59D) (Figure 15) or PtdCho-binding/transfer (C95T) (Figure 16). Since both the T59D and the C95A mutant were stable proteins (Figure 19), these data suggest that both PtdIns- and PtdCho-binding/transfer activity of PITPs are important for regulating the NSC pool in mouse embryonic neocortex (Figure 18).

2.4.4 Lipid binding/transfer activities are not sufficient for maintaining the NSC pool

A long-held model of PITP function, the lipid gradient model, is that these proteins support cell signaling by transferring the signaling substrate PtdIns from its site of synthesis (the endoplasmic reticulum) to the site of signaling (e.g., cis-Golgi membrane), thereby sustaining the PtdIns pool used for biosynthesis of phosphoinositides directly involved in signaling (Figure 20). The second model, known as the presentation model, suggests that PITPs, as a result of their interaction with membrane-bound PtdIns, make PtdIns more accessible to modification by PtdIns 4-OH kinase, enabling signaling that would otherwise be impossible due to inaccessibility of the substrate (Figure 20). Were the lipid gradient model a sufficient explanation for the role of PITPs, other PITPs with similar PtdIns-binding/transfer activities would be able to substitute PITPNA/PITPNB in the regulation of NSC self-renewal. To test this possibility, we performed *in utero* electroporation rescue experiments with a plasmid for expressing Sec14p, the major yeast PITP with similar lipid-binding/transfer activities to that of PITPNA/PITPNB (Figure 21) and a plasmid for expressing mouse PITPNC1, a homolog of PITPNA/PITPNB that also shows PtdIns-transfer activity but different second lipid, PtdOH, (Figure 22) to test PtdIns/PtdCho exchanging ability of presentation model. Neither Sec14p nor PITPNC1 restored the NSC pool in *Pitpna*$^{-/-}$

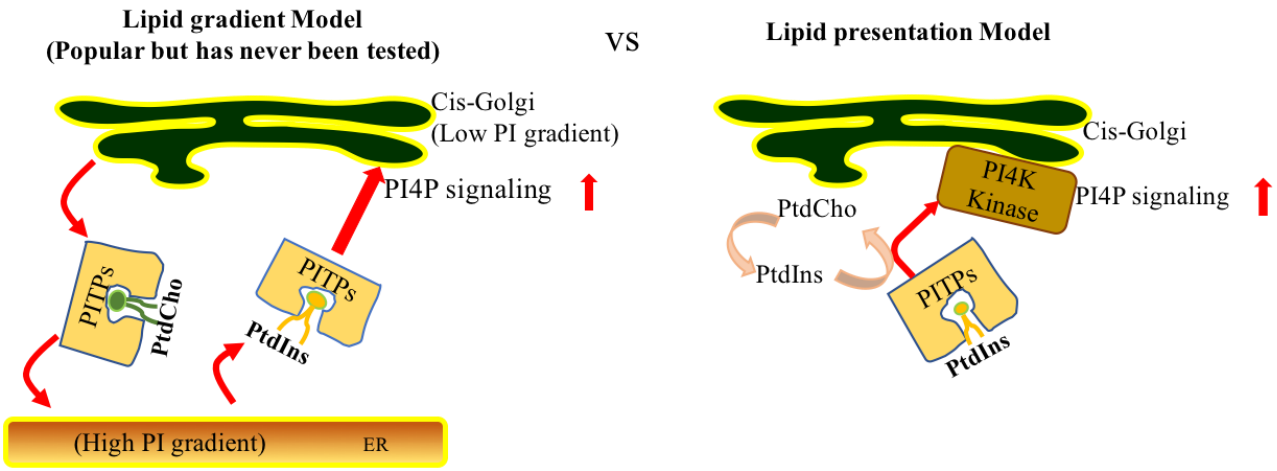

Figure 20. Two different models of how PITPs stimulate PI4P signaling in mammalian cells.

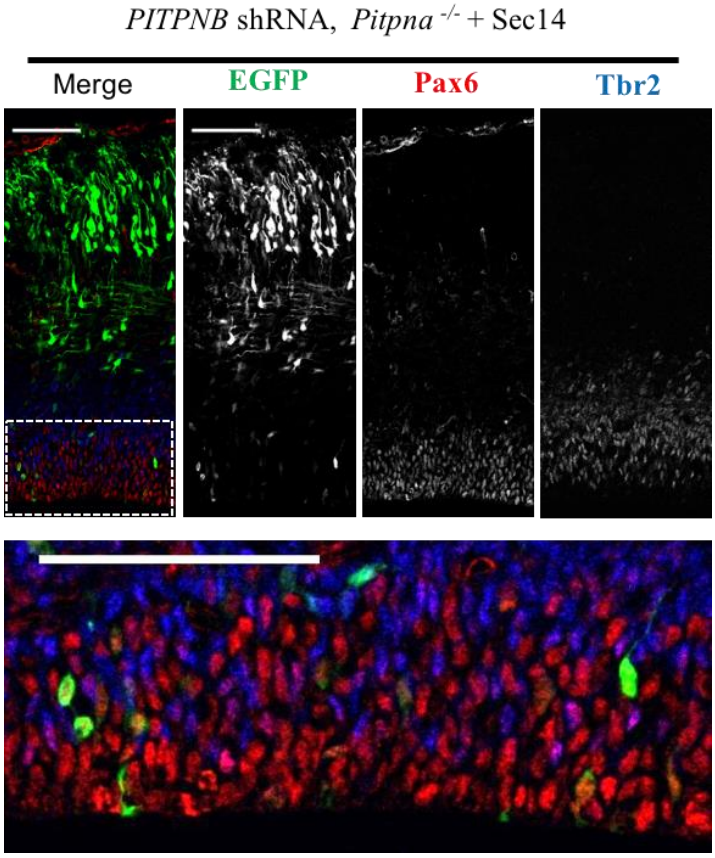

Figure 21. SEC14-like PITPs did not rescue double-PITP-deficiency-induced NSC reduction.

Mouse embryos (progeny of *Pitpna*$^{+/-}$) were co-electroporated with an EGFP plasmid and *Pitpnb* shRNA plasmid at E12.5 and sacrificed at E15.5. For the SEC14 rescue experiments, an intron-less plasmid expressing SEC14 was co-electroporated with PITPNB shRNA and EGFP plasmid and selected pups with genotype *Pitpna*. Representative confocal images of mouse embryonic neocortex. Area of the ventricular zone (Pax6^{+} layer) is shown at higher magnification in bottom panels. SEC14 failed to rescue double-PITP-deficiency-induced NSC reduction. Scale bars: 50μm.

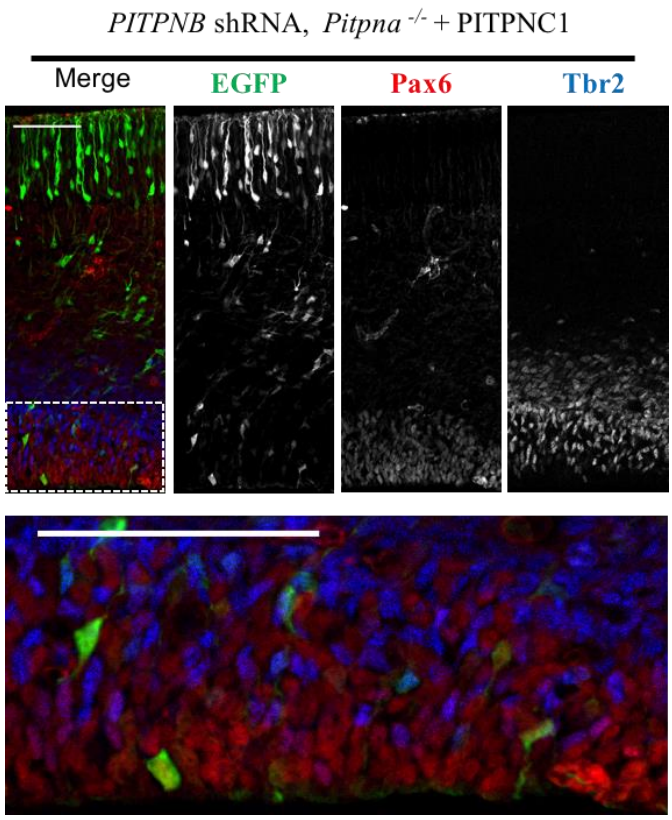

Figure 22. Class II StART-like PITPs did not rescue double-PITP-deficiency-induced NSC reduction.

Mouse embryos (progeny of *Pitpna*$^{+/-}$) were co-electroporated with an EGFP plasmid and *Pitpnb* shRNA plasmid at E12.5 and sacrificed at E15.5. For Class II StART-like PITPs (PtdIns and other second lipid transfer proteins) rescue experiments, PtdIns/PtdOH transfer protein, PITPNC1, was co-electroporated with PITPNB shRNA and EGFP plasmid and selected pups with genotype *Pitpna*$^{-/-}$. Representative confocal images of mouse embryonic neocortex. Area of the ventricular zone (Pax6^{+} layer) is shown at higher magnification in bottom panels. PITPNC1 failed to rescue double-PITP-deficiency-induced NSC reduction. Scale bars: 50μm.

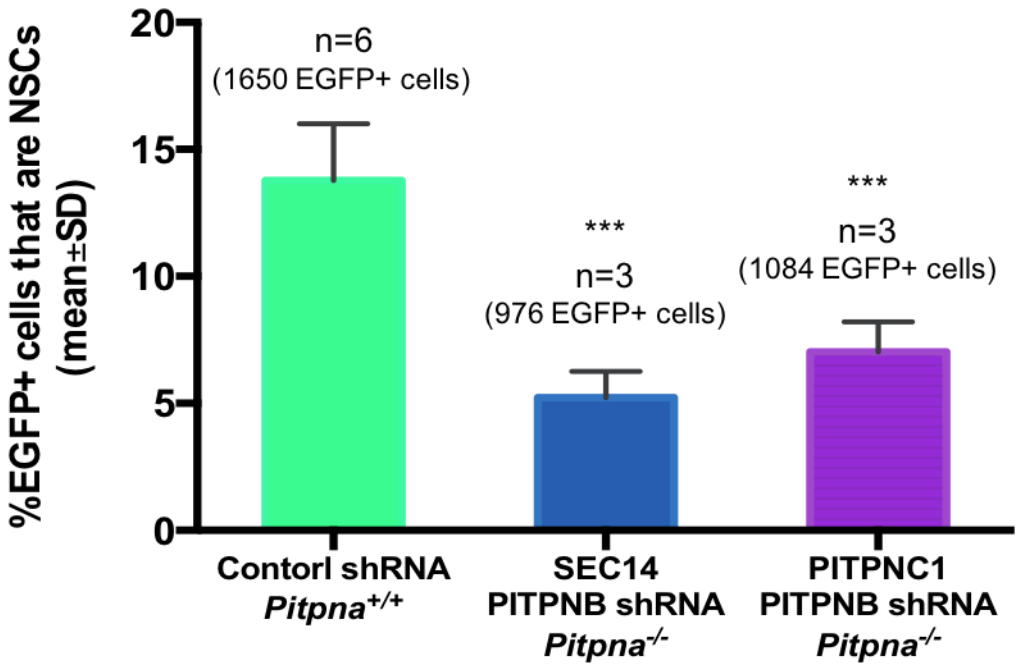

Figure 23. Neither SEC14-like PITPs nor Class II StART-like PITPs rescued double-PITP-deficiency-induced NSC reduction.

Mouse embryos (progeny of *Pitpna*$^{+/-}$) were co-electroporated with an EGFP plasmid and *Pitpnb* shRNA plasmid at E12.5 and sacrificed at E15.5. For the SEC14 rescue experiments, an intron-less plasmid expressing SEC14 or PITPNC1 was co-electroporated with PITPNB shRNA and EGFP plasmid and selected pups with genotype *Pitpna*$^{-/-}$. Quantification of EGFP+ NSCs. *** $p<0.001$, ** $P<0.01$, Student's t-test.

embryos expressing *Pitpnb* shRNA (Figure 23). These data reveal that PITPNA/PITPNB are specifically required for maintaining the NSC pool, meaning that the role of PITPNA/PITPNB in NSC self-renewing cannot be accounted for by a simple PtdIns-gradient model.

2.4.5 GOLPH3 knockdown causes diminished NSC pool via enhancing symmetric differentiating division

Our recent analysis of NSCs using Cre-mediated deletion of floxed *Pitpna* and *Pitpnb* revealed that simultaneous deletion of *Pitpna* and *Pitpnb* caused loss of apical distribution of Golgi fragments and reduced recruitment of GOLPH3, a PtdIns-4-P-binding protein, to the Golgi body (Xie et al., 2018). To test whether GOLPH3-dependent Golgi positioning is required for maintaining the NSC pool, we introduced an EGFP plasmid together with control or GOLPH3 small hairpin RNA (shRNA) into the neocortex of E12.5 mouse embryos by in utero electroporation, and sacrificed the electroporated embryos 3 days later to analyze the NSC pool. Compared with the control group (electroporated with control shRNA), a significant reduction of the NSC pool ($Pax6^{+}Tbr2^{-}$ pool) among $EGFP^{+}$ cells was observed in the GOLPH3 shRNA group (Figure 24). We tested the requirement of GOLPH3 binding to Ptdins-4-P for maintaining the NSC pool. We performed rescue of *golph3* shRNA knockdown with silencing-resistant rescue plasmids for expressing wild-type GOLPH3 and $GOLPH3^{R90L}$ (a Ptdins-4-binding-deficient mutant) (Figure 25). Quantification of Pax6 and Tbr2 immunoreactivity revealed that the NSC pool in *Pitpna*$^{-/-}$ embryos expressing *golph3* shRNA was restored by expression of either wild type GOLPH3 but not by expression of GOLPH3 deficient in PtdIns-4-P binding

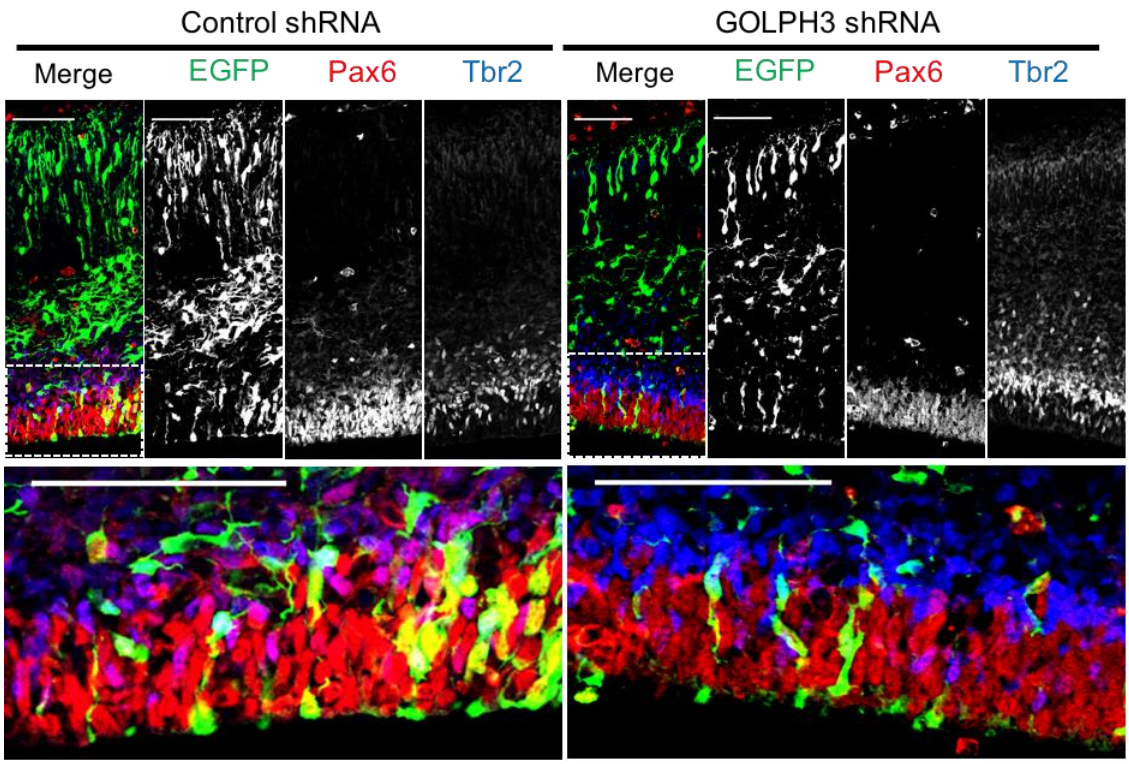

Figure 24. GOLPH3 deficiency decreased the size of the NSC pool in mouse embryonic neocortex.

Mouse embryos (C57BL6 wild-type) were co-electroporated with an EGFP plasmid, and either control or a GOLPH3 shRNA plasmid, at E12.5. The mice were sacrificed at E15.5. Left panel shows representative confocal images of mouse embryonic neocortex as a control and right panel shows representative confocal images of mouse embryonic neocortex with GOLPH3 deficiency to identify NSCs and IPCs. Areas of the ventricular zone ($Pax6^+$ layer) are shown at higher magnification in bottom panels. Scale bars: 20μm.

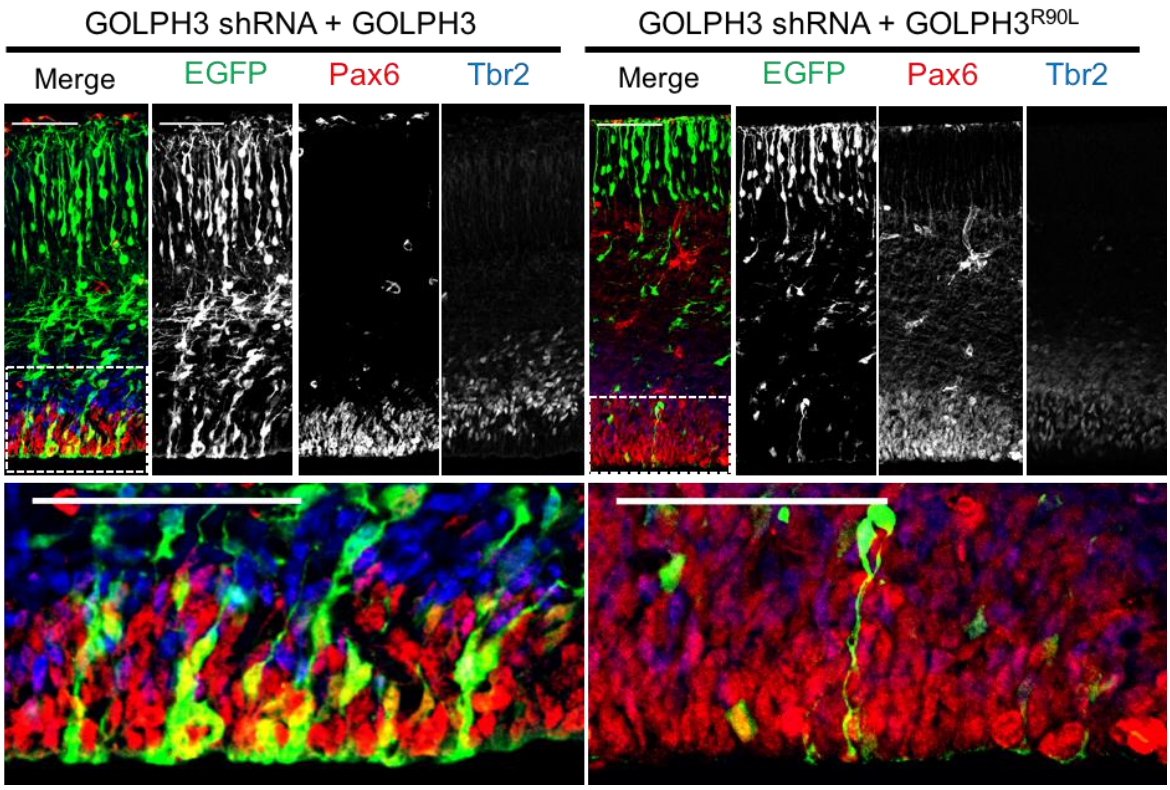

Figure 25. PtdIns-4-P dependent GOLPH3 regulates the size of the NSC pool in mouse embryonic neocortex. Mouse embryos (C57BL6 wild-type) were co-electroporated with an EGFP plasmid, and either control or a GOLPH3 shRNA plasmid, at E12.5. The mice were sacrificed at E15.5. For the GOLPH3 rescue experiments, either a plasmid expressing GOLPH3 or GOLPH3^{R90L} (PtdIns-4-P binding site mutant) was co-electroporated with GOLPH3 shRNA and EGFP plasmid. Representative confocal images of mouse embryonic neocortex. Area of the ventricular zone (Pax6^{+} layer) is shown at higher magnification in bottom panels. Left panel shows that Wild-type GOLPH3 rescued GOLPH3 deficiency-induced NSC reduction. Right panel shows that GOLPH3^{R90L} failed to rescue GOLPH3 deficiency-induced NSC reduction. Scale bars: 20μm.

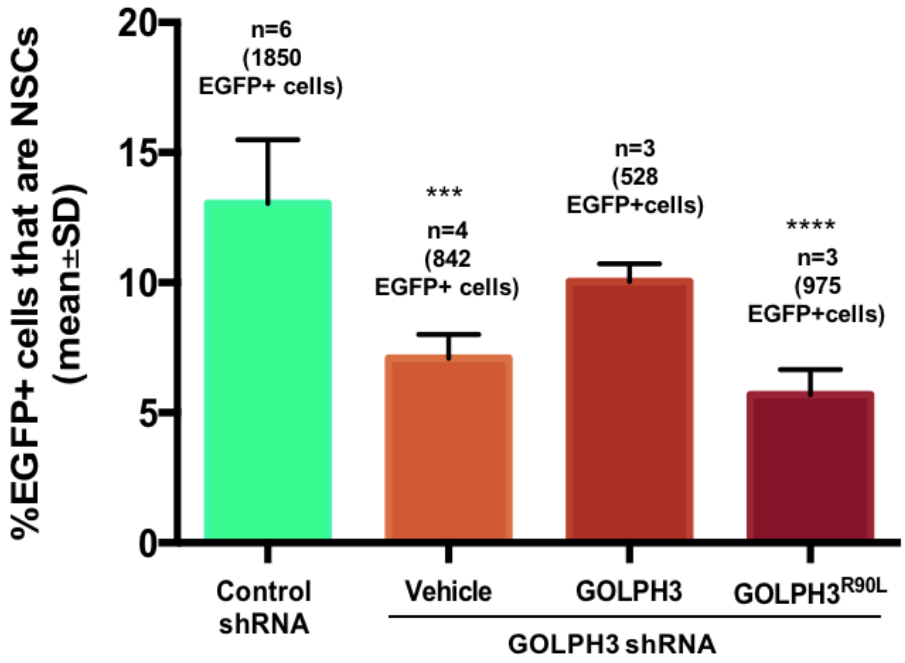

Figure 26. PtdIns-4-P dependent GOLPH3 regulates the size of the NSC pool in mouse embryonic neocortex.

Mouse embryos (C57BL6 wild-type) were co-electroporated with an EGFP plasmid, and either control or a GOLPH3 shRNA plasmid, at E12.5. The mice were sacrificed at E15.5. Quantification of EGFP+ NSCs ***$p<0.001$ compared to control, one-way ANOVA.

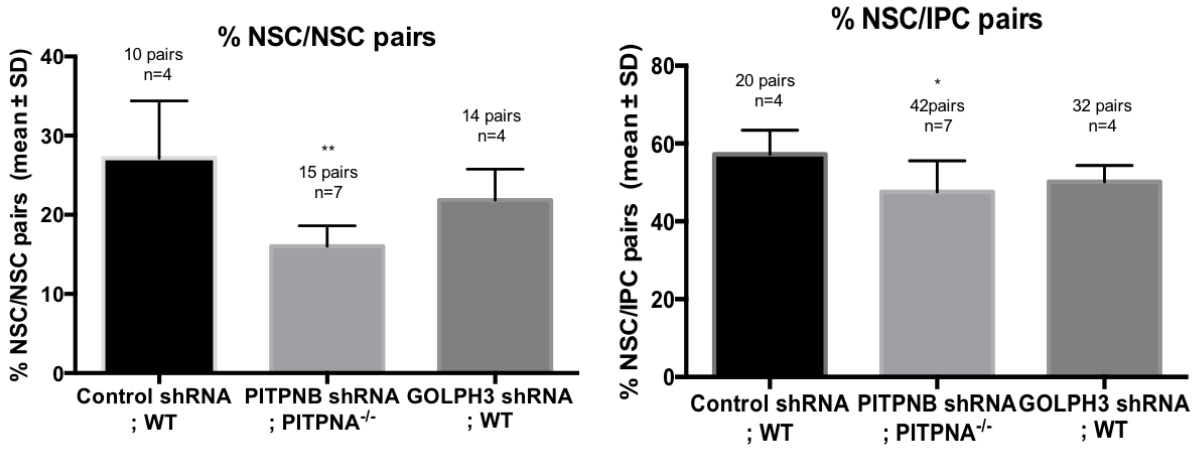

Figure 27. GOLPH3 deficiency accelerate symmetric differentiating division while GOLPH3 deficiency tend to inhibit symmetric self-renewing division and asymmetric division.

Attractene-mediated in vivo transfection was performed similarly as the in-utero electroporation procedure except that plasmid solution was mixed with Attractene reagent before being injected into the lateral ventricle of embryos and that no electric pulses were delivered after plasmid injection. In this experiment, a mixture of control or *Golph3* shRNA with EGFP plasmid was introduced into the neocortex of E13.5 mouse embryos via Attractene co-injection, and the injected embryos were harvested 20h later. Transfected forebrain hemispheres were fixed 2% paraformaldehyde (prepared in PBS) for 20min, and cryosections (30μm) were prepared and used for Pax6, Tbr2 and EGFP immunostaining. Cell identity was analyzed only for $EGFP^+$ cell pairs (which were derived from a single $EGFP^+$ cell via one round of division). Quantification of cell pairs. ****$p<0.0001$, ** $p<0.01$, * $p<0.05$ compared to control, one-way ANOVA.

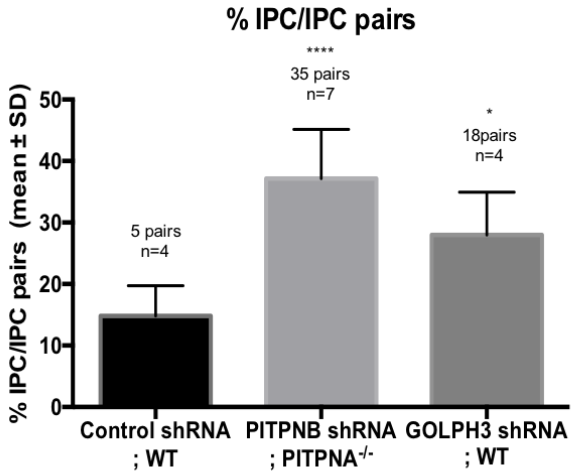

Figure 27. Continued

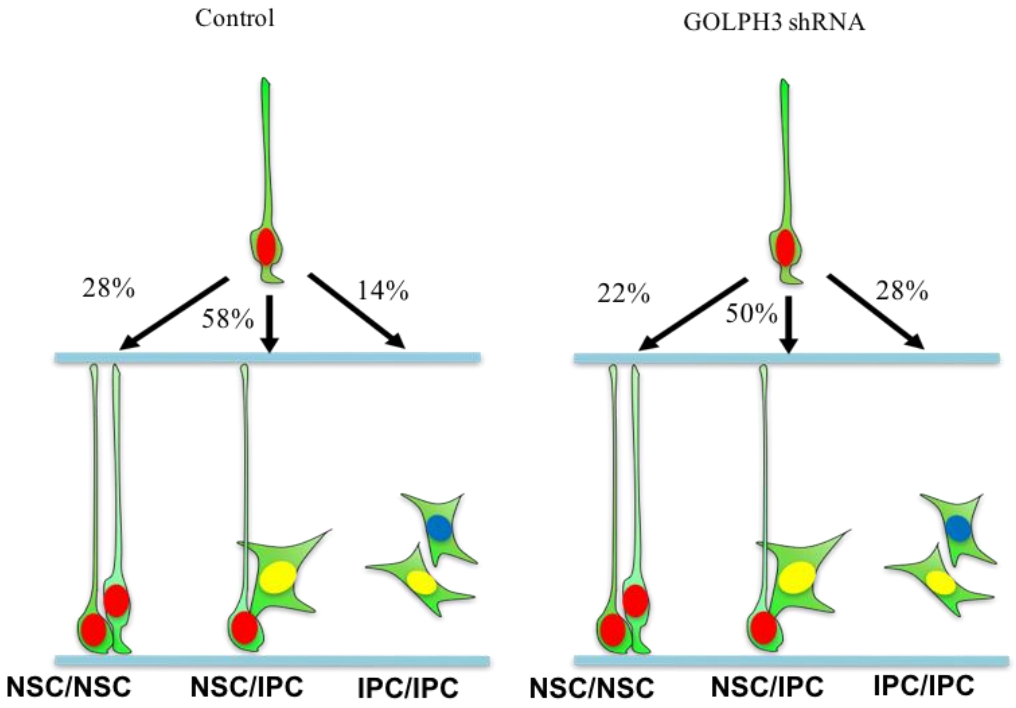

Figure 28. PtdIns-4-P dependent GOLPH3 regulates the modes of Neural Stem Cells division in mouse embryonic neocortex.

GOLPH3 deficiency (transfected with *Pitpnb* shRNA) led to marked increase in the fraction of IPC/IPC pairs (27.99 ± 3.11, n = 4 embryos, $p<0.05$ compared to control, one-way ANOVA). A corresponding decrease in the fraction of NSC/NSC pairs (21.85 ± 2.99, n=4 embryos) and a trend toward decreased fraction of NSC/IPC pairs (50.17 ± 7.06, n=4 embryos) was also observed in the GOLPH3 shRNA mice.

(R90L) (Figure 26). Moreover, we tested a daughter cell pair analysis to assess whether GOLPH3 deficiency affected the division mode of NSCs in the neocortex. In this experiment, a mixture of control or *GOLPH3* shRNA with EGFP plasmid was introduced into the neocortex of E13.5 mouse embryos via Attractene co-injection (Figure 27). GOLPH3 deficiency (transfected with *Pitpnb* shRNA) led to marked increase in the fraction of IPC/IPC pairs (27.99 ± 3.11, n = 4 embryos, $p<0.05$ compared to control, one-way ANOVA) (Figure 27 C). A corresponding decrease in the fraction of NSC/NSC pairs (21.85 ± 2.99, n=4 embryos) (Figure 27 A) and a trend toward decreased fraction of NSC/IPC pairs (50.17 ± 7.06, n=4 embryos) (Figure 27 B) was also observed in the GOLPH3 shRNA mice (Figure 28). We thus conclude that GOLPH3 binding to Ptdins-4-P is crucial for supporting the NSC pool via regulating NSC self-renewing in mouse embryonic neocortex.

2.4.6 NSCs in *Pitpna*$^{-/-}$ embryos expressing *Pitpnb* shRNA show altered distribution of Golgi body and diminished Golgi localization of GOLPH3

To investigate the mechanisms by which PITPNA/PITPNB regulate NSC self-renewal, we first assessed whether NSCs in *Pitpna*$^{-/-}$ embryos expressing *Pitpnb* shRNA recapitulated those defects. To this end, we co-electroporated a plasmid for expressing mCherry (to label the entire transfected cell), a plasmid for expressing EGFP-GM130 (to label the Golgi body), and either control or *Pitpnb* shRNA into E12.5 mouse embryos derived from *Pitpna*$^{+/-}$ heterozygous crosses, and sacrificed the electroporated embryos 3 days later. The Golgi body (indicated by

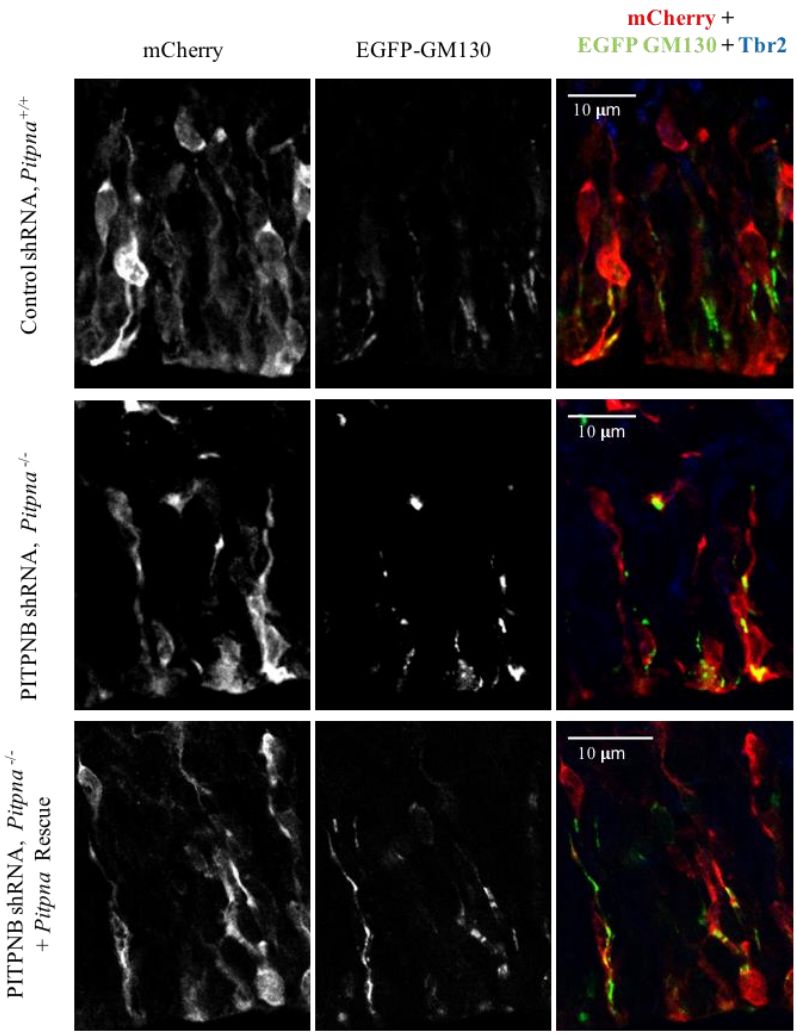

Figure 29. PITPNA/PITPNB regulate Golgi position.

Mouse embryos (progeny of *Pitpna*$^{+/-}$) were electroporated with plasmids expressing mCherry, EGFP-GM130 and PITPNB shRNA at E12.5, and were sacrificed 72h after electroporation. In rescue experiments, a plasmid expressing wild-type PITPNA was added to the plasmid mixture. Confocal z-series images were used for analysis of Golgi morphology and localization. Representative images are shown. Tbr2 immunofluorescence (Cy5 and Dylight 405, both pseudocolored to blue) were used to determine NSC identity (Tbr2^{-}). NSCs from three or more embryos in each experimental group were pooled together for analysis. Note that not all cells co-expressed mCherry and EGFP-GM130 because of the detection limit of our methods.

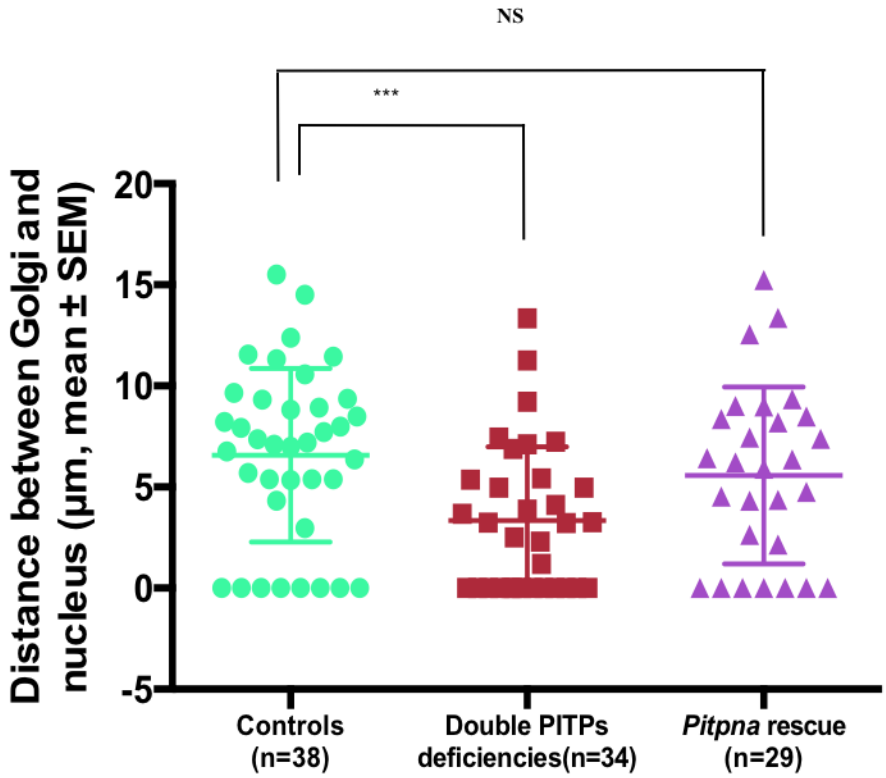

Figure 30. PITPNA/PITPNB deficiencies change Golgi position near nuclei.

the distance between the center of the EGFP-GM130 puncta/segments and the proximal edge of the nucleus was measured. If multiple EGFP-GM130 puncta/segments were present in a single NSC, the average distance for these puncta/segments was used to represent the data point for that NSC. *** P<0.001 compared to control, one-way ANOVA.

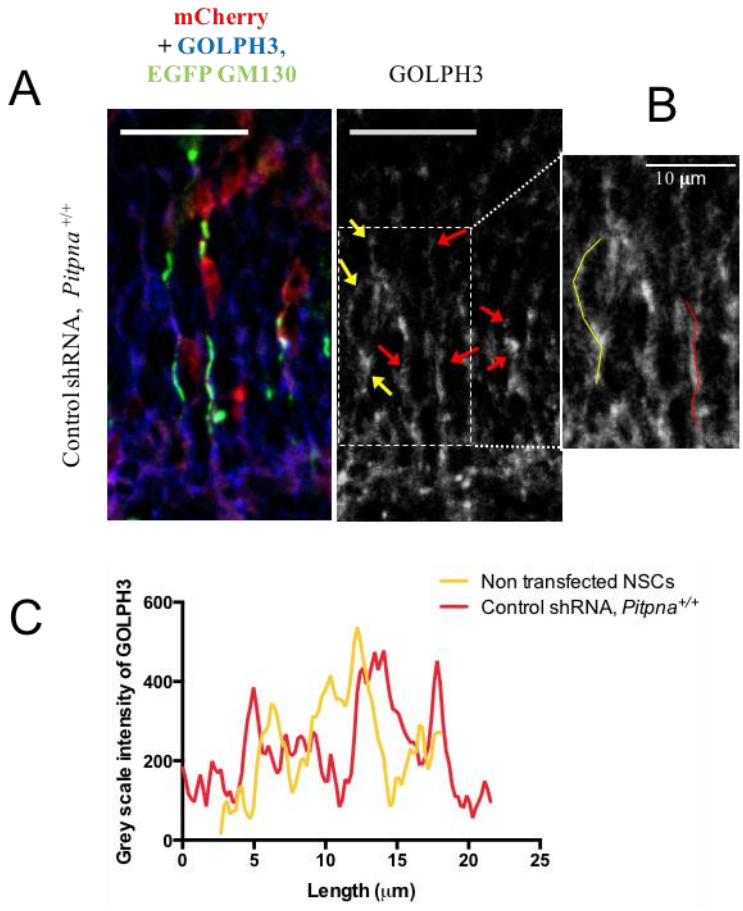

Figure 31. Golgi localization of GOLPH3 in wild-type NSCs were transfected with control shRNA did not alter that of GOLPH3 in non-transfected wild-type NSCs.

Mouse embryos (genotype: Pitpna$^{+/+}$ [control shRNA for control]) were electroporated with plasmids expressing mCherry and EGFP-GM130 at E12.5, and were sacrificed 90h after electroporation. Yellow arrows indicate Golgi localization of GOLPH3 in non-transfected NSCs and red arrows indicate that in transfected NSCs in (A). Higher magnification images are shown and, yellow line indicates Golgi localization of GOLPH3 in non-transfected NSCs and red line indicates that in transfected NSCs in (B). (C) quantification of the intensity of GOLPH3 on each line shown in (B). Scale bars: 20 μm.

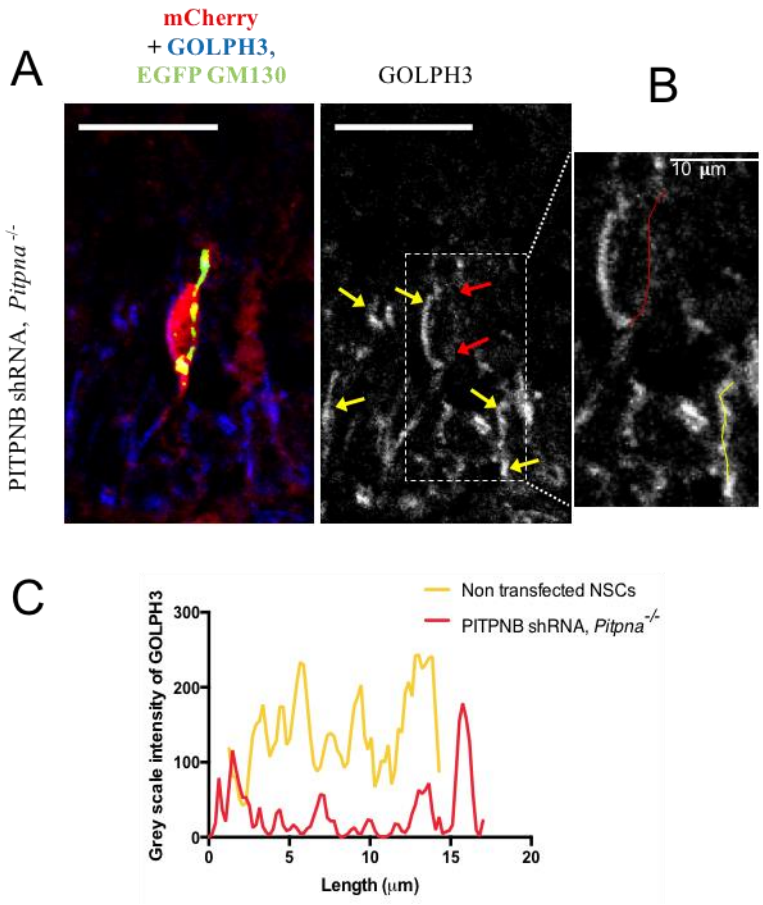

Figure 32. Golgi localization of GOLPH3 in *Pitpna*$^{-/-}$ NSCs were transfected with *Pitpnb* shRNA decreased that of GOLPH3 in non-transfected NSCs.

Mouse embryos (genotype: Pitpna$^{-/-}$ [*Pitpnb* shRNA]) were electroporated with plasmids expressing mCherry and EGFP-GM130 at E12.5, and were sacrificed 90h after electroporation. Yellow arrows indicate Golgi localization of GOLPH3 in non-transfected NSCs and red arrows indicate that in transfected NSCs in (A). Higher magnification images are shown and, yellow line indicates Golgi localization of GOLPH3 in non-transfected NSCs and red line indicates that in transfected NSCs in (B). (C) quantification of the intensity of GOLPH3 on each line shown in (B). Scale bars: 20 μm.

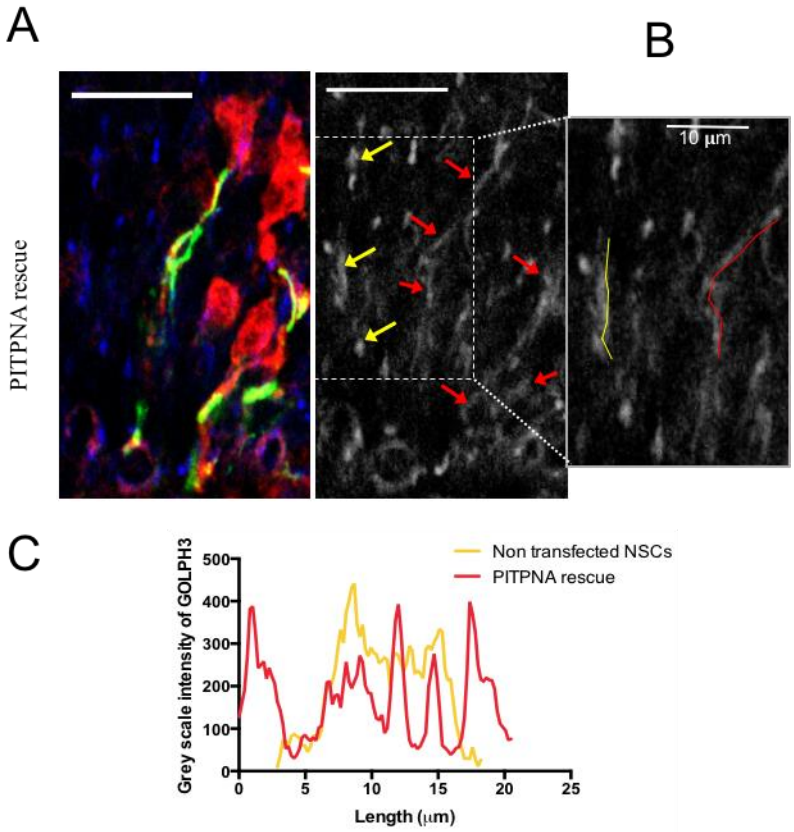

Figure 33. Golgi localization of GOLPH3 in PITPNA rescue NSCs did not alter that of GOLPH3 in non-transfected NSCs.

In rescue experiments, Mouse embryos (genotype: Pitpna$^{-/-}$ [*Pitpnb* shRNA and wild-type PITPNA for rescue]) were electroporated with plasmids expressing mCherry and EGFP-GM130 at E12.5, and were sacrificed 90h after electroporation. Yellow arrows indicate Golgi localization of GOLPH3 in non-transfected NSCs and red arrows indicate that in transfected NSCs in (A). Higher magnification images are shown and, yellow line indicates Golgi localization of GOLPH3 in non-transfected NSCs and red line indicates that in transfected NSCs in (B). (C) quantification of the intensity of GOLPH3 on each line shown in (B). Scale bars: 20 μm.

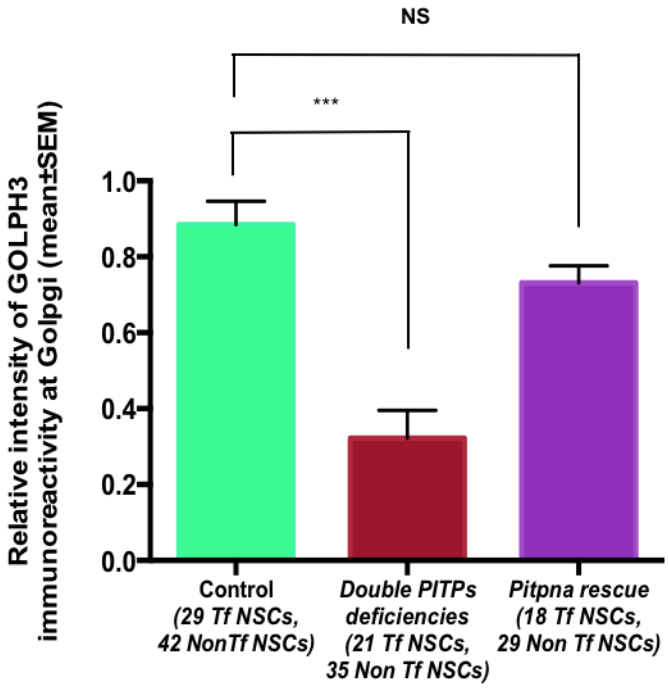

Figure 34. The ratio of the intensity of GOLPH3 labeling at the Golgi in transfected NSCs to that in bystander non-transfected NSCs is quantified as the relative intensity of GOLPH3 immunoreactivity in Golgi complex.

The relative intensity was significantly reduced in double-PITP-deficiency NSCs compared to control. Red and yellow arrows indicate GOLPH3 staining at the Golgi complex in transfected and non-transfected bystander NSCs. *** P<0.001 compared to control, one-way ANOVA.

EGFP-GM130) was typically in the form of short bullet-like segments distributed throughout the apical process in control NSCs (i.e. NSCs in *Pitpna*$^{+/+}$ embryos transfected with control shRNA), but as perinuclear puncta in PITPNA/PITPNB-deficient NSCs (i.e. NSCs in *Pitpna*$^{-/-}$ embryos expressing *Pitpnb* shRNA) (Figure 29). As a result, the nucleus-Golgi distance was significantly reduced in PITPNA/PITPNB-deficient NSCs (Figure 30). Immunostaining using a GOLPH3 antibody revealed that localization of GOLPH3 at the Golgi body (labled GM130) was diminished in PITPNA/PITPNB-deficient NSCs (Figures 32 and 34) while localization of GOLPH3 at the Golgi body was not significantly changed in both control and *Pitpna* rescued NSCs. (Figures 31, 33 and 34) Thus, NSCs in *Pitpna*$^{-/-}$ embryos expressing *Pitpnb* shRNA recapitulated both the Golgi positioning defect and the GOLPH3 localization defect.

2.4.7 Notch signaling pathways may be the key aberration underlying the NSC self-renewal defects induced by PITPNA/PITPNB-deficiency

Notch signaling players, such as Notch1 (a Notch receptor), Hes1 and Hes5 (Notch induced transcription factors), are highly expressed in the neocortex of the embryonic brain, and specifically in NSCs (Mizutani et al., 2007). Mutations in these genes lead to the depletion of NSCs and to aberrant neuronal differentiation in the embryonic mouse brain (de la Pompa et al., 1997; Handler et al., 2000; Hatakeyama et al., 2004; Mizutani et al., 2007). The connection between Notch signaling and embryonic NSC self-renewing has been well studied (Aguirre et al., 2010; Doe, 2008). Notch receptors are transported from Golgi to the plasma membrane after maturation of Notch receptors which is essential for the production of a functional receptor (Hicks et al., 2000; Okajima et al., 2008; Zhou et al., 2007).

To investigate the mechanisms by which altered distributions of the Golgi body induce NSCs self-renewal defects, we assessed whether Notch signaling is affected by PITPNA/PITPNB-deficiency. To test this prediction, we used *in utero* electroporation to introduce an EGFP plasmid together with control or *Pitpnb* shRNA into the neocortex of E12.5 mouse embryos derived from *Pitpna* heterozygous crosses, and sacrificed the electroporated embryos 3 days later to analyze Notch signaling in the NSC pool. Compared with the control group (*Pitpna*$^{+/+}$ embryos electroporated with control shRNA), a significant reduction of the Notch intracellular domain (NICD), which is cleaved from the Notch receptor as part of the Notch signaling cascade (Kopan and Ilagan, 2009), was observed among EGFP^{+} cells in the PITPNA/PITPNB double deficiency group (Figures 37 and 39), but not in any other groups (Figures 36, 38 and 39). To confirm our immunohistochemistry data, we immunoblotted neocortex tissue lysate from conditional PITPNA/PITPNB double knockout embryos as previously described (Xie et al., 2018) and wild-type embryos at E12.5 with each of the NICD antibodies and HES1 antibodies. One of the NSC self-renewal-related target genes, Hes1, in Notch signaling pathways (Iso et al., 2003; Kageyama and Ohtsuka, 1999; Sato et al., 2010) was significantly reduced in the PITPNA/PITPNB double deficiency group, compared with control group (Figure 35 A). Moreover, our recent immunoblotting shows that NOTCH1 protein expression, which is the whole cell membrane receptor contains NICD in Notch signaling pathways, is also reduced in the PITPNA/PITPNB double deficiency group, compared with control groups (Figure 35 B). This preliminary data show that NOTHCH1, NICD and HES1 protein concentrations are reduced in E12.5 neocortex of PITPNA/PITPNB double knockout embryos, raising the possibility that Notch signaling pathways may be the key aberration underlying the NSC self-renewal defects.

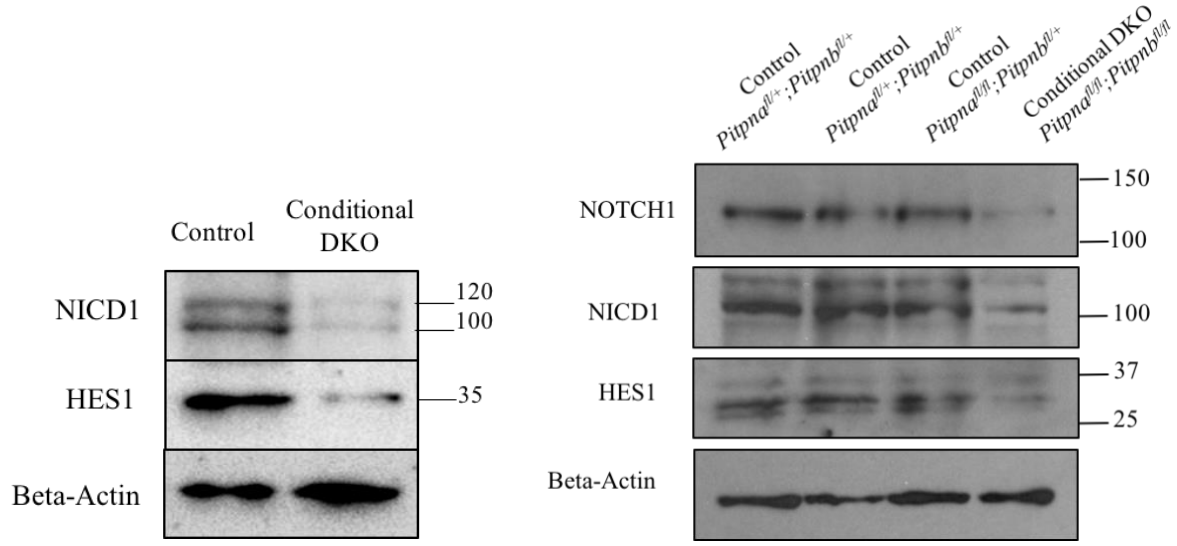

Figure 35. Notch activity of conditional PITPNA/PITPNB double knockout embryonic neocortex is reduced. (A) Control (Pitpna$^{fl/+}$ Pitpnb$^{fl/+}$ Emx1$^{Cre/+}$) or conditional DKO neocortex tissue lysate was analyzed by Western blot using a rabbit monoclonal anti-NICD and a rabbit polyclonal anti-HES1. The tissue-specific double knockout embryos characterized by Pitpna$^{fl/fl}$ Pitpnb$^{fl/fl}$ Emx1$^{Cre/+ \text{ or } Cre/Cre}$ genotypes. (B) Control or conditional DKO neocortex tissue lysate in RIPA buffer (to detect NOTCH1 receptor) was analyzed by Western blot using a rabbit monoclonal anti-NOTCH, monoclonal anti-NICD and a rabbit polyclonal anti-HES1.

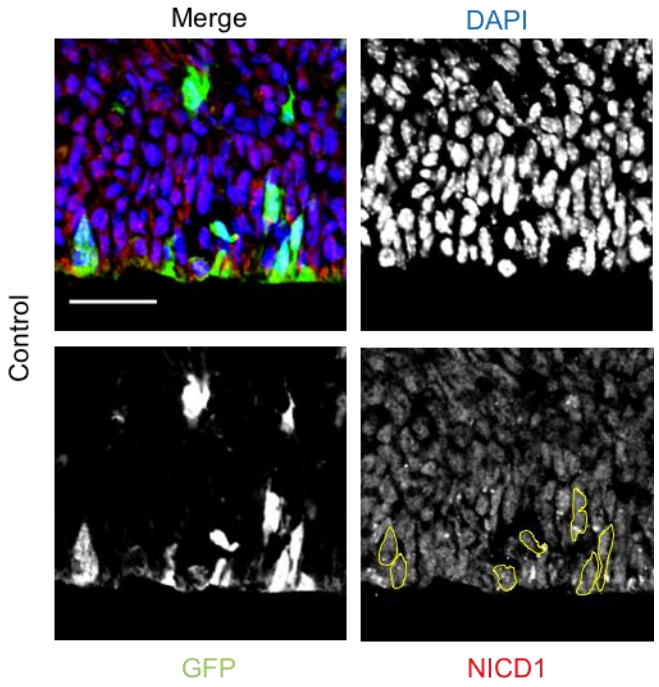

Figure 36. Notch activity in control Ventricular Zone NSCs is not reduced in the wild-type neocortex.

Mouse embryos (genotype: Pitpna$^{+/+}$ [control shRNA for control]) were co-electroporated with an EGFP plasmid and *control* shRNA plasmid at E12.5 and sacrificed at E15.5. NICD immunofluorescence(Cy3) were used to determine Notch signal activity on ventricular zone. Panels shows representative confocal images of mouse embryonic neocortex as a control to analyze intensity of NICD labeling in nuclei of NSCs. Scale bars: 20μm.

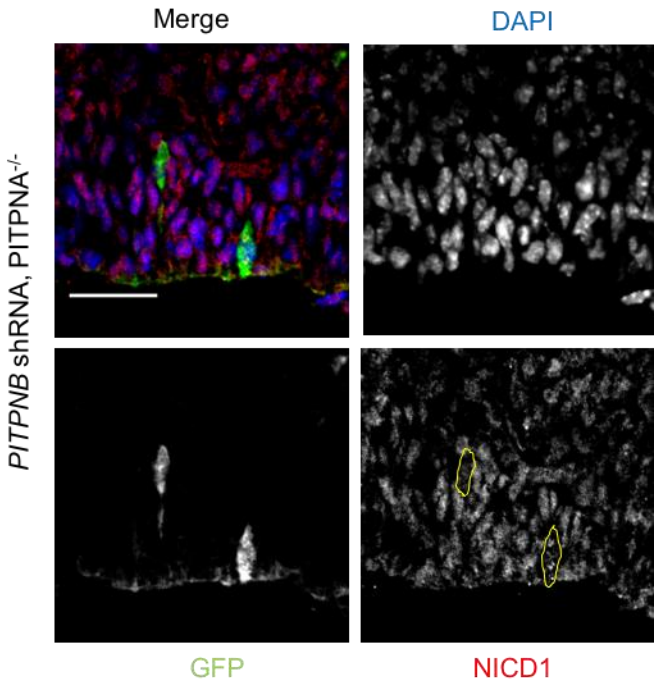

Figure 37. Notch activity in Ventricular Zone NSCs is reduced in the PITPNA/PITPNB-Deficient Neocortex. Mouse embryos (genotype: Pitpna$^{-/-}$ [PITPNB shRNA for double PITP deficiency] were co-electroporated with an EGFP plasmid and *Pitpnb* shRNA plasmid at E12.5 and sacrificed at E15.5. NICD immunofluorescence(Cy3) were used to determine Notch signal activity on ventricular zone. Panel shows representative confocal images of mouse embryonic neocortex with double PITP deficiency to analyze intensity of NICD labeling in nuclei of NSCs. Scale bars: 20μm.

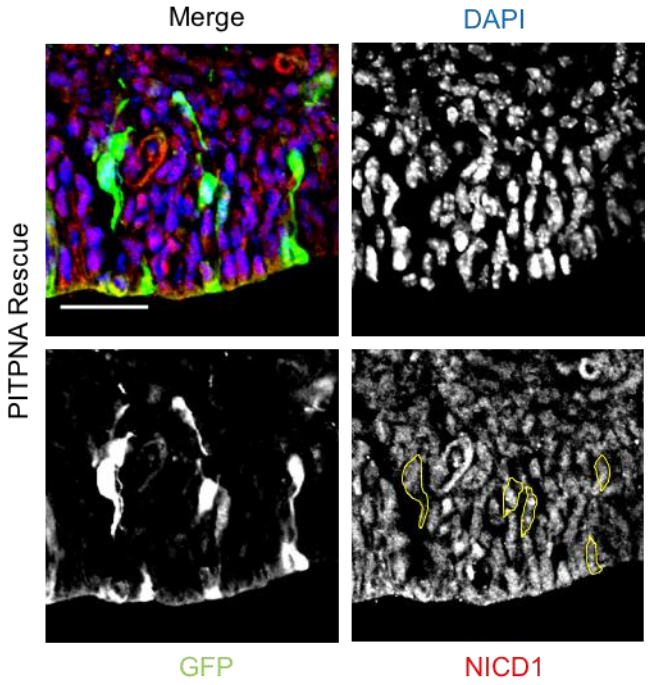

Figure 38. Notch activity in PITPNA rescue Ventricular Zone NSCs is not reduced in the neocortex.

Mouse embryos (genotype: Pitpna$^{-/-}$ [PITPNB shRNA for double PITP deficiency] were co-electroporated with an EGFP plasmid and *Pitpnb* shRNA plasmid at E12.5 and sacrificed at E15.5. In rescue experiments, a plasmid expressing wild-type PITPNA was added to the plasmid mixture. NICD immunofluorescence(Cy3) were used to determine Notch signal activity on ventricular zone. For the PITPNA rescue experiments, a plasmid expressing wild-type PITPNA was co-electroporated with PITPNB shRNA and EGFP plasmid. Representative confocal images of mouse embryonic neocortex. Scale bars: 20μm.

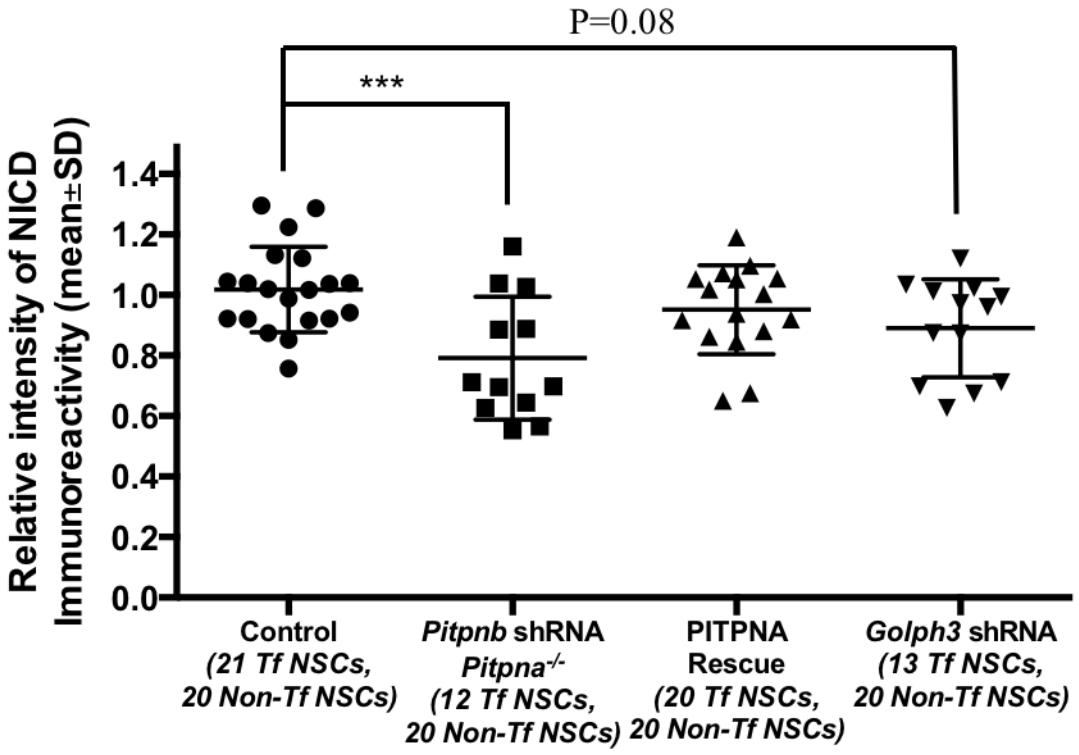

Figure 39. The relative intensity was reduced in double-PITP-deficient NSCs compared to control, but not significantly reduced in Golph3-deficient NSCs.

The ratio of the intensity of NICD labeling at the nuclei (indicated by DAPI) in transfected NSCs to that in non-transfected NSCs was quantified as the relative intensity of NICD immunoreactivity. *** $P<0.001$ compared to control, one-way ANOVA.

2.4.8 Notch signaling may not be the only pathway between PITP-dependent PtdIns-4-P signaling and NSC self-renewal

We already showed that *Golph3* shRNA expression diminished the NSC pool via enhancing asymmetric NSC division, and PITPNA/PITPNB double deficiency affected Golgi body distribution and Golgi localization of GOLPH3. To investigate whether Golgi body redistribution, which is induced by GOLPH3 knockdown, affected Notch signaling, we introduced an EGFP plasmid together with control or GOLPH3 shRNA into the neocortex of E12.5 mouse embryos by in utero electroporation, and sacrificed the electroporated embryos 3 days later to perform immunostaining with the NICD antibodies. GOLPH3 deficiency does not entirely abolish NICD activity in embryonic NSCs compared to quantified NICD activity in PITPs deficiency (Figure 39). However, our preliminary data shows that 4 out of 13 transfected cells with Golph3 shRNA induced 30% reduction in NICD activity in the NSCs (Figure 39). These data suggest that Notch signaling, while clearly affected by PITP-dependent, may not be the only pathway regulating NSC self-renewal, but that other signaling pathways might be involved in regulating cell fate. Future studies will aim to identify other pathways which are associated with PITP-dependent and GOLPH3-dependent signaling to support the NSC self-renewal.

CHAPTER III

CONCLUSIONS AND DISCUSSION

3.1 Key Findings

3.1.1 The START-like PITPs, PITPNA and PITPNB, are redundant, but required for neocortex/forebrain development

Our first two mice strategies, cre-mediated brain tissue-specific double-KO and whole-body PITBNA/PITPNB KO, demonstrated a requirement for either of these proteins to be present for proper embryonic development: brain tissue specific *Cre*-mediated PITPNA/PITPNB double knockout mice are born alive but fail to develop a neocortex, while PITPNA/PITNB double whole body knockout mice show early embryonic lethality. However, single-knockouts of either of these genes failed to develop a noticeable phenotype (Xie et al., 2018) suggesting that PITPNA/PITPNB may play a critical role and act in a functionally redundant manner as well in non-brain tissue development.

3.1.2 PITPNA and PITPNB are functionally redundant in determining stem cell fate

A significant reduction of the NSC pool was observed only in the case of PITPNA/PITPNB double deficiency, but not in any other groups (any single PITPNA or PITPNB deficiency) (Figure 11). Moreover, our cell pair analysis data also indicates that the mode of neural stem cell division was affected in only PITPNA/PITPNB double deficiency group (Figures 5-9). These data support very strongly that these two PITPs play in a functional redundant manner in neocortical development.

3.1.3 PITPNA and PITPNB are specifically required – similar exogenous proteins are insufficient for NSC self-renewal

In utero electroporation rescue experiments also showed that replacement of the PITPNA/PITPNB pair with an overexpressed PITPNA mutant that fails to bind either PtdIns or PtdCho were insufficient to restore functionality (Figure 15-16), suggesting that their ability to bind both lipids is a required factor for their function. Additionally, replacement of PITPNA/PITPNB with a yeast PITP, Sec14, which binds PtdIns and PtdCho and which localizes to the same areas within the cell, was insufficient to restore the NSC pool (Figure 20-23), suggesting that there are other intrinsic properties specific to PITPNA/PITPNB which are required for proper functionality, independent of lipid transfer (i.e., interactions with other proteins).

3.1.4 PtdIns-4-P-dependent signaling (via PITPNA/PITPNB) of GOLPH3 not only ensures proper Golgi positioning, but regulates NSC self-renewal

PtdIns-4-P-dependent recruitment of GOLPH3 was previously known to promote MYO18A and F-actin to regulate Golgi positioning in NSCs (Xie et al., 2018). However, the aforementioned studies showed that PtdIns-4-P-dependent GOLPH3 signaling regulates NSC self-renewal and, by extension, the NSC pool (Figure 24~28). The reduction of the NSC pool was rescued by re-expression of wild-type GOLPH3, but not of the mutant GOLPH3 R90L (defective in PtdIns-4-P binding). These data clearly demonstrated novel cellular roles of a PtdIns-4-P effector protein, GOLPH3, that (1) GOLPH3 is required for Golgi distribution and maintaining the NSCs pool, and (2) PtdIns-4-P binding manner is critical for GOLPH3 signaling for NSCs pool maintenance.

3.2 Future Directions

3.2.1 What is the role of PITPNA/PITPNB in non-neural stem cell differentiation?

PITPNA and PITPNB clearly play a significant role in neural stem cell differentiation and renewal, opening the possibility that these proteins could play a role in the development of other stem cell types. One method to determine stem cell populations thus affected would be to examine the precise time of early embryonic lethality displayed by PITPNA/PITPNB whole body double-KO mice and examine the stem cell populations that are active at that stage of development. Our preliminary data shows that of the 79 E12.5 embryos analyzed from intercross *Pitpna*$^{+/-}$ *Pitpnb*$^{+/-}$, there were none of recovered progenies exhibited either *Pitpna*$^{-/-}$ *Pitpnb*$^{-/-}$ or *Pitpna*$^{+/-}$ *Pitpnb*$^{-/-}$ genotypes (See 1.5). Our analysis of E11.5 embryos is ongoing (see 1.5). Thus, combined whole body PITPNA/PITPNB deficiency was not allowed for successful completion of early embryonic development in the mouse with the critical failure occurring prior to E12.5, and a single functional *Pitpna* allele was insufficient to rescue developmental failure. We will continue to analyze earlier embryonic stages (E8.5, E9.5, E10.5 and more E11.5 embryos) to identify the developmental failure. In lieu of a clear failure point, embryonic stem cells, or blastocysts could be good candidates for observation to determine the role of these PITPs in normal cellular activity.

3.2.2 What is the mechanism by which PITPNA/PITPNB carry out their role?

As mentioned previously, Sec14p, a yeast PITP which exhibits similar lipid-binding/transfer activities to that of PITPNA/PITPNB did not restore the NSC pool in PITPs

double deficient group (Figure 20). This result overturns a long-held model of PITP function, the PtdIns-gradient model, because the model cannot explain why PITPNA/PITPNB are specifically required for maintaining the NSC pool. However, the exchange model still holds weight: a rescue experiment with a plasmid for expressing mouse PITPNC1, a homolog of PITPNA/PITPNB that shows PtdIns-transfer activity but which exchanges with a different second lipid (PtdOH) failed to restore the NSC pool in PITPNA/PITPNB deficient group (Figure 22). Similarly, PITPNA PtdIns and PtdCho mutants similarly fail to restore the NSC pool (Figure 15-16). These data indicate that PtdIns/PtdCho exchange is absolutely necessary for the function of PITPNA/PITPNB, likely serving as the means whereby these PITPs stimulate the PtdIns-4 kinase.

To better understand this mechanism, with guidance from previous *in vitro* transfer-assay and molecular dynamics data, we aim to generate a catalogue of new candidate amino acid residues which are connected with PtdIns/PtdCho exchanging ability and membrane interaction. With each of these mutants, we will perform a rescue experiment of the NSC pool to test whether the mutant residues of PITPs, which inhibit membrane binding or PtdIns/PtdCho exchanging ability, can restore the NSC pool. These experiments will provide the greater insight into how PITPs bind with membranes and interact with the PtdIns-4 kinases to generate meaningful PtdIns-4-P signals.

3.2.3 Is the Notch signaling pathway the only connector between PITP dependent signaling and NSCs self-renewal?

Given that PITP deficiency induces a significant reduction in NICD activity and Hes1 expression in brain specific conditional PITPNA/PITPNB double Knockout embryo neocortex

(Figure 35), it is likely that PITP-dependent Golgi distribution is required to enable mature Notch receptors to travel to the plasma membrane, thereby serving as a regulator of NSC self-renewal (Blaumueller et al., 1997; Bruckner et al., 2000; Jang et al., 2014; Shen, 2007). To clarify how PITP-dependent PtdIns-4-P signaling could contribute to the Notch signaling pathway, we will measure quantified immunoreactivity of matured Notch receptor and activated NICD (Notch Intracellular domain) and look at their localizations in PITP-deficient NSCs. These data will provide beneficial information on whether PITP-dependent PtdIns-4-P signaling is associated either with the maturation of the Notch receptor within the Golgi, or with the process of Notch receptor trafficking to the plasma membrane for presentation.

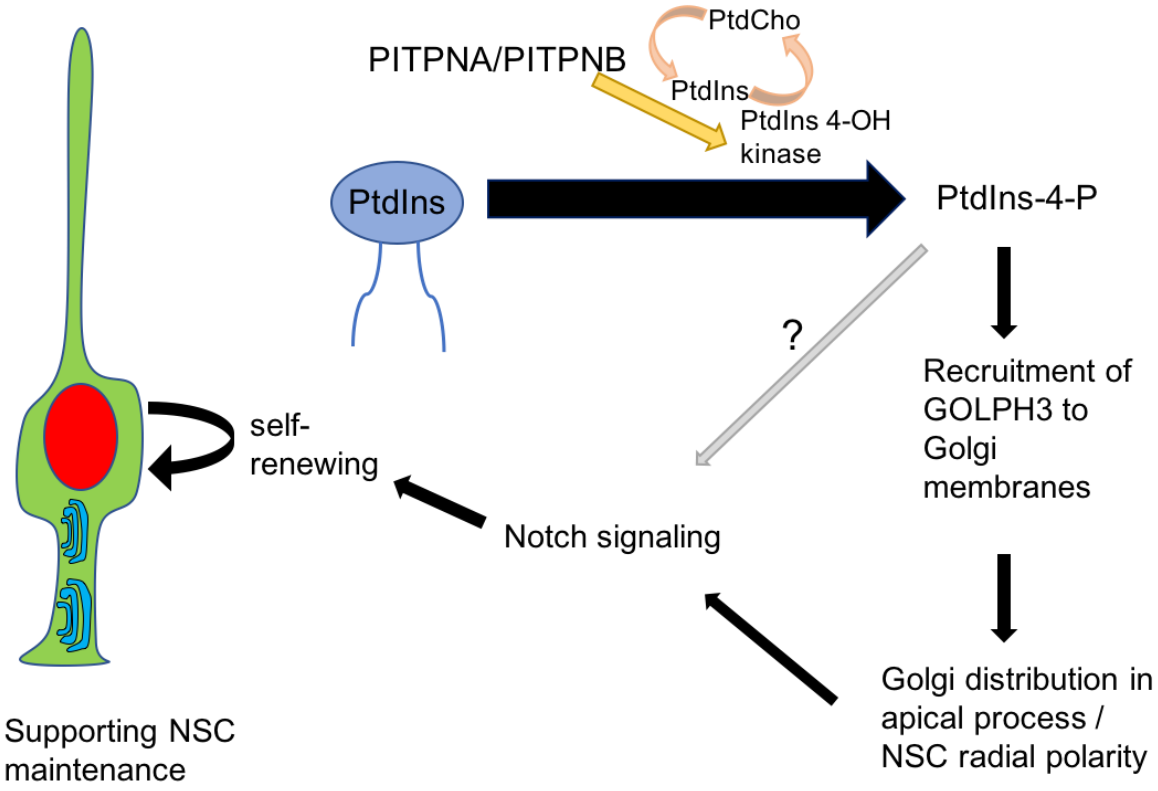

Figure 40. PtdIns-4-P dependent Golgi signaling pathway for NSCs self-renewing via Notch signaling.

PITPNA/PITPNB stimulate PtdIns 4-OH kinase to generate PtdIns-4-P which recruits GOLPH3 to Golgi membranes to modulate Golgi distribution in apical process of NSC. And then Golgi distribution contribute to Notch signaling activation to maintain NSCs self-renewal. Gray arrow indicates that a GOLPH3 independent pathway could help Notch signaling activation for NSCs self-renewing.

3.2.4 What are the roles of the PtdIns-4-P binding proteins GOLPH3, CERT?

In section 2.3.8, we tested whether GOLPH3-dependent PtdIns-4-P signaling is involved in the Notch signaling pathway. In our studies, GOLPH3 deficiency did not reduce NICD activity as much as PITP deficiency in NSCs, suggesting the existence of other relevant parallel signaling pathways unrelated to GOLPH3 (See Figure 40). Thus, PITP-dependent PtdIns-4-P signaling may not only use Notch signaling pathway but also other signaling pathways to regulate NSC self-renewal.

Similar to GOLPH3, ceramide transfer protein, (CERT) is another PtdIns-4-P dependent effector known to regulate NSC Golgi positioning and radial alignment (Xie et al., 2018). CERT is known to bind PtdIns-4-P, and is involved in diverse Golgi activities (Hanada et al., 2007). Given the functional and positional similarity to GOLPH3, CERT-mediated signaling is a likely candidate to explain the insufficient reduction of the NICD activity conferred by GOLPH3 deficiency experiments.

In addition to GOLPH3 and CERT, there is some evidence that the Wnt pathway is a likely effector of this pathway. The non-canonical Wnt-Planar Cell Polarity (PCP) pathway is known to affect the actin cytoskeleton rearrangement to generate planer polarity in tissues, playing a critical role in cell migration and cell divisions during neurogenesis (Mayor and Theveneau, 2014; Tissir and Goffinet, 2010), and regulating planar cell polarity behavior, such as neural tube closing, ciliary beating, and wound healing (Bayly and Axelrod, 2011; Mayor and Theveneau, 2014; Wada and Okamoto, 2009). Our previous study using conditional double-KO mice showed that PITP deficiency induced serious loss of polarity of NSCs (Xie et al., 2018), which is a known phenotype of blocked PCP signaling pathway (Beane et al., 2012). Given the similarity between the embryonic NSC polarity phenotype in forebrain-specific conditional

PITPNA/PITPNB double knockout mice, and the non-canonical Wnt-PCP pathway, the Wnt-PCP pathway is likely to be related with PITP-dependent PtdIns-4-P signaling.

To directly assess this activity, we screened readouts for another signaling pathway (canonical Wnt) to determine whether they might be directly or indirectly affected by PtdIns-4-P signaling. Our preliminary data showed that we did not find any abnormality in the canonical Wnt signaling pathway in neocortical development in PITP deficiency conditions. However, inhibition of the Wnt-PCP signaling pathway affects Golgi distribution (data not shown), yielding a similar Golgi phenotype to NSCs deficient in PITPNA/PITPNB (Figure 30). Thus, a connection between the Wnt-PCP signaling pathway should be examined to determine whether PITP-dependent PtdIns-4-P signaling is connected with Wnt-PCP signaling during neocortical development.

3.3 A comprehensive model for a PITP-mediated mechanism to control NSC self-renewal

These studies, which comprise my dissertation, demonstrate the novel role of type1 START-like PITPs during neocortical neurogenesis. PITPs stimulate PtdIns 4-OH kinases to generate PtdIns-4-P via PtdIns/PtdCho exchanging capability, and the resultant PtdIns-4-P recruits GOLPH3 to Golgi membranes to modulate Golgi distribution and NSCs radial polarity. Asymmetric Golgi distribution may contribute to maturation process of Notch receptor to maintain the NSC pool via controlling NSC self-renewing cell division (Figure 40). In addition, our data suggests that PITPs-dependent PtdIns-4-P signaling could activate pathways that are parallel to GOLPH3, such as CERT and the Wnt-PCP signaling pathway, to modulate NSCs polarity for NSC maintenance (Figure 41).

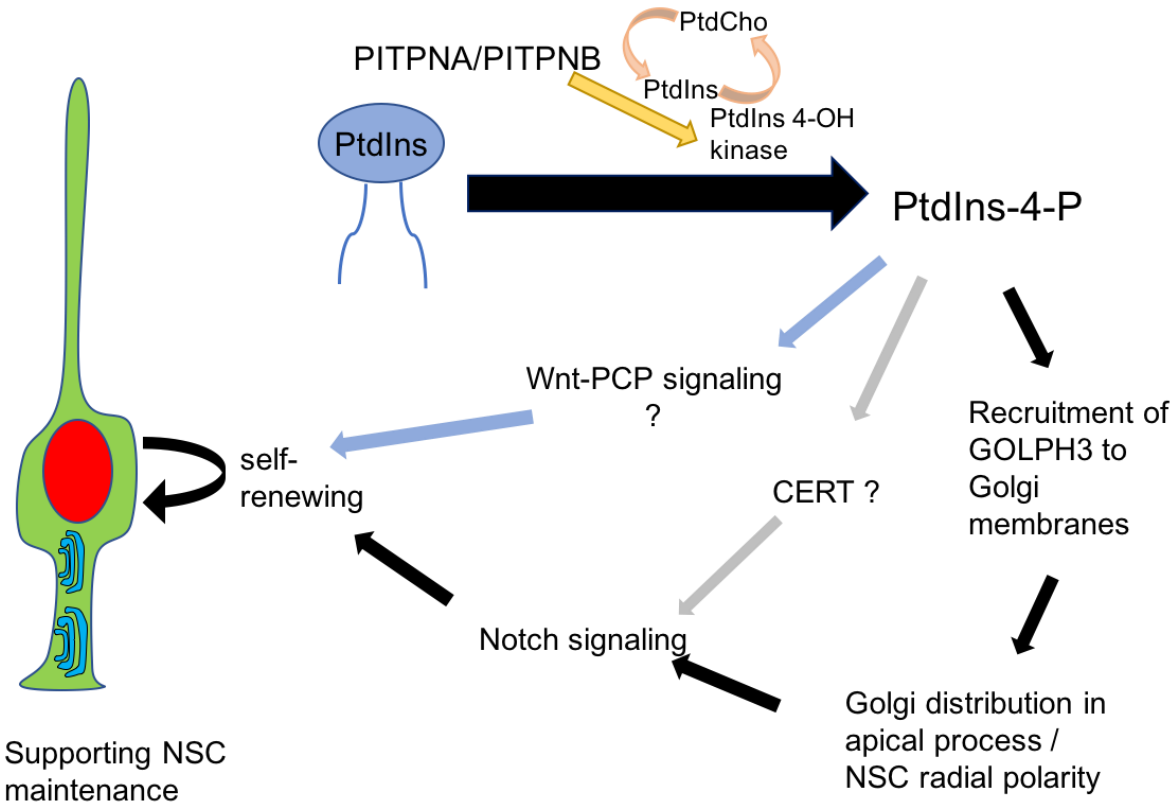

Figure 41. PITP-dependent PtdIns-4-P signaling regulates NSCs self-renewal through GOLPH3 stimulation, in addition to other pathways such as CERT and Wnt-PCP signaling.

PITPNA/PITPNB stimulate PtdIns 4-OH kinase to generate PtdIns-4-P at the Golgi membrane, which recruits GOLPH3 to modulate Golgi distribution in apical process of NSC. Golgi distribution is believed to enable Notch signaling activation to maintain NSC self-renewal. The gray arrow indicates that a GOLPH3-independent unknown pathway (i.e. CERT) could help Notch signaling activation for NSCs self-renewing, while the blue arrow indicates the possibility that PtdIns-4-P signaling could help to induce Wnt-PCP signaling to modulate NSC polarity, regulating NSC self-renewal.

REFERENCES

Aguirre, A., Rubio, M.E., and Gallo, V. (2010). Notch and EGFR pathway interaction regulates neural stem cell number and self-renewal. Nature *467*, 323-327.

Alb, J.G., Jr., Cortese, J.D., Phillips, S.E., Albin, R.L., Nagy, T.R., Hamilton, B.A., and Bankaitis, V.A. (2003). Mice lacking phosphatidylinositol transfer protein-alpha exhibit spinocerebellar degeneration, intestinal and hepatic steatosis, and hypoglycemia. J Biol Chem *278*, 33501-33518.

Alb, J.G., Jr., Gedvilaite, A., Cartee, R.T., Skinner, H.B., and Bankaitis, V.A. (1995). Mutant rat phosphatidylinositol/phosphatidylcholine transfer proteins specifically defective in phosphatidylinositol transfer: implications for the regulation of phospholipid transfer activity. Proc Natl Acad Sci U S A *92*, 8826-8830.

Alb, J.G., Jr., Phillips, S.E., Wilfley, L.R., Philpot, B.D., and Bankaitis, V.A. (2007). The pathologies associated with functional titration of phosphatidylinositol transfer protein alpha activity in mice. J Lipid Res *48*, 1857-1872.

Artegiani, B., Lange, C., and Calegari, F. (2012). Expansion of embryonic and adult neural stem cells by in utero electroporation or viral stereotaxic injection. J Vis Exp.

Balla, A., Vereb, G., Gulkan, H., Gehrmann, T., Gergely, P., Heilmeyer, L.M., Jr., and Antal, M. (2000). Immunohistochemical localisation of two phosphatidylinositol 4-kinase isoforms, PI4K230 and PI4K92, in the central nervous system of rats. Experimental brain research *134*, 279-288.

Balla, T. (2005). Inositol-lipid binding motifs: signal integrators through protein-lipid and protein-protein interactions. J Cell Sci *118*, 2093-2104.

Balla, T. (2013). Phosphoinositides: tiny lipids with giant impact on cell regulation. Physiol Rev *93*, 1019-1137.

Bankaitis, V.A., Aitken, J.R., Cleves, A.E., and Dowhan, W. (1990). An essential role for a phospholipid transfer protein in yeast Golgi function. Nature *347*, 561-562.

Bankaitis, V.A., Garcia-Mata, R., and Mousley, C.J. (2012). Golgi membrane dynamics and lipid metabolism. Curr Biol *22*, R414-424.

Bankaitis, V.A., Mousley, C.J., and Schaaf, G. (2010). The Sec14 superfamily and mechanisms for crosstalk between lipid metabolism and lipid signaling. Trends Biochem Sci *35*, 150-160.

Bayly, R., and Axelrod, J.D. (2011). Pointing in the right direction: new developments in the field of planar cell polarity. Nat Rev Genet *12*, 385-391.

Beane, W.S., Tseng, A.S., Morokuma, J., Lemire, J.M., and Levin, M. (2012). Inhibition of planar cell polarity extends neural growth during regeneration, homeostasis, and development. Stem Cells Dev *21*, 2085-2094.

Berridge, M.J., and Irvine, R.F. (1984). Inositol trisphosphate, a novel second messenger in cellular signal transduction. Nature *312*, 315.

Bjornsson, C.S., Apostolopoulou, M., Tian, Y., and Temple, S. (2015). It takes a village: constructing the neurogenic niche. Dev Cell *32*, 435-446.

Blaumueller, C.M., Qi, H., Zagouras, P., and Artavanis-Tsakonas, S. (1997). Intracellular cleavage of Notch leads to a heterodimeric receptor on the plasma membrane. Cell *90*, 281-291.

Boura, E., and Nencka, R. (2015). Phosphatidylinositol 4-kinases: Function, structure, and inhibition. Exp Cell Res *337*, 136-145.

Bourgeron, T. (2009). A synaptic trek to autism. Curr Opin Neurobiol *19*, 231-234.

Bruckner, K., Perez, L., Clausen, H., and Cohen, S. (2000). Glycosyltransferase activity of Fringe modulates Notch-Delta interactions. Nature *406*, 411-415.

Cao, X., Coskun, U., Rossle, M., Buschhorn, S.B., Grzybek, M., Dafforn, T.R., Lenoir, M., Overduin, M., and Simons, K. (2009). Golgi protein FAPP2 tubulates membranes. Proc Natl Acad Sci U S A *106*, 21121-21125.

Carvou, N., Holic, R., Li, M., Futter, C., Skippen, A., and Cockcroft, S. (2010). Phosphatidylinositol- and phosphatidylcholine-transfer activity of PITPbeta is essential for COPI-mediated retrograde transport from the Golgi to the endoplasmic reticulum. J Cell Sci *123*, 1262-1273.

Christian, S.L., Brune, C.W., Sudi, J., Kumar, R.A., Liu, S., Karamohamed, S., Badner, J.A., Matsui, S., Conroy, J., McQuaid, D., *et al.* (2008). Novel submicroscopic chromosomal abnormalities detected in autism spectrum disorder. Biol Psychiatry *63*, 1111-1117.

Clayton, E.L., Minogue, S., and Waugh, M.G. (2013). Phosphatidylinositol 4-kinases and PI4P metabolism in the nervous system: roles in psychiatric and neurological diseases. Mol Neurobiol *47*, 361-372.

Cleves, A., McGee, T., and Bankaitis, V. (1991). Phospholipid transfer proteins: a biological debut. Trends in Cell Biology *1*, 30-34.

Cockcroft, S., and Carvou, N. (2007). Biochemical and biological functions of class I phosphatidylinositol transfer proteins. Biochim Biophys Acta *1771*, 677-691.

Concepcion, D., Johannes, F., Lo, Y.H., Yao, J., Fong, J., and Hamilton, B.A. (2011). Modifier genes for mouse phosphatidylinositol transfer protein alpha (vibrator) that bypass juvenile lethality. Genetics *187*, 1185-1191.

Conti, L., Pollard, S.M., Gorba, T., Reitano, E., Toselli, M., Biella, G., Sun, Y., Sanzone, S., Ying, Q.L., Cattaneo, E., *et al.* (2005). Niche-independent symmetrical self-renewal of a mammalian tissue stem cell. PLoS Biol *3*, e283.

D'Angelo, G., Polishchuk, E., Di Tullio, G., Santoro, M., Di Campli, A., Godi, A., West, G., Bielawski, J., Chuang, C.C., van der Spoel, A.C., *et al.* (2007). Glycosphingolipid synthesis requires FAPP2 transfer of glucosylceramide. Nature *449*, 62-67.

D'Angelo, G., Vicinanza, M., Di Campli, A., and De Matteis, M.A. (2008). The multiple roles of PtdIns(4)P – not just the precursor of PtdIns(4,5)P₂. Journal of Cell Science *121*, 1955-1963.

de la Pompa, J.L., Wakeham, A., Correia, K.M., Samper, E., Brown, S., Aguilera, R.J., Nakano, T., Honjo, T., Mak, T.W., Rossant, J., *et al.* (1997). Conservation of the Notch signalling pathway in mammalian neurogenesis. Development *124*, 1139-1148.

De Vries, D.D., Went, L.N., Bruyn, G.W., Scholte, H.R., Hofstra, R.M., Bolhuis, P.A., and van Oost, B.A. (1996). Genetic and biochemical impairment of mitochondrial complex I activity in a family with Leber hereditary optic neuropathy and hereditary spastic dystonia. Am J Hum Genet *58*, 703-711.

de Vries, D.J., and Beart, P.M. (1995). Fishing for drugs from the sea: status and strategies. Trends Pharmacol Sci *16*, 275-279.

Demmel, L., Gravert, M., Ercan, E., Habermann, B., Müller-Reichert, T., Kukhtina, V., Haucke, V., Baust, T., Sohrmann, M., Kalaidzidis, Y., *et al.* (2008). The Clathrin Adaptor Gga2p Is a Phosphatidylinositol 4-phosphate Effector at the Golgi Exit. Molecular biology of the cell *19*, 1991-2002.

Di Paolo, G., and De Camilli, P. (2006). Phosphoinositides in cell regulation and membrane dynamics. Nature *443*, 651.

Dippold, H.C., Ng, M.M., Farber-Katz, S.E., Lee, S.-K., Kerr, M.L., Peterman, M.C., Sim, R., Wiharto, P.A., Galbraith, K.A., Madhavarapu, S., *et al.* (2009a). GOLPH3 Bridges Phosphatidylinositol-4- Phosphate and Actomyosin to Stretch and Shape the Golgi to Promote Budding. Cell *139*, 337-351.

Dippold, H.C., Ng, M.M., Farber-Katz, S.E., Lee, S.K., Kerr, M.L., Peterman, M.C., Sim, R., Wiharto, P.A., Galbraith, K.A., Madhavarapu, S., *et al.* (2009b). GOLPH3 bridges phosphatidylinositol-4- phosphate and actomyosin to stretch and shape the Golgi to promote budding. Cell *139*, 337-351.

Doe, C.Q. (2008). Neural stem cells: balancing self-renewal with differentiation. Development *135*, 1575-1587.

Dumaresq-Doiron, K., Savard, M.-F., Akam, S., Costantino, S., and Lefrancois, S. (2010). The phosphatidylinositol 4-kinase PI4KIIIα is required for the recruitment of GBF1 to Golgi membranes. Journal of Cell Science *123*, 2273-2280.

Fruman, D.A., Meyers, R.E., and Cantley, L.C. (1998). Phosphoinositide kinases. Annu Rev Biochem *67*, 481-507.

Gage, Fred H., and Temple, S. (2013). Neural Stem Cells: Generating and Regenerating the Brain. Neuron *80*, 588-601.

Garner, K., Hunt, A.N., Koster, G., Somerharju, P., Groves, E., Li, M., Raghu, P., Holic, R., and Cockcroft, S. (2012). Phosphatidylinositol transfer protein, cytoplasmic 1 (PITPNC1) binds and transfers phosphatidic acid. J Biol Chem *287*, 32263-32276.

Glaser, T., and Brustle, O. (2005). Retinoic acid induction of ES-cell-derived neurons: the radial glia connection. Trends Neurosci *28*, 397-400.

Godi, A., Di Campli, A., Konstantakopoulos, A., Di Tullio, G., Alessi, D.R., Kular, G.S., Daniele, T., Marra, P., Lucocq, J.M., and De Matteis, M.A. (2004). FAPPs control Golgi-to-cell-surface membrane traffic by binding to ARF and PtdIns(4)P. Nat Cell Biol *6*, 393-404.

Grabon, A., Khan, D., and Bankaitis, V.A. (2015). Phosphatidylinositol transfer proteins and instructive regulation of lipid kinase biology. Biochim Biophys Acta *1851*, 724-735.

Grabon, A., Orlowski, A., Tripathi, A., Vuorio, J., Javanainen, M., Rog, T., Lonnfors, M., McDermott, M.I., Siebert, G., Somerharju, P., *et al.* (2017). Dynamics and energetics of the mammalian phosphatidylinositol transfer protein phospholipid exchange cycle. J Biol Chem *292*, 14438-14455.

Groszer, M., Erickson, R., Scripture-Adams, D.D., Lesche, R., Trumpp, A., Zack, J.A., Kornblum, H.I., Liu, X., and Wu, H. (2001). Negative regulation of neural stem/progenitor cell proliferation by the Pten tumor suppressor gene in vivo. Science *294*, 2186-2189.

Gu, F., Crump, C.M., and Thomas, G. (2001). Trans-Golgi network sorting. Cell Mol Life Sci *58*, 1067-1084.

Halberg, N., Sengelaub, C.A., Navrazhina, K., Molina, H., Uryu, K., and Tavazoie, S.F. (2016). PITPNC1 Recruits RAB1B to the Golgi Network to Drive Malignant Secretion. Cancer Cell *29*, 339-353.

Hama, H., Schnieders, E.A., Thorner, J., Takemoto, J.Y., and DeWald, D.B. (1999). Direct involvement of phosphatidylinositol 4-phosphate in secretion in the yeast Saccharomyces cerevisiae. J Biol Chem *274*, 34294-34300.

Hamilton, B.A., Smith, D.J., Mueller, K.L., Kerrebrock, A.W., Bronson, R.T., van Berkel, V., Daly, M.J., Kruglyak, L., Reeve, M.P., Nemhauser, J.L., *et al.* (1997). The vibrator mutation causes neurodegeneration via reduced expression of PITP alpha: positional complementation cloning and extragenic suppression. Neuron *18*, 711-722.

Hammond, G.R., Machner, M.P., and Balla, T. (2014). A novel probe for phosphatidylinositol 4-phosphate reveals multiple pools beyond the Golgi. J Cell Biol *205*, 113-126.

Hammond, G.R., Schiavo, G., and Irvine, R.F. (2009). Immunocytochemical techniques reveal multiple, distinct cellular pools of PtdIns4P and PtdIns(4,5)P(2). Biochem J *422*, 23-35.

Hanada, K., Kumagai, K., Tomishige, N., and Kawano, M. (2007). CERT and intracellular trafficking of ceramide. Biochim Biophys Acta *1771*, 644-653.

Hanada, K., Kumagai, K., Yasuda, S., Miura, Y., Kawano, M., Fukasawa, M., and Nishijima, M. (2003). Molecular machinery for non-vesicular trafficking of ceramide. Nature *426*, 803-809.

Handler, M., Yang, X., and Shen, J. (2000). Presenilin-1 regulates neuronal differentiation during neurogenesis. Development *127*, 2593-2606.

Hatakeyama, J., Bessho, Y., Katoh, K., Ookawara, S., Fujioka, M., Guillemot, F., and Kageyama, R. (2004). Hes genes regulate size, shape and histogenesis of the nervous system by control of the timing of neural stem cell differentiation. Development *131*, 5539-5550.

Hay, J.C., Fisette, P.L., Jenkins, G.H., Fukami, K., Takenawa, T., Anderson, R.A., and Martin, T.F. (1995). ATP-dependent inositide phosphorylation required for Ca(2+)-activated secretion. Nature *374*, 173-177.

Hay, J.C., and Martin, T.F. (1993). Phosphatidylinositol transfer protein required for ATP-dependent priming of Ca(2+)-activated secretion. Nature *366*, 572-575.

Heldwein, E.E., Macia, E., Wang, J., Yin, H.L., Kirchhausen, T., and Harrison, S.C. (2004). Crystal structure of the clathrin adaptor protein 1 core. Proc Natl Acad Sci U S A *101*, 14108-14113.

Hicks, C., Johnston, S.H., diSibio, G., Collazo, A., Vogt, T.F., and Weinmaster, G. (2000). Fringe differentially modulates Jagged1 and Delta1 signalling through Notch1 and Notch2. Nat Cell Biol *2*, 515-520.

Huang, J., Ghosh, R., and Bankaitis, V.A. (2016). Sec14-like phosphatidylinositol transfer proteins and the biological landscape of phosphoinositide signaling in plants. Biochim Biophys Acta *1861*, 1352-1364.

Ile, K.E., Kassen, S., Cao, C., Vihtehlic, T., Shah, S.D., Mousley, C.J., Alb, J.G., Jr., Huijbregts, R.P., Stearns, G.W., Brockerhoff, S.E., *et al.* (2010). Zebrafish class 1 phosphatidylinositol transfer proteins: PITPbeta and double cone cell outer segment integrity in retina. Traffic *11*, 1151-1167.

Ile, K.E., Schaaf, G., and Bankaitis, V.A. (2006). Phosphatidylinositol transfer proteins and cellular nanoreactors for lipid signaling. Nat Chem Biol *2*, 576-583.

Imai, H., Tanaka, S., Fukusato, T., Yamashita, S., and Hosaka, K. (1997). Differential distribution of mRNAs encoding phosphatidylinositol transfer proteins alpha and beta in the central nervous system of the rat. Brain Res Mol Brain Res *46*, 256-264.

Iso, T., Kedes, L., and Hamamori, Y. (2003). HES and HERP families: multiple effectors of the Notch signaling pathway. J Cell Physiol *194*, 237-255.

Jacoby, M., Cox, J.J., Gayral, S., Hampshire, D.J., Ayub, M., Blockmans, M., Pernot, E., Kisseleva, M.V., Compere, P., Schiffmann, S.N., *et al.* (2009). INPP5E mutations cause primary

cilium signaling defects, ciliary instability and ciliopathies in human and mouse. Nat Genet *41*, 1027-1031.

Jang, J., Byun, S.H., Han, D., Lee, J., Kim, J., Lee, N., Kim, I., Park, S., Ha, S., Kwon, M., *et al.* (2014). Notch intracellular domain deficiency in nuclear localization activity retains the ability to enhance neural stem cell character and block neurogenesis in mammalian brain development. Stem Cells Dev *23*, 2841-2850.

Kageyama, R., and Ohtsuka, T. (1999). The Notch-Hes pathway in mammalian neural development. Cell Res *9*, 179-188.

Kakuk, A., Friedlander, E., Vereb, G., Jr., Kasa, A., Balla, A., Balla, T., Heilmeyer, L.M., Jr., Gergely, P., and Vereb, G. (2006). Nucleolar localization of phosphatidylinositol 4-kinase PI4K230 in various mammalian cells. Cytometry A *69*, 1174-1183.

Kauffmann-Zeh, A., Thomas, G.M., Ball, A., Prosser, S., Cunningham, E., Cockcroft, S., and Hsuan, J.J. (1995). Requirement for phosphatidylinositol transfer protein in epidermal growth factor signaling. Science *268*, 1188-1190.

Kopan, R., and Ilagan, M.X. (2009). The canonical Notch signaling pathway: unfolding the activation mechanism. Cell *137*, 216-233.

Kriegstein, A., and Alvarez-Buylla, A. (2009). The glial nature of embryonic and adult neural stem cells. Annu Rev Neurosci *32*, 149-184.

Lemmon, M.A. (2008). Membrane recognition by phospholipid-binding domains. Nat Rev Mol Cell Biol *9*, 99-111.

Li, X., Routt, S.M., Xie, Z., Cui, X., Fang, M., Kearns, M.A., Bard, M., Kirsch, D.R., and Bankaitis, V.A. (2000). Identification of a novel family of nonclassic yeast phosphatidylinositol

transfer proteins whose function modulates phospholipase D activity and Sec14p-independent cell growth. Molecular biology of the cell *11*, 1989-2005.

LoTurco, J., Manent, J.B., and Sidiqi, F. (2009). New and improved tools for in utero electroporation studies of developing cerebral cortex. Cereb Cortex *19 Suppl 1*, i120-125.

Mayor, R., and Theveneau, E. (2014). The role of the non-canonical Wnt-planar cell polarity pathway in neural crest migration. Biochem J *457*, 19-26.

McLaughlin, S., and Murray, D. (2005). Plasma membrane phosphoinositide organization by protein electrostatics. Nature *438*, 605-611.

Mellman, I. (1996). Endocytosis and molecular sorting. Annu Rev Cell Dev Biol *12*, 575-625.

Michell, R.H. (2008). Inositol derivatives: evolution and functions. Nat Rev Mol Cell Biol *9*, 151-161.

Miyama, S., Takahashi, T., Nowakowski, R.S., and Caviness, V.S., Jr. (1997). A gradient in the duration of the G1 phase in the murine neocortical proliferative epithelium. Cereb Cortex *7*, 678-689.

Mizutani, K., Yoon, K., Dang, L., Tokunaga, A., and Gaiano, N. (2007). Differential Notch signalling distinguishes neural stem cells from intermediate progenitors. Nature *449*, 351-355.

Morgan, C.P., Allen-Baume, V., Radulovic, M., Li, M., Skippen, A., and Cockcroft, S. (2006). Differential expression of a C-terminal splice variant of phosphatidylinositol transfer protein beta lacking the constitutive-phosphorylated Ser262 that localizes to the Golgi compartment. Biochem J *398*, 411-421.

Nakatsu, F., Baskin, J.M., Chung, J., Tanner, L.B., Shui, G., Lee, S.Y., Pirruccello, M., Hao, M., Ingolia, N.T., Wenk, M.R., *et al.* (2012). PtdIns4P synthesis by PI4KIIIalpha at the plasma membrane and its impact on plasma membrane identity. J Cell Biol *199*, 1003-1016.

Nile, A.H., Bankaitis, V.A., and Grabon, A. (2010). Mammalian diseases of phosphatidylinositol transfer proteins and their homologs. Clin Lipidol *5*, 867-897.

Nyquist, D.A., and Helmkamp, G.M., Jr. (1989). Developmental patterns in rat brain of phosphatidylinositol synthetic enzymes and phosphatidylinositol transfer protein. Biochim Biophys Acta *987*, 165-170.

Odom, A.R., Stahlberg, A., Wente, S.R., and York, J.D. (2000). A Role for Nuclear Inositol 1,4,5-Trisphosphate Kinase in Transcriptional Control. Science *287*, 2026-2029.

Ohashi, M., Jan de Vries, K., Frank, R., Snoek, G., Bankaitis, V., Wirtz, K., and Huttner, W.B. (1995). A role for phosphatidylinositol transfer protein in secretory vesicle formation. Nature *377*, 544-547.

Okajima, T., Reddy, B., Matsuda, T., and Irvine, K.D. (2008). Contributions of chaperone and glycosyltransferase activities of O-fucosyltransferase 1 to Notch signaling. BMC Biol *6*, 1.

Phillips, S.E., Ile, K.E., Boukhelifa, M., Huijbregts, R.P., and Bankaitis, V.A. (2006a). Specific and nonspecific membrane-binding determinants cooperate in targeting phosphatidylinositol transfer protein beta-isoform to the mammalian trans-Golgi network. Molecular biology of the cell *17*, 2498-2512.

Phillips, S.E., Vincent, P., Rizzieri, K.E., Schaaf, G., Bankaitis, V.A., and Gaucher, E.A. (2006b). The diverse biological functions of phosphatidylinositol transfer proteins in eukaryotes. Crit Rev Biochem Mol Biol *41*, 21-49.

Png, K.J., Halberg, N., Yoshida, M., and Tavazoie, S.F. (2011). A microRNA regulon that mediates endothelial recruitment and metastasis by cancer cells. Nature *481*, 190-194.

Rhee, S.G. (2001). Regulation of Phosphoinositide-Specific Phospholipase C. Annual Review of Biochemistry *70*, 281-312.

Roth, M.G. (2004). Phosphoinositides in constitutive membrane traffic. Physiol Rev *84*, 699-730.

Routt, S.M., Ryan, M.M., Tyeryar, K., Rizzieri, K.E., Mousley, C., Roumanie, O., Brennwald, P.J., and Bankaitis, V.A. (2005). Nonclassical PITPs activate PLD via the Stt4p PtdIns-4-kinase and modulate function of late stages of exocytosis in vegetative yeast. Traffic *6*, 1157-1172.

Saito, K., Tautz, L., and Mustelin, T. (2007). The lipid-binding SEC14 domain. Biochim Biophys Acta *1771*, 719-726.

Salazar, G., Craige, B., Wainer, B.H., Guo, J., De Camilli, P., and Faundez, V. (2005). Phosphatidylinositol-4-Kinase Type II α Is a Component of Adaptor Protein-3-derived Vesicles. Molecular biology of the cell *16*, 3692-3704.

Sato, T., Shimazaki, T., Naka, H., Fukami, S., Satoh, Y., Okano, H., Lax, I., Schlessinger, J., and Gotoh, N. (2010). FRS2alpha regulates Erk levels to control a self-renewal target Hes1 and proliferation of FGF-responsive neural stem/progenitor cells. Stem Cells *28*, 1661-1673.

Sauer, M.E., and Walker, B.E. (1959). Radioautographic study of interkinetic nuclear migration in the neural tube. Proc Soc Exp Biol Med *101*, 557-560.

Schaaf, G., Ortlund, E.A., Tyeryar, K.R., Mousley, C.J., Ile, K.E., Garrett, T.A., Ren, J., Woolls, M.J., Raetz, C.R., Redinbo, M.R., *et al.* (2008). Functional anatomy of phospholipid binding and regulation of phosphoinositide homeostasis by proteins of the sec14 superfamily. Mol Cell *29*, 191-206.

Schouten, A., Agianian, B., Westerman, J., Kroon, J., Wirtz, K.W., and Gros, P. (2002). Structure of apo-phosphatidylinositol transfer protein alpha provides insight into membrane association. EMBO J *21*, 2117-2121.

Serajee, F.J., Nabi, R., Zhong, H., and Mahbubul Huq, A.H. (2003). Association of INPP1, PIK3CG, and TSC2 gene variants with autistic disorder: implications for phosphatidylinositol signalling in autism. J Med Genet *40*, e119.

Shen, M.M. (2007). Nodal signaling: developmental roles and regulation. Development *134*, 1023-1034.

Sidman, R.L., Miale, I.L., and Feder, N. (1959). Cell proliferation and migration in the primitive ependymal zone: an autoradiographic study of histogenesis in the nervous system. Exp Neurol *1*, 322-333.

Sridhar, S., Patel, B., Aphkhazava, D., Macian, F., Santambrogio, L., Shields, D., and Cuervo, A.M. (2013). The lipid kinase PI4KIIIbeta preserves lysosomal identity. EMBO J *32*, 324-339.

Suh, P.G., Park, J.I., Manzoli, L., Cocco, L., Peak, J.C., Katan, M., Fukami, K., Kataoka, T., Yun, S., and Ryu, S.H. (2008). Multiple roles of phosphoinositide-specific phospholipase C isozymes. BMB Rep *41*, 415-434.

Sun, T., and Hevner, R.F. (2014). Growth and folding of the mammalian cerebral cortex: from molecules to malformations. Nat Rev Neurosci *15*, 217-232.

Taverna, E., Gotz, M., and Huttner, W.B. (2014). The cell biology of neurogenesis: toward an understanding of the development and evolution of the neocortex. Annu Rev Cell Dev Biol *30*, 465-502.

Tilley, S.J., Skippen, A., Murray-Rust, J., Swigart, P.M., Stewart, A., Morgan, C.P., Cockcroft, S., and McDonald, N.Q. (2004). Structure-function analysis of human [corrected] phosphatidylinositol transfer protein alpha bound to phosphatidylinositol. Structure *12*, 317-326.

Tissir, F., and Goffinet, A.M. (2010). Planar cell polarity signaling in neural development. Curr Opin Neurobiol *20*, 572-577.

Toth, B., Balla, A., Ma, H., Knight, Z.A., Shokat, K.M., and Balla, T. (2006). Phosphatidylinositol 4-kinase IIIbeta regulates the transport of ceramide between the endoplasmic reticulum and Golgi. J Biol Chem *281*, 36369-36377.

Utsunomiya, A., Owada, Y., Yoshimoto, T., and Kondo, H. (1997). Localization of gene expression for phosphatidylinositol transfer protein in the brain of developing and mature rats. Brain Res Mol Brain Res *45*, 349-352.

Wada, H., and Okamoto, H. (2009). Roles of noncanonical Wnt/PCP pathway genes in neuronal migration and neurulation in zebrafish. Zebrafish *6*, 3-8.

Walch-Solimena, C., and Novick, P. (1999). The yeast phosphatidylinositol-4-OH kinase pik1 regulates secretion at the Golgi. Nat Cell Biol *1*, 523-525.

Wang, J., Sun, H.Q., Macia, E., Kirchhausen, T., Watson, H., Bonifacino, J.S., and Yin, H.L. (2007). PI4P promotes the recruitment of the GGA adaptor proteins to the trans-Golgi network and regulates their recognition of the ubiquitin sorting signal. Molecular biology of the cell *18*, 2646-2655.

Wang, Y.J., Wang, J., Sun, H.Q., Martinez, M., Sun, Y.X., Macia, E., Kirchhausen, T., Albanesi, J.P., Roth, M.G., and Yin, H.L. (2003). Phosphatidylinositol 4 phosphate regulates targeting of clathrin adaptor AP-1 complexes to the Golgi. Cell *114*, 299-310.

Waugh, M.G., Minogue, S., Anderson, J.S., Balinger, A., Blumenkrantz, D., Calnan, D.P., Cramer, R., and Hsuan, J.J. (2003). Localization of a highly active pool of type II phosphatidylinositol 4-kinase in a p97/valosin-containing-protein-rich fraction of the endoplasmic reticulum. Biochemical Journal *373*, 57-63.

Weimar, W.R., Lane, P.W., and Sidman, R.L. (1982). Vibrator (vb): a spinocerebellar system degeneration with autosomal recessive inheritance in mice. Brain Res *251*, 357-364.

Wirtz, K.W. (1991). Phospholipid transfer proteins. Annu Rev Biochem *60*, 73-99.

Wirtz, K.W. (2006). Phospholipid transfer proteins in perspective. FEBS Lett *580*, 5436-5441.

Wood, C.S., Schmitz, K.R., Bessman, N.J., Setty, T.G., Ferguson, K.M., and Burd, C.G. (2009). PtdIns4P recognition by Vps74/GOLPH3 links PtdIns 4-kinase signaling to retrograde Golgi trafficking. The Journal of Cell Biology *187*, 967-975.

Xie, Y., Ding, Y.Q., Hong, Y., Feng, Z., Navarre, S., Xi, C.X., Zhu, X.J., Wang, C.L., Ackerman, S.L., Kozlowski, D., *et al.* (2005). Phosphatidylinositol transfer protein-alpha in netrin-1-induced PLC signalling and neurite outgrowth. Nat Cell Biol *7*, 1124-1132.

Xie, Z., Hur, S.K., Zhao, L., Abrams, C.S., and Bankaitis, V.A. (2018). A Golgi Lipid Signaling Pathway Controls Apical Golgi Distribution and Cell Polarity during Neurogenesis. Dev Cell *44*, 725-740 e724.

Xie, Z., Jones, A., Deeney, J.T., Hur, S.K., and Bankaitis, V.A. (2016). Inborn Errors of Long-Chain Fatty Acid beta-Oxidation Link Neural Stem Cell Self-Renewal to Autism. Cell Rep *14*, 991-999.

Yoder, M.D., Thomas, L.M., Tremblay, J.M., Oliver, R.L., Yarbrough, L.R., and Helmkamp, G.M., Jr. (2001). Structure of a multifunctional protein. Mammalian phosphatidylinositol transfer protein complexed with phosphatidylcholine. J Biol Chem *276*, 9246-9252.

Zhou, J., and Parada, L.F. (2012). PTEN signaling in autism spectrum disorders. Curr Opin Neurobiol *22*, 873-879.

Zhou, Y., Atkins, J.B., Rompani, S.B., Bancescu, D.L., Petersen, P.H., Tang, H., Zou, K., Stewart, S.B., and Zhong, W. (2007). The mammalian Golgi regulates numb signaling in asymmetric cell division by releasing ACBD3 during mitosis. Cell *129*, 163-178.